Electronic Supplementary Material (ESI) for Dalton Transactions.

Bi- and trinuclear coinage metal complexes of a PNNP ligand featuring metallophilic interactions and an unusual charge separation

- Supporting information -

Milena Dahlen,[a] Max Kehry,[b] Sergei Lebedkin,[c] Manfred M. Kappes,[b,d] Wim Klopper[b] and Peter W. Roesky[a]*

a Institute of Inorganic Chemistry; Karlsruhe Institute of Technology (KIT); Engesserstr. 15, 76131 Karlsruhe (Germany); roesky@kit.edu)
b Institute of Nanotechnology; Karlsruhe Institute of Technology (KIT); Hermann-von-Helmholtz-Platz 1, 76344 Eggenstein-Leopoldshafen (Germany)
c Institute for Physical Chemistry (Theoretical Chemistry); Kaiserstraße 12, 76131 Karlsruhe
d Institute for Physical Chemistry; Karlsruhe Institute of Technology (KIT); Fritz-Haber-Weg 2, 76131 Karlsruhe (Germany)

Content

1 General procedures 3
2 Synthetic procedures 4
2.0 Potassium *N,N*'-bis[(2-diphenylphosphino)phenyl]-formamidinate (Kdpfam)[5-7] 4
2.1 Binuclear complexes 6
2.1.1 Synthesis of [$dpfam_2Cu_2$] (**1**) 6
2.1.2 Synthesis of [$dpfam_2Ag_2$] (**2**) 7
2.1.3 Synthesis of [$dpfam_2Au_2$] (**3**) 7
2.2 Synthesis of the trinuclear complexes 8
2.2.1 [$dpfam_2Cu_3(MeCN)][PF_6$] (**4**) 8
2.2.2 [$dpfam_2Cu_3][PF_6$] (**4a**) 9
2.2.3 [$dpfam_2Ag_3(thf)_2][BF_4$] (**5**) 10
3 Photoluminescence measurements 11
4 Quantum mechanical calculations 12
4.1 Calculated singlet excitation energies of bimetallic complexes **1**-**3** 13
4.2 Calculated singlet excitation energies of trimetallic complexes **4**, **4a** and **5** 20
4.3 Non-relaxed difference densities for **1**-**3** 33
4.4 Non-relaxed difference densities for **4**, **4a** and **5** 34
4.5 Calculated triplet excitation energies of bimetallic complexes **1**-**3** 35
4.6 Calculated triplet excitation energies of trimetallic complexes **4**, **4a** and **5** 36
5 Spectra 37
5.0 Kdpfam 37
5.1 [$dpfam_2Cu_2$] (**1**) 40
5.2 [$dpfam_2Ag_2$] (**2**) 43
5.3 [$dpfam_2Au_2$] (**3**) 46
5.4 [$dpfam_2Cu_3(MeCN)][PF_6$] (**4**) 50
5.5 [$dpfam_2Cu_3][PF_6$] (**4a**) 54
5.6 [$dpfam_2Ag_3(thf)_2][BF_4$] (**5**) 59
6 Crystallographic Data 62
7 References 69

Synthesis and analytics

1 General procedures

All manipulations of air-sensitive materials were carried out under exclusion of oxygen and moisture using common Schlenk technique on a dual manifold Schlenk line (inert gas: N_2, vacuum up to $1 \cdot 10^{-3}$ mbar) or an MBraun glove box (argon atmosphere). All reactions/substances comprising silver or gold were handled and crystallized in the dark (using aluminum foil).
Dry diethyl ether, toluene, *n*-pentane and *n*-heptane were obtained from a MBraun solvent purification system (SPS-800). THF was dried through distillation over potassium and benzophenone, dichloromethane was distilled over P_2O_5. All dried solvents were stored under nitrogen atmosphere.
Deuterated solvents were commercially obtained and dried over NaK alloy (THF-d_8,C_6D_6 stored over NaK) or CaH_2 (DMSO-d_6, stored over molecular sieve 4 Å) and degassed by freeze-pump-thaw cycles.
NMR spectra were recorded on a Bruker Avance III 300 MHz, Avance III 400 MHz or Avance 400 MHz. Chemical shifts were reported in parts per million (ppm) relative to tetramethylsilane (^{1}H,^{13}C) or 85% H_3PO_4 (^{31}P) and referenced to the proton rest signal of the deuterated solvent.[1] The multiplicities were abbreviated as the following: s = singlet, d = doublet, vd = virtual doublet, t = triplet, vt = virtual triplet, q = quartet, bs = broad singlet, m = multiplet. If not stated otherwise, all NMR spectra were recorded at 298 K.
IR spectra were obtained on a Bruker Tensor 37 FTIR spectrometer (DLaTGS detector and diamond ATR (attenuated total reflection) unit) equipped with a nitrogen flushed chamber. The spectra were prior to analysis flattened in baseline and intensity of signals was classified into the categories vs = very strong, s = strong, m = medium, w = weak and vw = very weak.
ESI mass spectra were obtained using a LTQ Orbitrap XL Q Exactive mass spectrometer (Thermo Fisher Scientific, San Jose, CA, USA) equipped with a HESI II probe. The instrument was calibrated in the m/z range 74-1822 using premixed calibration solutions (Thermo Scientific).
Elemental analyses were carried out on a Vario MICRO cube instrument from *Elementar Analysensysteme GmbH*.
N,N'-bis(2-fluorophenyl)formimidamide (FFormH)[2] was prepared according to literature procedures.
The following chemicals were obtained from common commercial sources and used without further purification: diphenylphosphine ($HPPh_2$), potassium chunks, 2-fluoroaniline, $AgBF_4$, $[Cu(MeCN)_4][PF_6]$.
Note that, if not otherwise stated, crystals used for single crystal diffraction analysis were taken from the crystallization mother liquor. For all other analytical methods, the crystalline product was isolated from the mother liquor and dried under reduced pressure. If not otherwise depicted, spectra were recorded at room temperature.

2 Synthetic procedures

Tetrahydrothiophene gold chloride [AuCl(tht)][3, 4]

Gold (4.827 g, 245 mmol) was dissolved in 120 mL boiling aqua regia (nitrohydrochloric acid) and the resulting red orange solution concentrated to around 25 mL. Remaining nitric acid was removed by repeated addition of concentrated hydrochloric acid (50 mL, 25 mL, 25 mL) and boiling the solution until the resulting vapor was colorless. After concentration to ~25 mL and cooling down to room temperature, 150 mL ethanol (technical) and 10 mL of water were added. The solution was heated to 50 °C and 15 mL of tetrahydrothiophene were added resulting in precipitation of the product as white colorless needle crystals. Crystallization was completed by storing the mother liquor in a fridge. After filtration, the obtained white crystals were washed with cold ethanol and cold diethylether (15 mL each) and dried under reduced pressure in the dark. The obtained product was used without further analytics. Yield: 7.42 g, 23.1 mmol, 94%.

2.0 Potassium *N,N'*-bis[(2-diphenylphosphino)phenyl]-formamidinate (Kdpfam)[5-7]

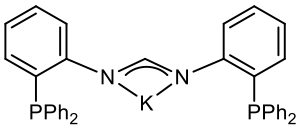

Potassium (2.08 g, 53.2 mmol, 3.00 eq) was provided in dry toluene at room temperature. Diphenylphosphine (9.30 mL, 9.95 g, 53.4 mmol, 3.00 eq) was added and the mixture was heated to 140 °C (oil bath temperature) until the potassium was fully consumed (~6h). *N,N*'-bis(2-fluorophenyl)formimidamide (4.01 g, 17.7 mmol, 1.00 eq) was added and the deep red suspension was stirred overnight at room temperature and refluxed for another 6–8 h (140 °C oil bath temperature) until a dull dark yellow suspension was obtained. The resulting brownish yellow suspension was submitted to a warm filtration over celite (P4 frit) and the solvent was removed *in vacuo* (while heating with a bath at 50 °C). The yellow semifluid residue was stirred overnight with/in heptane (300 mL) until a suspension with yellow free flowing solids is obtained. Filtration and intense washing of the yellow precipitate with pentane yielded the product as a water sensitive yellow powder (7.29 g, 12.1 mmol, 68%). Single crystals suitable for X-ray diffraction could be obtained by layering a solution of Kdpfam in 1:5 THF/toluene with *n*-heptane.

^{1}H NMR (400 MHz, THF-d_8): δ (ppm) = 8.65 – 8.55 (bs, 1H, NCN), 7.27 – 7.14 (m, 20H, H^{Ph}), 7.06 (ddd, $J_{H,H}$ = 8.5 Hz, 6.9 Hz, 1.9 Hz, 2H, H^{Ar}), 6.82 (ddd, $^{3}J_{H,H}$ = 8.2 Hz, $^{3}J_{H,H}$ = 5.1 Hz, $^{4}J_{H,H}$ = 1.1 Hz, 2H, H^{Ar}), 6.53 – 6.47 (m, 2H, H^{Ar}), 6.47 – 6.43 (m, 2H, H^{Ar}). – **^{13}C{^{1}H} NMR** (101 MHz, THF-d_8): δ (ppm) = 160.0 – 159.7 (m, N*C*HN), 140.8 (d, $J_{C,P}$ = 12.7 Hz, C_q), 134.8 (d, $J_{C,P}$ = 19.3 Hz, HC^{Ph}), 133.7 (HC^{Ar}), 130.5 (HC^{Ar}), 129.0 (d, $J_{C,P}$ = 6.4 Hz, HC^{Ph}), 128.7 (HC^{Ph}), 128.5 (C_q), 119.1 (HC^{Ar}), 116.6 (d, $J_{C,P}$ = 2.5 Hz, HC^{Ar}). – **^{31}P{^{1}H} NMR** (162 MHz, THF-d_8): δ (ppm) = -14.3 (s). – **IR** (ATR): $\tilde{\nu}$ (cm^{-1}) = 3049 (vw), 1583 (vw), 1558 (vw), 1530 (s), 1510 (vs), 1476 (vw), 1452 (s), 1427 (vs), 1334 (vs), 1277 (vw), 1263 (vw), 1217 (m), 1157 (vw), 1126 (vw), 1089 (vw), 1026 (vw), 989 (vw), 919 (vw), 771 (vw), 739 (m), 698 (s), 504 (m), 487 (m), 428(vw). – **EA:** $C_{37}H_{29}N_4P_4K$: calc. C 73.74; H 4.85; N 4.65; found C 73.21; N 4.75; H 4.55.

The ^{31}P NMR showed some minor remaining impurities of diphenyl phosphine and diphenyl phosphine oxide (<1 % each). In the $^{13}C\{^{1}H\}$ NMR spectrum, one resonance of a quaternary carbon atom is missing probably due to overlapping with another resonance.

If the protonated product is desired, the following aqueous work-up can be carried out: Saturated sodium bicarbonate solution was added to dry Kdpfam and the mixture was extracted 5 times with dichloromethane. The colorless organic phase was concentrated and the product was precipitated by

adding pentane (at least two times the former volume). After filtration, the resulting white powder was three times washed with pentane and dried under reduced pressure.

2.1 Binuclear complexes

2.1.1 Synthesis of [dpfam$_2$Cu$_2$] (1)

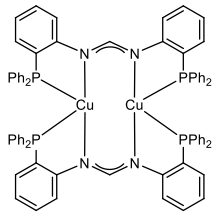

Kdpfam (100 mg, 166 µmol, 1.00 eq) and tetrakisacetonitrile copper hexafluorophosphate (61.8 mg, 166 µmol, 1.00 eq) were stirred in 12 mL of THF for 1.5 h. The solvent was removed under reduced pressure and the resulting residues extracted with toluene (8 mL). The obtained intensely colored yellow suspension was filtered and toluene was removed in vacuo. The yellow solid was dissolved in THF and the product was crystallized by slow diffusion of pentane into it. The product was obtained as intense yellow crystals (34.5 mg, 26.0 µmol, 31%, calculated including 1 molecule of THF) which were partially suitable for X-ray diffraction. Note that a direct crystallization from the concentrated toluene extraction solution also leads to the desired product (co-crystallized with toluene). An extraction with dichloromethane was not possible as it led to a chlorine bridged $Cu^{I/II}$-Cl-$Cu^{I/II}$ product hence a partial oxidation of the copper atoms occured.

^{1}H NMR (400 MHz, C_6D_6): δ (ppm) = 9.51 (s, 1H, NC*H*N), 7.52 (bs, 4H, H^{Ph}), 7.33 – 7.22 (mj, 2H, H^{Ar}), 7.12 – 7.05 (m, 2H, H^{Ar}), 7.06 – 6.81 (m, 6H, 2 H^{Ar} + 4H^{Ph}), 6.80 – 6.72 (m, 6H, 2H^{Ar} + 4H^{Ph}), 6.59 (app. t, $J_{H,H}$ = 7.5 Hz, 8H, H^{Ph}). – **^{1}H NMR{^{31}P (-18.4 ppm)}** (400 MHz, C_6D_6): δ (ppm) = 9.51 (s, 1H, NC*H*N), 7.52 (bs, 4H, H^{Ph}), 7.28 (dd, $^3J_{H,H}$ = 7.6 Hz, $^4J_{H,H}$ = 1.6 Hz, 2H, H^{Ar}), 7.09 (ddd, $^3J_{H,H}$ = 8.5 Hz, $^3J_{H,H}$ = 7.0 Hz, $^4J_{H,H}$ = 1.7 Hz, 2H, H^{Ar}), 7.08 – 6.79 (m, 6H, 2H^{Ar}+4H^{Ph}), 6.80 – 6.72 (m, 6H, H^{Ph}), 6.59 (app. t, $J_{H,H}$ = 7.6 Hz, 8H, H^{Ph}). – **^{13}C{^{1}H} NMR** (75 MHz, C_6D_6): δ (ppm) = 159.9 (N*C*HN), 156.6 (virtual t, $^nJ_{C,P}$ = 20.4 Hz, C_q), 134.6 (H*C*^{Ar}), 133.8 (bs, C_q), 132.0 (bs, C_q), 130.7 (H*C*^{Ar}), 127.8 (H*C*^{Ph}), 120.2 (H*C*^{Ar}), 115.2 (H*C*^{Ar}). – **^{31}P{^{1}H} NMR** (162 MHz, C_6D_6): δ (ppm) = -18.4 (s). – **MS** (ESI): m/z (%) = 1286.211 $[M+2O]^+$ (calc. 1286.208), 1302.206 $[M+3O]^+$ (calc. 1302.203), 1318.198 $[M+4O]^+$(calc. 1318.198). – **IR** (ATR): $\tilde{\nu}$ (cm^{-1}) = 3051 (vw), 1584 (vw), 1546 (vw), 1511 (vs), 1479 (m), 1453 (vs), 1431 (vs), 1310 (vs), 1263 (s), 1212 (s), 1157 (w), 1125 (vw), 1093 (vw), 1065 (vw), 1027 (vw), 955 (s), 916 (vw), 840 (vw), 815 (vw), 754 (w), 738 (s), 715 (vw), 691 (s), 547 (vw), 509 (w), 497 (m), 479 (m). – **EA:** $C_{74}H_{58}N_4P_4Cu_2$: calculated C 70.86; N 4.47; H 4.66; found C 70.67; N 4.35; H 4.72.

Both ^{1}H NMR and the ^{13}C{^{1}H} NMR spectra show signals for remaining THF (1 to 1.5 molecules) which was originally present in the crystals used for analytics although the product was dried under high vacuum. Due to some overlaps with the solvent signal and the broad signals, not all resonances for the diphenyl phosphine moieties could be identified. Integration in proton NMR was done for ½ molecule (= 1 ligand).

2.1.2 Synthesis of [dpfam$_2$Ag$_2$] (2)

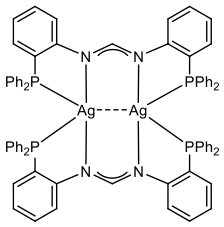

Kdpfam (100 mg, 166 µmol, 1.00 eq) and $AgBF_4$ (32.3 mg, 166 µmol, 1.00 eq) were stirred in 12 mL of THF for 1.5 h. After filtration of the light yellow suspension, pentane was diffused into it. The product was obtained as pale yellow crystals (88 mg, 60.6 µmol, 73%; calculated including 1.5 molecules of THF) which were partially suitable for X-ray diffraction.

We did not observe remaining metathesis salt in the obtained product (confirmed by elemental analysis). However, an extraction with dichloromethane or toluene prior to crystallization is possible.

^{1}H NMR (400 MHz, C_6D_6): δ (ppm) = 9.78 – 9.69 (m, 1H, NC*H*N), 7.40 – 7.33 (m, 4H, H^{Ar}), 7.29 (bs, 8H, H^{Ph}), 7.15 – 7.11 (m, 2H, H^{Ar}), 6.79 – 6.72 (m, 6H, $2H^{Ar}$+$4H^{Ph}$), 6.59 (app. t, $J_{H,H}$ = 7.6 Hz, 8H, H^{Ph}). – **^{1}H{^{31}P (-16.7 ppm)} NMR** (400 MHz, C_6D_6): δ (ppm) = 9.73 (pseudo t, $^3J_{H,107/109Ag}$ = 4.2 Hz, 1H, NC*H*N), 7.37 – 7.36 (m, 2H, H^{Ar}), 7.35 – 7.33 (m, 2H, H^{Ar}), 7.33 – 7.26 (m, 8H, H^{Ph}), 7.15 – 7.11 (m, 2H, H^{Ar}), 6.80 – 6.72 (m, 6H, $2H^{Ar}$+$4H^{Ph}$), 6.59 (app. t, $J_{H,H}$ = 7.6 Hz, 8H, H^{Ph}). – **^{13}C{^{1}H} NMR** (75 MHz, C_6D_6): δ (ppm) = 160.2 (NC*H*N), 157.2 – 157.1 (m, C_q), 136.3 (C_q), 135.5 (HC^{Ar}), 133.8 (bs, HC^{Ph}), 131.4 (HC^{Ar}), 128.2 (HC^{Ph}), 127.9 (HC^{Ph}), 120.3 (HC^{Ar}), 119.0 (C_q), 116.9 (HC^{Ar}). – **^{31}P{^{1}H}* NMR** (162 MHz, C_6D_6): δ (ppm) = -16.8 (superimposed pseudo tt, $J_{P,109Ag}$ = 184.2 Hz, $J_{P,107Ag}$ = 160.0 Hz. – **MS** (ESI): m/z (%) = 671.092 [1/2 M+H]$^+$ (calc. 671.093). – **IR** (ATR): $\tilde{\nu}$ (cm^{-1}) = 3050 (vw), 2953 (vw), 2923 (vw), 1583 (w), 1556 (w), 1535 (w), 1502 (vs), 1479 (m), 1453 (s), 1430 (s), 1334 (m), 1309 (s), 1286 (m), 1260 (m), 1213 (m), 1158 (w), 1124 (w), 1093 (w), 1055 (vw), 1036 (w), 961 (w), 918 (vw), 845 (vw), 815 (vw), 755 (w), 739 (m), 693 (m), 615 (vw), 543 (vw), 504 (w), 498 (w), 479 (w). – **EA:** $C_{78}H_{65}N_4OP_4Ag_2$ (M+1.5THF): calculated C 66.22; N 3.86; H 4.86; found C 66.43; N 3.95; H 4.59.

Both ^{1}H NMR and the ^{13}C{^{1}H} NMR spectra show signals for remaining THF (1 to 1.5 molecules) which was originally present in the crystals used for analytics although the product was dried under high vacuum. Integration in proton NMR was done for ½ molecule (= 1 ligand).

2.1.3 Synthesis of [dpfam$_2$Au$_2$] (3)

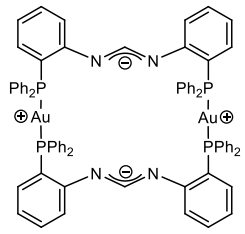

Kdpfam (200 mg, 332 µmol, 1.00 eq) and tetrahydrothiophene gold chloride (106 mg, 332 µmol, 1.00 eq) were stirred in 12 mL of THF overnight. After evaporation of the solvent in vacuum, 7 mL of toluene were added resulting in a yellow suspension. After filtration (PTFE syringe filter) and diffusion of pentane into the solution, the product was obtained as yellow crystals (164 mg, 102 µmol, 61% calculated including 1 molecule of toluene) which were partially suitable for X-ray diffraction.

For the use as metalloligand, **3** was not crystallized but directly obtained by removing the solvent from the filtered toluene extract.

^{1}H NMR (400 MHz, THF-d_8, 213 K): δ (ppm) = 8.33 – 8.26 (m, 1H, H^{Ar1}), 7.65 (s, 1H, NC*H*N), 7.57 – 7.33 (m, 16H, H^{Ph}), 7.34 – 7.26 (m, 2H, $2H^{Ph}$), 7.26 – 7.19 (m, 1H, $H_{Ar}{}^{Tol}$), 7.18 – 7.14 (m, 1H, H^{Ar2}), 7.14 – 7.08 (m, 1.5H, $H_{Ar}{}^{Tol}$), 6.98 – 6.88 (m, 3H, H^{Ar1}+$2H^{Ph}$), 6.78 – 6.70 (m, 1H, H^{Ar2}), 6.67 – 6.60 (m, 1H, H^{Ar1}), 6.58 – 6.52 (m, 1H, H^{Ar2}), 6.52 – 6.48 (m, 1H, H^{Ar2}), 6.46 – 6.39 (m, 1H, H^{Ar1}), 2.93 (s, 1.5H, $H_{Me}{}^{Tol}$). – **^{31}P{^{1}H} NMR** (121 MHz, THF-d_8): δ (ppm) = 35.9* (d, $^2J_{P,P}$ = 339.3 Hz), 27.6* (d, $^2J_{P,P}$ = 338.8 Hz). – **^{13}C{^{1}H} NMR** (75 MHz, THF-d_8): δ (ppm) = 158.6 (C_q), 157.4 (N(*C*H)N), 155.3 (C_q), 138.5 ($C_q{}^{Tol}$), 136.1 (bs, HC^{Ar}) 134.8

(HC^{Ar}), 134.7 (HC^{Ar}), 134.0 (bs, HC^{Ar}), 133.2 (bs, HC^{Ar}), 132.7 (bs, HC^{Ar}), 130.9 (HC^{Ar}), 130.3 (HC^{Ar}), 129.7 (HC^{Tol}), 129.2 (HC^{Ar}), 129.1 (HC^{Ar}), 128.9 (HC^{Tol}), 126.1 (HC^{Tol}), 125.7 (HC^{Ar}), 119.4 (HC^{Ar}), 118.7 (HC^{Ar}), 117.2 (HC^{Ar}), 21.5 (H_3C^{Tol}). – **MS** (ESI): m/z (%) = 1521.302 $[M+H]^+$ (cal. 1521.302). – **IR** (ATR): $\tilde{\nu}$ (cm^{-1}) = 3049 (w), 1635 (vw), 1576 (w), 1501 (vs), 1469 (w), 1450 (w), 1426 (vs), 1396 (s), 1344 (m), 1308 (w), 1262 (m), 1218 (w), 1181 (vw), 1157 (w), 1120 (w), 1098 (m), 1059 (w), 1027 (w), 999 (s), 980 (w), 900 (vw), 846 (vw), 745 (s), 732 (m), 690 (s), 547 (w), 508 (m), 490 (m), 415 (vw). – **EA:** $C_{81}H_{66}N_4P_4Au_2$ (M+toluene): calc. C 60.31; H 4.12; N 3.47; found C 59.83; H 4.007; N 3.45.

*Resonance show a strong roof effect probably being caused by higher order effects.

Both ^1H NMR and the $^{13}C\{^1H\}$ NMR spectra show signals for remaining toluene (1 molecule) which was originally present in the crystals used for analytics although the product was dried under high vacuum. Additionally, some remaining trace amounts of pentane (1.36 – 1.20 (m), 0.89 (t, *J* = 7.0 Hz)) (originating from the crystallization procedure) and tetrahydrothiophene (from the starting material) were detected. Due to dynamic behavior at room temperature, $^{13}C\{^1H\}$ NMR resonances could not be assigned thoroughly and some quaternary carbon signals could not be detected or identified.

2.2 Synthesis of the trinuclear complexes

2.2.1 $[dpfam_2Cu_3(MeCN)][PF_6]$ (4)

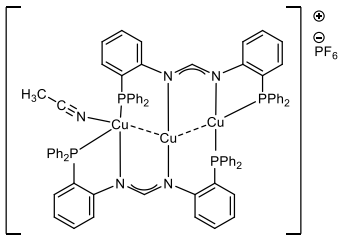

Kdpfam (100 mg, 166 µmol, 1.00 eq) and $[Cu(MeCN)_4][PF_6]$ (92.7 mg, 249 µmol, 1.50 eq) were stirred in 12 mL of THF for 1.5 h before the solvent was removed in vacuo. The yellow residues were extracted with dichloromethane (8 mL), the suspension was filtered and the solvent again removed under reduced pressure. After taking up the yellow solids in THF, one drop of MeCN was added and diffusion of pentane into the solution led to the product as yellow crystals (103 mg, 65.3 µmol, 79 ; calculated including one molecule of THF and one molecule of MeCN) which were partially suitable for X-ray diffraction.

$^1H\{^{31}P$(-18.2 ppm)$\}$ NMR (400 MHz, THF-d_8): δ (ppm) = 9.03 (s, 1H, NC*H*N), 7.95 – 7.83 (m, 1H; H^{Ar1}), 7.59 – 7.52 (m, 1H, H^{Ar1}), 7.50 – 7.44 (m, 1H, H^{Ar2}), 7.28 (dd, $^3J_{H,H}$ = 7.7 Hz, $^4J_{H,H}$ = 1.6 Hz, 1H, H^{Ar1}), 7.20 – 7.13 (m, 5H, $1H^{Ar2}$ + $4H^{Ph}$), [7.11 – 7.5 (m, H^{Ar1} +H^{Ph}) + 7.05 (bs, H^{Ph}), 9H], 6.98 – 6.93 (m, H^{Ar2}), 6.92 – 6.81 (m, 6H, H^{Ph}), 6.74 (dd, $^3J_{H,H}$ = 7.7 Hz, $^4J_{H,H}$ = 1.6 Hz, 1H, H^{Ar2}), 1.87 (s, 1.5H, MeCN). – **$^{13}C\{^1H,^{31}P$ (-18.2 ppm)$\}$ NMR** (101 MHz, THF-d_8): δ (ppm) = 162.3 (N(*C*H)N), 155.3 (C_q), 154.0 (C_q), 136.0 (HC^{Ar1}), 135.9 (HC^{Ar2}), 134.3 (HC^{Ph}), 133.6 (HC^{Ar1}), 132.9 (HC^{Ar2}), 130.8 (HC^{Ph} oder HC^{Ar2}), 129.9 (HC^{Ph} oder $H^{Ar1/2}$), 129.7 (HC^{Ph}), 127.3 (C_q), 125.4 (HC^{Ar2} oder HC^{Ph}), 124.4 (HC^{Ar1} oder HC^{Ph}), 124.3 (HC^{Ar2}), 123.5 (C_q), 117.8 (HC^{Ar1}), 117.3 (C_q^{MeCN}), 0.8 (H_3C^{MeCN}). – **$^{31}P\{^1H\}$ NMR** (162 MHz, THF-d_8): δ (ppm) = -17.0* (d, ^nJ = 109.2 Hz), -19.5* (d, ^nJ = 109.7 Hz), -141.9 (hept, $^1J_{P,F}$ = 709.6 Hz, PF_6^-) – **MS** (ESI): m/z (%) = 1317.150 $[M]^+$ (calc. 1317.148). – **IR** (ATR): $\tilde{\nu}$ (cm^{-1}) =3053 (vw), 1583 (vw), 1565 (vw), 1526 (vs), 1460 (s), 1433 (s), 1323 (s), 1269 (w), 1202 (w), 1164 (vw), 1094 (vw), 1064 (vw), 970 (vw), 834 (vs), 740 (m), 690 (s), 556 (m), 508 (m), 491 (m). – **EA:** $C_{74}H_{58}N_4P_5Cu_3F_6$ (+1 MeCN): calculated C 60.70; H 4.09; N 4.66; found C 60.56; H 4.45; N 4.00.

*The resonances show a strong Dach effect hinting higher order coupling.

Both ^{1}H NMR and the ^{13}C{^{1}H} NMR spectra show signals for remaining THF (1 molecule) and acetonitrile (1 molecule) which were originally present in the crystals used for analytics although the product was dried under high vacuum. Proton signals in the ligand backbone could be assigned to the two different aromatic rings (Ar1 and Ar2) using ^{1}H-COSY NMR. Probably due to some overlaps and broad signals for the diphenyl phosphine groups, not all carbon atom resonances of this moiety could be detected in ^{13}C NMR. Integration in proton NMR was done for ½ molecule (= 1 ligand). As both ^{1}H and ^{13}C nuclei show in parts strong coupling with the ^{31}P nuclei only phosphorous decoupled spectra are given. For coupled spectra see below.

2.2.2 [dpfam$_2$Cu$_3$][PF$_6$] (4a)

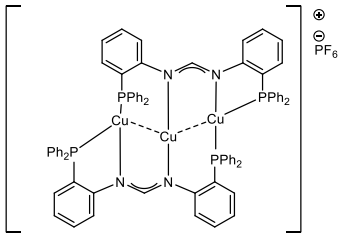

Kdpfam (100 mg, 166 µmol, 1.00 eq) and [Cu(MeCN)$_4$][PF$_6$] (92.7 mg, 249 µmol, 1.50 eq) were stirred in 12 mL of THF for 1.5 h before the solvent was removed in vacuo. The yellow residues were extracted with dichloromethane (8 mL), the suspension was filtered and the solvent again removed under reduced pressure. After taking up the yellow solids in THF, pentane was allowed to diffuse into the solution leading to the product as yellow crystals (64.5 mg, 44.1 µmol, 53%; calculated including half a molecule of THF) which were partially suitable for X-ray diffraction.

^{1}H{^{31}P (-18.3 ppm)} NMR (400 MHz, THF-d_8): δ (ppm) = 9.07 (s, 1H, NC*H*N), 7.92 (d, $^{3}J_{H,H}$ = 8.4 Hz, 1H, H^{Ar1}), 7.56 (ddd, $^{3}J_{H,H}$ = 8.6 Hz, $^{3}J_{H,H}$ = 7.1 Hz, $^{4}J_{H,H}$ = 1.6 Hz, 1H, H^{Ar1}), 7.54 – 7.46 (m, H^{Ar2}), 7.28 (dd, $^{3}J_{H,H}$ = 7.7 Hz, $^{4}J_{H,H}$ = 1.6 Hz, 1H, H^{Ar1}), 7.24 – 7.19 (m, H^{Ar2}), 7.16 (app. t, $J_{H,H}$ = 7.3 Hz, H^{Ph}), 7.12 – 7.06 (m, 1H, H^{Ar1}), 7.04 (bs, H^{Ph}), 6.95 (td, $^{3}J_{H,H}$ = 7.5 Hz, $^{4}J_{H,H}$ = 1.1 Hz, H^{Ar2}), 6.93 – 6.86 (m, H^{Ph}), 6.75 (dd, $^{3}J_{H,H}$ = 7.7 Hz, $^{4}J_{H,H}$ = 1.6 Hz, 1H, H^{Ar2}). – **^{13}C{^{1}H,^{31}P(-18.3 ppm)} NMR** (101 MHz, THF-d_8): δ (ppm) = 162.3 (N(*C*H)N), 155.3 (C$_q$), 153.9 (C$_q$), 136.0 (HC^{Ar1}), 135.8 (HC^{Ar2}), 134.3 (HC^{Ph}), 133.7 (HC^{Ar1}), 133.0 (HC^{Ar2}), 130.8 (HC^{Ph}), 130.0 (HC^{Ph}), 129.7 (HC^{Ph}), 127.3 (C$_q$), 125.5 (HC^{Ar2}), 124.4 (HC^{Ar1}), 124.3 (HC^{Ar2}), 123.6 (C$_q$), 117.8 (HC^{Ar1}). – **^{31}P{^{1}H} NMR** (121 MHz, THF-d_8): δ (ppm) = -17.0* (d, $^{n}J_{P,P}$ = 110.0 Hz), -19.6* (d, $^{n}J_{P,P}$ = 109.8 Hz), -144.1 (hept, $^{1}J_{P,F}$ = 709.6 Hz). – **MS** (ESI): m/z (%) = 1353.168 [M+2H$_2$O]$^{+}$ (calc. 1353.169). – **IR** (ATR): $\tilde{\nu}$ (cm^{-1}) = 3053 (w), 1633 (w), 1583 (w), 1565 (w), 1566 (vs), 1474 (m), 1461 (s), 1434 (vs), 1322 (s), 1286 (m), 1270 (m), 1218 (vw), 1202 (m), 1163 (w), 1131 (vw), 1095 (w), 1064 (vw), 974 (vw), 875 (vw), 832 (vs), 757 (w), 740 (s), 690 (s), 556 (m), 508 (w), 491 (m). – **EA:** $C_{74}H_{58}N_4P_5Cu_3F_6$: calculated C 60.76; H 4.00; N 3.83; found C 61.23; H 3.98; N 4.01.

*The resonances show a strong Dach effect hinting higher order coupling.

Both ^{1}H NMR and the ^{13}C{^{1}H} NMR spectra show signals for remaining THF (0.5 molecules) and pentane which were originally present in the crystals used for analytics although the product was dried under high vacuum. Due to a high baseline in the aromatic region of the ^{1}H NMR spectrum, integrals could not be determined adequately. However, proton signals in the ligand backbone could be assigned to the two different aromatic rings (Ar1 and Ar2) by using ^{1}H-COSY NMR. Probably due to some overlaps and broad signals for the diphenyl phosphine groups, eventually not all carbon atom resonances of this moiety could be detected in ^{13}C NMR. Integration in proton NMR was done for ½ molecule (= 1 ligand).

2.2.3 [dpfam$_2$Ag$_3$(*thf*)$_2$][BF$_4$] (5)

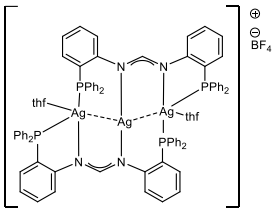

The ligand Kdpfam (150 mg, 249 µmol, 1.00 eq) and $AgBF_4$ (73 mg, 373 µmol, 1.50 eq) were stirred in 12 mL of THF overnight before the yellow suspension was filtrated. Through diffusion of pentane into the solution, the product was obtained as colorless to light yellow crystals (29.0 mg, 18.0 µmol, 14%) which were partially suitable for X-ray diffraction.

We did not observe remaining metathesis salt in the obtained product (confirmed by elemental analysis); However, an extraction with dichloromethane prior to crystallization is possible.

^{1}H NMR (400 MHz, DMSO-d_6): δ (ppm) = 7.61 – 7.52 (m, 1H, NC*H*N), 7.46 – 7.39 (m, 4H, H^{Ph}), 7.38 – 7.33 (m, 2H, H^{Ar}), 7.35 – 7.26 (m, 8H, H^{Ph}), 7.16 – 7.09 (m, 8H, H^{Ph}), 7.07 – 7.00 (m, 2H, H^{Ar}), 6.86 – 6.81 (m, 2H, H^{Ar}), 6.53 – 6.46 (m, 2H, H^{Ar}). – **^{13}C{^{1}H} NMR** (101 MHz, DMSO-d_6): δ (ppm) = 162.6 (N*C*HN), 154.6 (C$_q$), 133.3 (HC^{Ph}), 133.0 (HC^{Ar}), 132.1 (C$_q$), 131.5 (HC^{Ar}), 130.1 (HC^{Ph}), 128.9 (HC^{Ph}), 122.9 (HC^{Ar}), 122.7 (HC^{Ar}). – **^{31}P{^{1}H} NMR** (162 MHz, DMSO-d_6): δ (ppm) = -10.8* (bs), -13.2* (bs). – **MS** (ESI): m/z = 1451.078 [M]$^+$ (calc. 1451.075). – **IR** (ATR): $\tilde{\nu}$ (cm^{-1}) = 3053 (vw), 1586 (w), 1563 (w), 1541 (vw), 1456 (m), 1433 (s), 1351 (m), 1309 (m), 1269 (w), 1213 (w), 1205 (w), 1183 (m), 1160 (vw), 1094 (w), 1052 (vs), 1029 (m), 995 (vw), 972 (vw), 927 (vw), 892 (vw), 784 (w), 749 (m), 741 (m), 696 (s), 528 (vw), 505 (m), 471 (m), 464 (vw), 443 (vw). – **EA:** $C_{74}H_{58}N_4P_4Ag_3BF_4$ (+4THF: $C_{90}H_{89}Ag_3BF_4N_4O_4P_4$): calculated C 59.20; H 4.97; N 3.07; found C 59.47; H 4.43; N 3.44.

*The resonances shape hints higher order coupling.

Due to low solubility the NMR tube was heated over several days while THF formerly present in crystal structure evaporated out of the solution. Probably due to some overlapping with another resonance and the low intensity in ^{13}C NMR spectrum (low solubility), one quaternary carbon signal could not be detected. Integration in proton NMR was done for ½ molecule (= 1 ligand).

3 Photoluminescence measurements

PL measurements in the solid state were performed with a Horiba Jobin Yvon Fluorolog-322 spectrometer equipped with a closed-cycle optical cryostat (Leybold) operating within a temperature range of ca. 15-300 K. Solid samples (crystalline powders) were measured as dispersions in a thin layer of viscous polyfluoroester oil (ABCR GmbH) placed between two 1 mm thin quartz plates. The latter were mounted on the cold finger of the cryostat. Sample emission was collected at *ca*. 30° angle relative to the excitation light beam. All emission spectra were corrected for the wavelength-dependent response of the spectrometer and detector (in relative photon flux units). Emission decay traces were recorded by connecting a photomultiplier to a 500 MHz oscilloscope (via a 50, 500 or 2.500 Ohm load, depending on the decay time scale) and using a nitrogen laser (~2 ns, ~5 μJ per pulse) for pulsed excitation at 337 nm. Several hundred traces were usually acquired and averaged. PL quantum yields at ambient temperature were determined using an integrating sphere out of optical PTFE, which was installed into the sample chamber of the spectrometer, according to the method of de Mello et al.[8] The uncertainty of these measurements was estimated to be ± 10%.

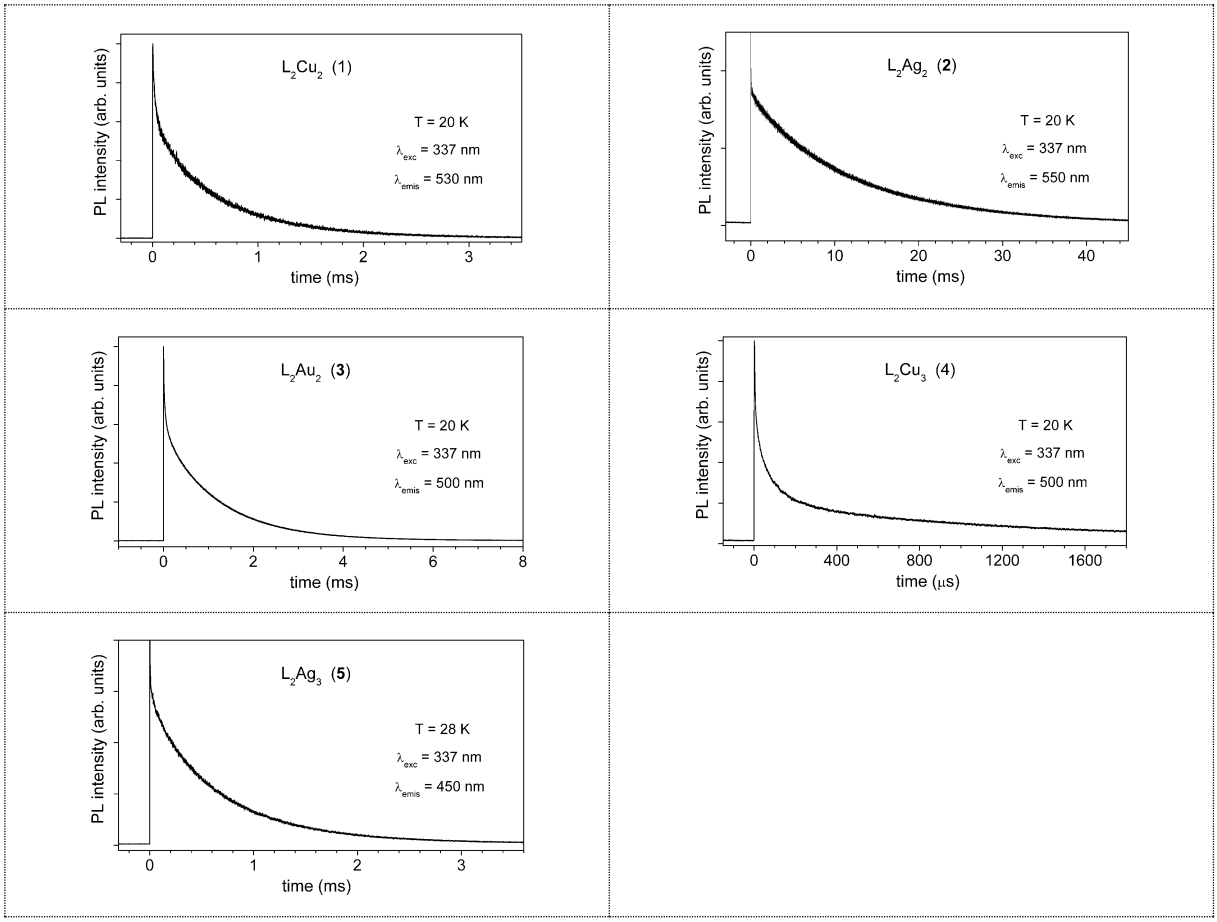

Figure S 3-1: Low-temperature PL decay of solid (polycrystalline) complexes **1**-**5** excited with a ns-pulsed nitrogen laser at 337 nm and recorded at indicated emission wavelengths. The decay traces can be fit with monoexponential/ biexponential curves with the following parameters (relative weights of biexponential components are denoted in brackets):

1 (T = 20 K, λ_{em} = 530 nm) : τ = 0.61 ms
2 (T = 20 K, λ_{em} = 554 nm) : τ = 11.9 ms
3 (T = 20 K, λ_{em} = 504 nm) : τ = 1.2 ms

4 (T = 20 K, λ_{em} =500 nm): τ1 =68 μs (67%), τ2 =840 μs (33%); **4a** (not shown): τ1 = 45 μs (67%), τ2 = 140 μs (33%)
5 (T = 28 K, λ_{em} = 430 nm) : τ = 0.69 ms

4 Quantum mechanical calculations

In the Following sections calculated excited state energies are presented for Cu, Ag and Au coinage metal complexes supported by the dpfam ligand system. The excited state calculations were done using time-dependent density functional theory employing the PBE0[9, 10] functional in combination with the dhf-TZVPP basis set for metal atoms Cu, Ag, Au, including effective core potentials (ECPs) by Stoll and co-workers for the latter two, while the smaller dhf-SVP (def2-SVP) basis set was chosen for all lighter elements.[11-13] All calculations were carried out using the TURBOMOLE program suite.[14-16] A fine grid (gridsize 4 in TURBOMOLE) was used for the numerical evaluation of terns arising from the exchange-correlation functional.[17] Geometries were assumed to be converged with the threshold for the gradient norm reaching 10^{-3} E_H/a_0 and 10^{-6} for the energy change. The optimization was carried out in C_1 symmetry. The ground states were optimized at least to 10^{-8} E_H in the energy (scfconv 8) and 10^{-7} in the root mean square density (denconv 10^{-7}). For excited states the residuals were converged to at least 10^{-4} (rpaconv 4). The RI-*J* approximation was used throughout, employing suitable auxiliary basis sets.[18, 19] Further computational speed-ups were achieved using the senex approximation the evaluation of the exact-exchange terms in excited state calculations using the default parameters and gridsizes.[20, 21] The effect of the coordinating solvent molecules is estimated by removal of the MeCN or THF units. From the calculated absorption spectrum the effects for **5** appear relatively small. For the trinuclear Cu complexes the change in structure upon relaxation appears more pronounced, as **4a** has two equivalent Cu atoms, except for minor structural differences, enabling a slightly different mixing of the (3d-)states. The 5 lowest lying triplet excitations in ground state geometry are given in subsections 4.5 and 4.6. While a complete relaxation of the respective first triplet excited state geometries is beyond the scope of this study, due to the associated high computational demands, the general trend among the systems appear already present in this simple picture. Oscillator strength are given in length gauge.

4.1 Calculated singlet excitation energies of bimetallic complexes 1-3

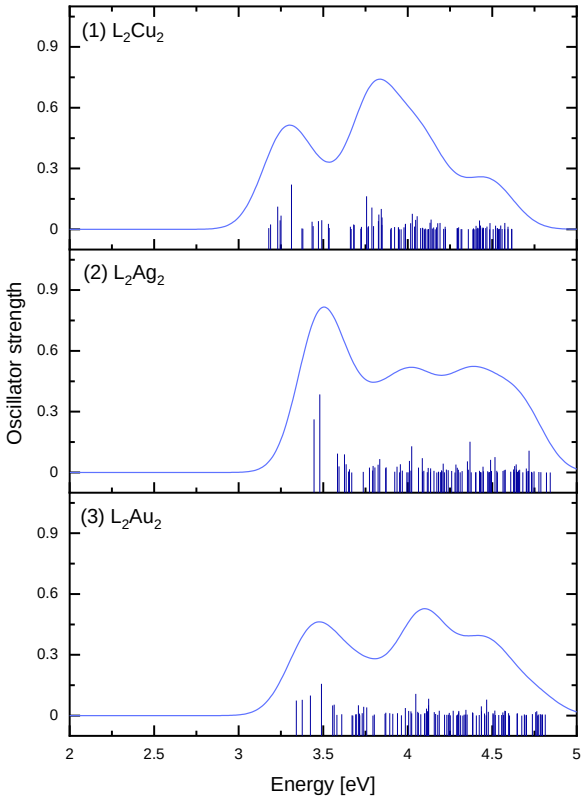

Figure S 4.1-1: Simulated absorptions spectra for complexes 1, 2 and 3 (top to bottom). Stick spectra shown in dark blue were broadened by superimposing Gaussians with a full width at half maximum of 0.3 eV and depicted in blue. Here L refers to the dpfam ligand system. The supporting dpfam ligand is abbreviated as L.

Table S 4.1-1: Lowest 100 roots (singlet excitations) of $dpfam_2Cu_2$ (**1**) as obtained using TDDFT.

Excitation	Energy [eV]	Oscillator strength
1	3.18	5.95×10^{-3}
2	3.19	2.40×10^{-2}
3	3.23	1.11×10^{-1}
4	3.24	4.44×10^{-2}
5	3.25	6.78×10^{-2}
6	3.31	2.21×10^{-1}
7	3.37	4.46×10^{-3}
8	3.38	2.99×10^{-3}
9	3.43	3.72×10^{-2}
10	3.44	1.60×10^{-2}
11	3.47	4.03×10^{-2}
12	3.49	4.51×10^{-2}
13	3.53	2.66×10^{-2}
14	3.54	6.99×10^{-3}
15	3.66	1.29×10^{-2}
16	3.67	1.27×10^{-3}
17	3.68	2.40×10^{-2}
18	3.68	2.13×10^{-2}
19	3.72	3.10×10^{-3}
20	3.73	1.21×10^{-2}
21	3.76	1.63×10^{-1}
22	3.76	9.77×10^{-3}
23	3.77	1.50×10^{-2}
24	3.79	1.08×10^{-1}
25	3.8	1.59×10^{-2}
26	3.83	4.04×10^{-2}
27	3.83	7.30×10^{-2}
28	3.84	1.00×10^{-1}
29	3.85	2.20×10^{-2}
30	3.85	5.82×10^{-2}
31	3.90	1.52×10^{-4}
32	3.90	6.94×10^{-3}
33	3.92	1.08×10^{-2}
34	3.94	9.43×10^{-3}
35	3.95	8.84×10^{-3}
36	3.95	5.29×10^{-5}
37	3.96	3.30×10^{-5}
38	3.98	9.32×10^{-3}
39	3.99	2.49×10^{-2}
40	3.99	2.71×10^{-2}
41	4.02	3.01×10^{-2}
42	4.03	7.62×10^{-2}
43	4.04	1.34×10^{-2}
44	4.05	4.66×10^{-2}
45	4.06	6.42×10^{-2}
46	4.08	6.25×10^{-3}
47	4.09	7.62×10^{-3}
48	4.09	4.49×10^{-3}
49	4.10	2.21×10^{-4}
50	4.10	3.96×10^{-3}
51	4.11	1.52×10^{-4}
52	4.12	1.18×10^{-3}
53	4.13	3.25×10^{-2}
54	4.14	4.78×10^{-2}
55	4.15	3.53×10^{-3}
56	4.15	8.95×10^{-3}
57	4.16	3.76×10^{-5}
58	4.17	9.90×10^{-3}
59	4.18	3.02×10^{-2}
60	4.19	3.13×10^{-2}

61	4.21	2.26×10^{-3}
62	4.22	1.29×10^{-2}
63	4.22	1.35×10^{-3}
64	4.29	5.28×10^{-3}
65	4.29	5.73×10^{-3}
66	4.30	1.03×10^{-3}
67	4.30	9.51×10^{-3}
68	4.32	9.68×10^{-4}
69	4.32	7.99×10^{-4}
70	4.36	9.95×10^{-4}
71	4.39	1.08×10^{-4}
72	4.39	4.13×10^{-3}
73	4.40	9.40×10^{-5}
74	4.40	1.74×10^{-2}
75	4.41	2.25×10^{-3}
76	4.41	7.51×10^{-3}
77	4.42	4.59×10^{-3}
78	4.42	4.37×10^{-2}
79	4.43	1.85×10^{-2}
80	4.44	8.13×10^{-3}
81	4.44	4.12×10^{-4}
82	4.45	7.46×10^{-3}
83	4.46	6.13×10^{-3}
84	4.47	1.34×10^{-2}
85	4.48	2.38×10^{-4}
86	4.49	3.08×10^{-2}
87	4.51	5.99×10^{-4}
88	4.52	1.78×10^{-2}
89	4.53	4.10×10^{-3}
90	4.53	5.69×10^{-3}
91	4.54	4.57×10^{-4}
92	4.54	2.33×10^{-3}
93	4.55	1.84×10^{-2}
94	4.56	1.07×10^{-3}
95	4.57	3.54×10^{-4}
96	4.57	3.12×10^{-2}
97	4.59	9.08×10^{-4}
98	4.59	1.25×10^{-2}
99	4.61	1.87×10^{-3}
100	4.62	5.11×10^{-4}

Table S 4.1-2: Lowest 100 roots (singlet excitations) of $dpfam_2Ag_2$ (**2**) as obtained using TDDFT.

Excitation	Energy [eV]	Oscillator strength
1	3.45	2.62×10^{-1}
2	3.48	3.85×10^{-1}
3	3.59	9.28×10^{-2}
4	3.59	2.99×10^{-2}
5	3.63	8.94×10^{-2}
6	3.64	4.01×10^{-2}
7	3.65	4.62×10^{-3}
8	3.66	1.55×10^{-2}
9	3.67	1.61×10^{-4}
10	3.74	2.97×10^{-3}
11	3.77	2.35×10^{-2}
12	3.79	9.49×10^{-3}
13	3.80	3.23×10^{-2}
14	3.81	2.44×10^{-2}
15	3.82	3.81×10^{-2}
16	3.83	6.57×10^{-2}
17	3.87	2.13×10^{-2}
18	3.87	2.51×10^{-2}
19	3.92	3.76×10^{-3}
20	3.94	2.82×10^{-2}
21	3.95	6.46×10^{-4}
22	3.96	4.03×10^{-2}
23	3.97	9.21×10^{-3}
24	3.99	3.09×10^{-4}
25	4.00	5.65×10^{-4}
26	4.01	5.69×10^{-2}
27	4.02	8.66×10^{-3}
28	4.02	1.29×10^{-1}
29	4.06	2.36×10^{-2}
30	4.09	7.03×10^{-2}
31	4.09	2.51×10^{-3}
32	4.10	8.50×10^{-3}
33	4.12	1.43×10^{-3}
34	4.12	2.22×10^{-2}
35	4.13	1.66×10^{-3}
36	4.14	1.98×10^{-2}
37	4.16	7.88×10^{-3}
38	4.17	1.01×10^{-4}
39	4.18	3.29×10^{-3}
40	4.18	1.52×10^{-3}
41	4.20	1.30×10^{-3}
42	4.20	1.06×10^{-2}
43	4.20	6.23×10^{-3}
44	4.21	4.38×10^{-2}
45	4.22	7.31×10^{-4}
46	4.23	1.44×10^{-2}
47	4.24	1.13×10^{-2}
48	4.26	7.52×10^{-3}
49	4.28	2.27×10^{-4}
50	4.29	3.89×10^{-2}
51	4.29	2.31×10^{-2}
52	4.30	1.34×10^{-2}
53	4.31	4.97×10^{-4}
54	4.32	6.78×10^{-3}
55	4.35	5.47×10^{-2}
56	4.36	1.33×10^{-2}
57	4.37	1.52×10^{-1}
58	4.38	7.38×10^{-4}
59	4.40	1.66×10^{-4}
60	4.40	1.55×10^{-3}

61	4.42	8.37×10^{-3}
62	4.43	1.65×10^{-3}
63	4.43	1.01×10^{-3}
64	4.43	5.01×10^{-4}
65	4.45	2.84×10^{-2}
66	4.45	6.21×10^{-3}
67	4.47	5.55×10^{-3}
68	4.48	9.90×10^{-4}
69	4.48	1.76×10^{-3}
70	4.49	6.22×10^{-2}
71	4.50	7.66×10^{-3}
72	4.52	7.60×10^{-2}
73	4.53	8.38×10^{-3}
74	4.53	2.84×10^{-4}
75	4.56	7.59×10^{-3}
76	4.57	1.11×10^{-2}
77	4.58	1.33×10^{-2}
78	4.61	3.57×10^{-3}
79	4.63	1.48×10^{-2}
80	4.63	1.89×10^{-3}
81	4.63	3.17×10^{-2}
82	4.64	3.99×10^{-2}
83	4.64	1.43×10^{-2}
84	4.65	2.96×10^{-3}
85	4.66	9.99×10^{-3}
86	4.66	1.69×10^{-4}
87	4.66	1.37×10^{-2}
88	4.68	6.07×10^{-4}
89	4.70	1.95×10^{-2}
90	4.70	1.32×10^{-3}
91	4.71	7.54×10^{-3}
92	4.72	7.26×10^{-3}
93	4.72	1.07×10^{-1}
94	4.73	3.20×10^{-3}
95	4.74	2.25×10^{-4}
96	4.75	5.19×10^{-3}
97	4.78	2.05×10^{-3}
98	4.79	1.72×10^{-3}
99	4.82	2.14×10^{-4}
100	4.84	5.13×10^{-5}

Table S 4.1-3: Lowest 100 roots (singlet excitations) of $dpfam_2Au_2$ (**3**) as obtained using TDDFT.

Excitation	Energy [eV]	Oscillator strength
1	3.34	7.45×10^{-2}
2	3.38	7.77×10^{-2}
3	3.42	9.92×10^{-2}
4	3.49	1.57×10^{-1}
5	3.56	4.98×10^{-2}
6	3.56	5.42×10^{-2}
7	3.58	3.54×10^{-3}
8	3.61	6.76×10^{-3}
9	3.67	1.50×10^{-3}
10	3.68	2.02×10^{-4}
11	3.69	5.89×10^{-3}
12	3.70	6.57×10^{-3}
13	3.71	5.12×10^{-2}
14	3.71	9.63×10^{-3}
15	3.72	1.22×10^{-3}
16	3.73	1.20×10^{-2}
17	3.74	4.37×10^{-2}
18	3.76	4.02×10^{-2}
19	3.79	6.49×10^{-5}
20	3.80	5.40×10^{-3}
21	3.87	8.61×10^{-3}
22	3.87	1.41×10^{-2}
23	3.89	1.22×10^{-2}
24	3.91	9.17×10^{-3}
25	3.94	1.17×10^{-2}
26	3.96	1.08×10^{-3}
27	3.99	3.71×10^{-2}
28	4.01	2.34×10^{-2}
29	4.02	2.06×10^{-2}
30	4.02	1.11×10^{-2}
31	4.05	1.07×10^{-1}
32	4.06	1.85×10^{-2}
33	4.06	1.23×10^{-2}
34	4.08	6.35×10^{-3}
35	4.10	8.80×10^{-3}
36	4.10	1.28×10^{-2}
37	4.11	3.43×10^{-2}
38	4.12	2.15×10^{-2}
39	4.12	5.09×10^{-2}
40	4.12	8.29×10^{-2}
41	4.16	1.72×10^{-2}
42	4.16	7.96×10^{-3}
43	4.18	3.41×10^{-3}
44	4.19	2.41×10^{-2}
45	4.22	4.23×10^{-3}
46	4.23	3.40×10^{-3}
47	4.24	4.56×10^{-3}
48	4.25	1.34×10^{-2}
49	4.25	1.47×10^{-3}
50	4.27	2.41×10^{-2}
51	4.29	1.25×10^{-3}
52	4.30	4.96×10^{-3}
53	4.30	1.53×10^{-2}
54	4.30	2.34×10^{-2}
55	4.31	1.75×10^{-3}
56	4.33	3.94×10^{-5}
57	4.33	4.68×10^{-3}
58	4.34	5.02×10^{-3}
59	4.34	2.84×10^{-2}
60	4.35	5.27×10^{-3}

61	4.38	1.53×10^{-2}
62	4.39	1.27×10^{-2}
63	4.41	3.36×10^{-4}
64	4.42	2.68×10^{-3}
65	4.44	4.56×10^{-2}
66	4.44	2.17×10^{-2}
67	4.45	1.05×10^{-2}
68	4.46	1.37×10^{-3}
69	4.47	7.90×10^{-2}
70	4.48	1.85×10^{-2}
71	4.50	1.21×10^{-2}
72	4.51	6.74×10^{-3}
73	4.52	2.50×10^{-2}
74	4.52	3.17×10^{-3}
75	4.54	3.21×10^{-3}
76	4.56	2.94×10^{-3}
77	4.56	1.57×10^{-2}
78	4.57	3.23×10^{-3}
79	4.57	2.42×10^{-2}
80	4.58	2.26×10^{-2}
81	4.60	1.20×10^{-2}
82	4.60	7.43×10^{-4}
83	4.65	9.64×10^{-3}
84	4.65	1.10×10^{-2}
85	4.67	2.45×10^{-4}
86	4.69	6.22×10^{-3}
87	4.69	1.70×10^{-3}
88	4.70	3.36×10^{-3}
89	4.70	1.21×10^{-3}
90	4.74	7.38×10^{-3}
91	4.76	1.70×10^{-2}
92	4.76	2.20×10^{-2}
93	4.77	7.70×10^{-4}
94	4.77	4.93×10^{-3}
95	4.78	7.59×10^{-3}
96	4.79	3.81×10^{-3}
97	4.80	6.06×10^{-3}
98	4.80	4.15×10^{-3}
99	4.80	1.23×10^{-3}
100	4.81	4.84×10−3

4.2 Calculated singlet excitation energies of trimetallic complexes 4, 4a and 5

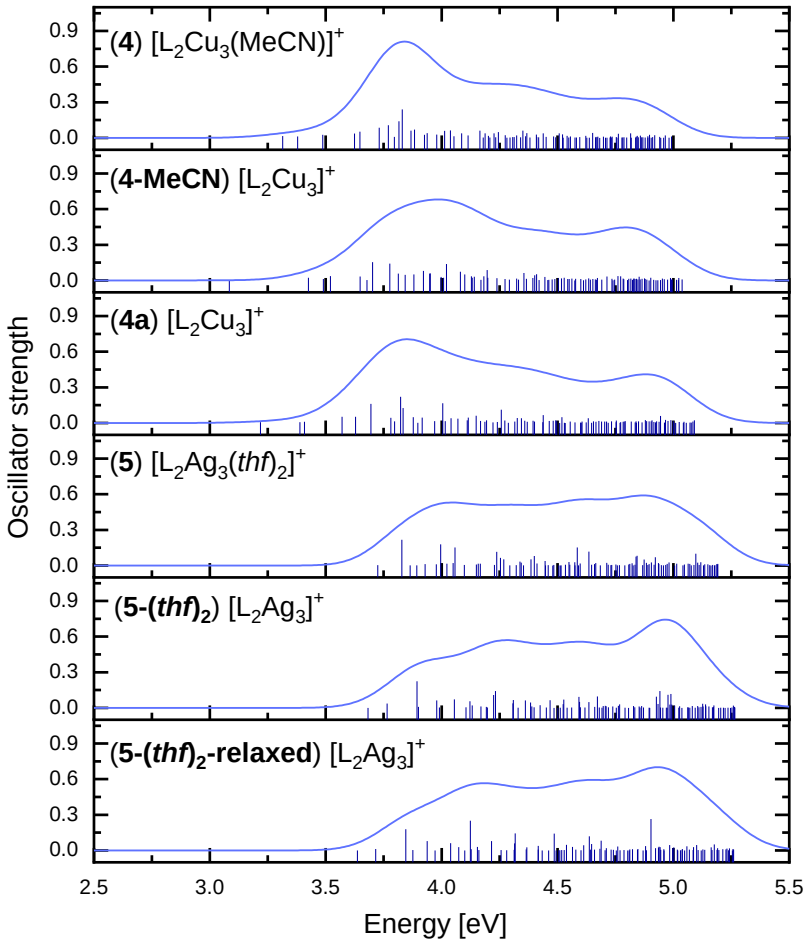

Figure S 4.2-1: Simulated absorptions spectra for complexes **4**, **4a** and **5**, as well as derivatives without the coordinating solvent atoms in relaxed and unrelaxed geometries. Note that (**4a**) already corresponds to the relaxed geometry of (**4**), where the MeCN equivalent is removed. Stick spectra shown in dark blue were broadened by superimposing Gaussians with a full width at half maximum of 0.3 eV and depicted in blue. Here L refers to the dpfam ligand system. The supporting dpfam ligand is abbreviated as L.

Table S 4.2-1: Lowest 100 roots (singlet excitations) of $[dpfam_2Cu_3(MeCN)]^+$ (**4**) as obtained using TDDFT.

Excitation	Energy [eV]	Oscillator strength
1	3.31	1.60×10^{-2}
2	3.38	1.16×10^{-2}
3	3.49	2.66×10^{-2}
4	3.62	3.60×10^{-2}
5	3.65	5.18×10^{-2}
6	3.73	8.56×10^{-2}
7	3.77	1.07×10^{-1}
8	3.80	8.58×10^{-3}
9	3.82	1.40×10^{-1}
10	3.83	2.40×10^{-1}
11	3.87	6.06×10^{-2}
12	3.88	6.95×10^{-2}
13	3.93	2.62×10^{-2}
14	3.94	3.96×10^{-2}
15	3.98	2.86×10^{-2}
16	4.01	5.97×10^{-2}
17	4.04	6.24×10^{-2}
18	4.05	1.37×10^{-2}
19	4.09	3.81×10^{-2}
20	4.11	2.03×10^{-2}
21	4.17	6.04×10^{-2}
22	4.18	2.67×10^{-3}
23	4.19	3.85×10^{-2}
24	4.20	1.79×10^{-2}
25	4.21	3.51×10^{-3}
26	4.23	3.78×10^{-2}
27	4.23	5.25×10^{-3}
28	4.24	4.95×10^{-2}
29	4.27	2.25×10^{-2}
30	4.28	1.40×10^{-3}
31	4.30	2.92×10^{-3}
32	4.31	6.97×10^{-3}
33	4.31	7.13×10^{-3}
34	4.32	2.14×10^{-2}
35	4.34	4.49×10^{-3}
36	4.35	6.06×10^{-2}
37	4.36	1.37×10^{-2}
38	4.37	3.95×10^{-2}
39	4.38	2.99×10^{-3}
40	4.41	2.76×10^{-2}
41	4.41	7.53×10^{-3}
42	4.42	5.60×10^{-3}
43	4.44	3.89×10^{-2}
44	4.45	9.41×10^{-3}
45	4.48	1.28×10^{-2}
46	4.49	5.51×10^{-3}
47	4.51	3.78×10^{-2}
48	4.52	2.92×10^{-2}
49	4.52	1.80×10^{-3}
50	4.54	1.75×10^{-2}
51	4.55	3.66×10^{-3}
52	4.56	1.18×10^{-2}
53	4.58	2.79×10^{-3}
54	4.58	3.25×10^{-3}
55	4.60	7.34×10^{-3}
56	4.62	1.81×10^{-2}
57	4.63	1.35×10^{-3}
58	4.64	2.43×10^{-3}
59	4.65	4.21×10^{-2}
60	4.66	3.61×10^{-3}

61	4.67	8.62×10^{-3}
62	4.67	4.80×10^{-3}
63	4.67	9.92×10^{-3}
64	4.68	6.11×10^{-4}
65	4.70	1.06×10^{-2}
66	4.71	1.25×10^{-3}
67	4.71	2.20×10^{-3}
68	4.73	3.25×10^{-3}
69	4.73	1.17×10^{-2}
70	4.73	4.07×10^{-3}
71	4.74	1.08×10^{-2}
72	4.75	6.40×10^{-3}
73	4.76	2.18×10^{-3}
74	4.76	3.48×10^{-2}
75	4.78	2.52×10^{-3}
76	4.78	4.23×10^{-3}
77	4.79	4.94×10^{-3}
78	4.80	3.93×10^{-3}
79	4.82	3.88×10^{-2}
80	4.82	8.26×10^{-4}
81	4.84	3.14×10^{-3}
82	4.84	1.08×10^{-2}
83	4.84	1.69×10^{-2}
84	4.85	4.82×10^{-3}
85	4.86	1.97×10^{-2}
86	4.86	5.88×10^{-3}
87	4.87	5.28×10^{-3}
88	4.88	3.91×10^{-3}
89	4.89	1.14×10^{-3}
90	4.89	1.46×10^{-2}
91	4.90	2.62×10^{-2}
92	4.90	1.06×10^{-3}
93	4.91	7.35×10^{-3}
94	4.92	2.25×10^{-2}
95	4.94	8.12×10^{-3}
96	4.95	5.85×10^{-4}
97	4.96	2.20×10^{-3}
98	4.97	2.14×10^{-2}
99	4.98	2.06×10^{-3}
100	4.99	1.20×10^{-2}

Table S 4.2-2: Lowest 100 roots (singlet excitations) of $[dpfam_2Cu_3]^+$ (**4-MeCN**) as obtained using TDDFT. The MeCN molecule was removed, while the geometry of **4** was kept frozen

Excitation	Energy [eV]	Oscillator strength
1	3.31	1.60×10^{-2}
2	3.38	1.16×10^{-2}
3	3.49	2.66×10^{-2}
4	3.62	3.60×10^{-2}
5	3.65	5.18×10^{-2}
6	3.73	8.56×10^{-2}
7	3.77	1.07×10^{-1}
8	3.80	8.58×10^{-3}
9	3.82	1.40×10^{-1}
10	3.83	2.40×10^{-1}
11	3.87	6.06×10^{-2}
12	3.88	6.95×10^{-2}
13	3.93	2.62×10^{-2}
14	3.94	3.96×10^{-2}
15	3.98	2.86×10^{-2}
16	4.01	5.97×10^{-2}
17	4.04	6.24×10^{-2}
18	4.05	1.37×10^{-2}
19	4.09	3.81×10^{-2}
20	4.11	2.03×10^{-2}
21	4.17	6.04×10^{-2}
22	4.18	2.67×10^{-3}
23	4.19	3.85×10^{-2}
24	4.20	1.79×10^{-2}
25	4.21	3.51×10^{-3}
26	4.23	3.78×10^{-2}
27	4.23	5.25×10^{-3}
28	4.24	4.95×10^{-2}
29	4.27	2.25×10^{-2}
30	4.28	1.40×10^{-3}
31	4.30	2.92×10^{-3}
32	4.31	6.97×10^{-3}
33	4.31	7.13×10^{-3}
34	4.32	2.14×10^{-2}
35	4.34	4.49×10^{-3}
36	4.35	6.06×10^{-2}
37	4.36	1.37×10^{-2}
38	4.37	3.95×10^{-2}
39	4.38	2.99×10^{-3}
40	4.41	2.76×10^{-2}
41	4.41	7.53×10^{-3}
42	4.42	5.60×10^{-3}
43	4.44	3.89×10^{-2}
44	4.45	9.41×10^{-3}
45	4.48	1.28×10^{-2}
46	4.49	5.51×10^{-3}
47	4.51	3.78×10^{-2}
48	4.52	2.92×10^{-2}
49	4.52	1.80×10^{-3}
50	4.54	1.75×10^{-2}
51	4.55	3.66×10^{-3}
52	4.56	1.18×10^{-2}
53	4.58	2.79×10^{-3}
54	4.58	3.25×10^{-3}
55	4.60	7.34×10^{-3}
56	4.62	1.81×10^{-2}
57	4.63	1.35×10^{-3}
58	4.64	2.43×10^{-3}
59	4.65	4.21×10^{-2}

60	4.66	3.61×10^{-3}
61	4.67	8.62×10^{-3}
62	4.67	4.80×10^{-3}
63	4.67	9.92×10^{-3}
64	4.68	6.11×10^{-4}
65	4.70	1.06×10^{-2}
66	4.71	1.25×10^{-3}
67	4.71	2.20×10^{-3}
68	4.73	3.25×10^{-3}
69	4.73	1.17×10^{-2}
70	4.73	4.07×10^{-3}
71	4.74	1.08×10^{-2}
72	4.75	6.40×10^{-3}
73	4.76	2.18×10^{-3}
74	4.76	3.48×10^{-2}
75	4.78	2.52×10^{-3}
76	4.78	4.23×10^{-3}
77	4.79	4.94×10^{-3}
78	4.80	3.93×10^{-3}
79	4.82	3.88×10^{-2}
80	4.82	8.26×10^{-4}
81	4.84	3.14×10^{-3}
82	4.84	1.08×10^{-2}
83	4.84	1.69×10^{-2}
84	4.85	4.82×10^{-3}
85	4.86	1.97×10^{-2}
86	4.86	5.88×10^{-3}
87	4.87	5.28×10^{-3}
88	4.88	3.91×10^{-3}
89	4.89	1.14×10^{-3}
90	4.89	1.46×10^{-2}
91	4.90	2.62×10^{-2}
92	4.90	1.06×10^{-3}
93	4.91	7.35×10^{-3}
94	4.92	2.25×10^{-2}
95	4.94	8.12×10^{-3}
96	4.95	5.85×10^{-4}
97	4.96	2.20×10^{-3}
98	4.97	2.14×10^{-2}
99	4.98	2.06×10^{-3}
100	4.99	1.20×10^{-2}

Table S 4.2-3: Lowest 100 roots (singlet excitations) of $[dpfam_2Cu_3]^+$ (**4a**) as obtained using TDDFT. Note that the crystal structure of **4a** used as a starting point does not include the MeCN molecule, as it was obtained from the solution of DCM. This results in a more symmetric structural motif when compared to **4**.

Excitation	Energy [eV]	Oscillator strength
1	3.22	5.73×10^{-4}
2	3.39	2.05×10^{-2}
3	3.51	3.50×10^{-3}
4	3.58	1.93×10^{-2}
5	3.62	1.56×10^{-1}
6	3.71	3.63×10^{-1}
7	3.73	7.77×10^{-2}
8	3.82	2.24×10^{-3}
9	3.85	2.07×10^{-2}
10	3.85	1.49×10^{-2}
11	3.90	9.71×10^{-2}
12	3.94	1.71×10^{-1}
13	3.95	6.93×10^{-3}
14	3.99	1.03×10^{-4}
15	4.00	2.70×10^{-2}
16	4.01	3.73×10^{-2}
17	4.02	1.05×10^{-2}
18	4.04	6.90×10^{-3}
19	4.11	7.58×10^{-6}
20	4.15	1.32×10^{-2}
21	4.16	6.65×10^{-2}
22	4.17	1.65×10^{-2}
23	4.17	1.03×10^{-1}
24	4.21	1.46×10^{-2}
25	4.24	1.63×10^{-2}
26	4.25	2.34×10^{-2}
27	4.26	3.48×10^{-2}
28	4.29	9.55×10^{-3}
29	4.29	4.50×10^{-4}
30	4.33	1.58×10^{-3}
31	4.33	9.61×10^{-4}
32	4.36	1.11×10^{-2}
33	4.36	3.67×10^{-2}
34	4.39	1.64×10^{-2}
35	4.40	1.23×10^{-2}
36	4.40	7.33×10^{-2}
37	4.41	1.19×10^{-3}
38	4.47	7.94×10^{-2}
39	4.47	1.14×10^{-1}
40	4.49	4.06×10^{-3}
41	4.50	3.62×10^{-2}
42	4.50	1.47×10^{-2}
43	4.51	3.05×10^{-3}
44	4.52	1.03×10^{-2}
45	4.53	1.47×10^{-5}
46	4.56	3.23×10^{-2}
47	4.56	4.26×10^{-2}
48	4.60	4.89×10^{-3}
49	4.60	2.75×10^{-3}
50	4.61	7.44×10^{-4}
51	4.62	2.34×10^{-3}
52	4.62	2.52×10^{-4}
53	4.65	2.10×10^{-4}
54	4.65	2.42×10^{-2}
55	4.67	2.92×10^{-4}
56	4.68	8.88×10^{-3}
57	4.69	3.80×10^{-5}
58	4.70	4.18×10^{-2}

59	4.70	6.60×10^{-2}
60	4.71	2.08×10^{-3}
61	4.71	8.98×10^{-5}
62	4.71	6.43×10^{-3}
63	4.72	4.85×10^{-3}
64	4.72	7.09×10^{-4}
65	4.73	4.48×10^{-2}
66	4.77	7.27×10^{-3}
67	4.78	4.92×10^{-3}
68	4.79	2.58×10^{-3}
69	4.81	1.15×10^{-4}
70	4.81	6.03×10^{-5}
71	4.82	1.07×10^{-2}
72	4.83	3.75×10^{-3}
73	4.84	8.70×10^{-3}
74	4.86	4.42×10^{-3}
75	4.86	5.82×10^{-3}
76	4.87	1.87×10^{-2}
77	4.87	1.64×10^{-3}
78	4.88	4.30×10^{-3}
79	4.90	2.87×10^{-2}
80	4.91	6.80×10^{-4}
81	4.92	3.37×10^{-2}
82	4.94	2.37×10^{-4}
83	4.94	2.36×10^{-2}
84	4.94	2.73×10^{-2}
85	4.95	2.68×10^{-5}
86	4.96	1.12×10^{-3}
87	4.97	5.08×10^{-3}
88	4.98	4.34×10^{-3}
89	4.98	4.73×10^{-3}
90	5.01	2.56×10^{-3}
91	5.01	8.81×10^{-3}
92	5.01	5.18×10^{-3}
93	5.02	2.09×10^{-3}
94	5.03	5.11×10^{-3}
95	5.03	1.98×10^{-2}
96	5.04	3.18×10^{-3}
97	5.04	2.19×10^{-2}
98	5.05	6.24×10^{-3}
99	5.05	5.58×10^{-3}
100	5.07	8.74×10^{-4}

Table S 4.2-4: Lowest 100 roots (singlet excitations) of $[dpfam_2Ag_3(thf)_2]^+$ (**5**) as obtained using TDDFT.

Excitation	Energy [eV]	Oscillator strength
1	3.72	2.77×10^{-3}
2	3.83	2.17×10^{-1}
3	3.86	2.27×10^{-3}
4	3.89	2.29×10^{-3}
5	3.93	1.15×10^{-2}
6	3.98	1.11×10^{-2}
7	4.00	1.79×10^{-1}
8	4.02	1.51×10^{-2}
9	4.05	2.08×10^{-2}
10	4.06	1.52×10^{-1}
11	4.10	5.54×10^{-3}
12	4.15	8.90×10^{-3}
13	4.16	1.58×10^{-2}
14	4.17	1.55×10^{-2}
15	4.23	4.97×10^{-3}
16	4.24	1.15×10^{-1}
17	4.25	6.55×10^{-2}
18	4.27	5.33×10^{-2}
19	4.29	2.36×10^{-3}
20	4.32	3.68×10^{-3}
21	4.34	3.33×10^{-2}
22	4.34	2.47×10^{-2}
23	4.35	1.64×10^{-3}
24	4.39	5.29×10^{-2}
25	4.40	7.99×10^{-2}
26	4.41	1.78×10^{-2}
27	4.45	3.86×10^{-2}
28	4.45	1.58×10^{-3}
29	4.46	4.21×10^{-3}
30	4.48	7.62×10^{-5}
31	4.48	4.93×10^{-3}
32	4.51	2.26×10^{-3}
33	4.51	1.45×10^{-4}
34	4.52	2.35×10^{-3}
35	4.53	7.17×10^{-3}
36	4.55	2.88×10^{-2}
37	4.55	6.98×10^{-3}
38	4.57	2.87×10^{-2}
39	4.58	1.72×10^{-3}
40	4.59	1.53×10^{-1}
41	4.59	1.10×10^{-3}
42	4.60	1.72×10^{-2}
43	4.64	1.18×10^{-1}
44	4.65	6.86×10^{-3}
45	4.66	1.19×10^{-2}
46	4.67	2.02×10^{-2}
47	4.68	7.62×10^{-4}
48	4.71	2.28×10^{-2}
49	4.72	7.30×10^{-3}
50	4.73	3.31×10^{-3}
51	4.73	5.40×10^{-3}
52	4.75	7.97×10^{-3}
53	4.76	8.51×10^{-4}
54	4.77	3.72×10^{-3}
55	4.79	8.61×10^{-4}
56	4.81	8.20×10^{-3}
57	4.81	1.34×10^{-2}
58	4.82	1.89×10^{-2}
59	4.83	1.62×10^{-3}
60	4.83	6.53×10^{-3}

61	4.84	7.60×10^{-2}
62	4.84	8.19×10^{-2}
63	4.87	3.07×10^{-3}
64	4.87	5.11×10^{-2}
65	4.88	2.24×10^{-2}
66	4.89	4.67×10^{-3}
67	4.90	1.25×10^{-2}
68	4.90	2.64×10^{-2}
69	4.92	7.73×10^{-3}
70	4.92	6.91×10^{-2}
71	4.94	2.09×10^{-2}
72	4.94	1.32×10^{-2}
73	4.95	4.20×10^{-3}
74	4.96	1.19×10^{-3}
75	4.97	5.62×10^{-3}
76	4.97	1.44×10^{-2}
77	4.98	2.59×10^{-2}
78	5.01	6.50×10^{-4}
79	5.01	1.63×10^{-2}
80	5.04	9.73×10^{-4}
81	5.05	7.94×10^{-3}
82	5.06	1.49×10^{-2}
83	5.07	1.39×10^{-2}
84	5.08	2.13×10^{-3}
85	5.09	4.93×10^{-3}
86	5.10	9.94×10^{-2}
87	5.10	2.40×10^{-2}
88	5.11	4.69×10^{-3}
89	5.12	2.71×10^{-2}
90	5.13	8.85×10^{-4}
91	5.14	1.06×10^{-2}
92	5.15	1.10×10^{-2}
93	5.16	3.78×10^{-3}
94	5.16	6.45×10^{-4}
95	5.17	5.45×10^{-3}
96	5.18	4.21×10^{-4}
97	5.18	4.09×10^{-3}
98	5.19	1.13×10^{-2}
99	5.19	9.26×10^{-3}
100	5.19	1.37×10^{-2}

Table S 4.2-5: Lowest 100 roots (singlet excitations) of $[dpfam_2Ag_3]^+$ (**5-(*thf*)$_2$**) as obtained using TDDFT. The 2 THF molecules were removed, while the geometry was kept frozen.

Excitation	Energy [eV]	Oscillator strength
1	3.68	4.10×10^{-4}
2	3.76	3.75×10^{-2}
3	3.89	2.25×10^{-1}
4	3.90	8.75×10^{-3}
5	3.98	6.29×10^{-2}
6	3.99	3.70×10^{-3}
7	4.05	7.11×10^{-2}
8	4.11	5.70×10^{-3}
9	4.12	5.66×10^{-2}
10	4.13	2.10×10^{-2}
11	4.17	1.26×10^{-2}
12	4.19	8.24×10^{-3}
13	4.20	2.51×10^{-3}
14	4.22	1.09×10^{-1}
15	4.23	1.41×10^{-1}
16	4.31	3.91×10^{-2}
17	4.31	6.59×10^{-2}
18	4.33	1.76×10^{-3}
19	4.36	6.38×10^{-2}
20	4.38	4.62×10^{-2}
21	4.39	1.20×10^{-2}
22	4.40	5.15×10^{-3}
23	4.43	2.25×10^{-2}
24	4.45	2.81×10^{-3}
25	4.47	6.52×10^{-2}
26	4.49	5.68×10^{-4}
27	4.50	3.40×10^{-4}
28	4.51	2.12×10^{-3}
29	4.52	3.07×10^{-2}
30	4.53	6.94×10^{-2}
31	4.54	1.82×10^{-3}
32	4.56	2.70×10^{-3}
33	4.59	9.33×10^{-2}
34	4.60	5.14×10^{-2}
35	4.60	4.65×10^{-3}
36	4.62	2.63×10^{-3}
37	4.64	4.86×10^{-2}
38	4.66	8.75×10^{-3}
39	4.67	9.63×10^{-2}
40	4.68	3.95×10^{-3}
41	4.69	1.36×10^{-3}
42	4.70	1.63×10^{-2}
43	4.71	1.81×10^{-2}
44	4.71	1.45×10^{-2}
45	4.72	4.73×10^{-3}
46	4.74	1.21×10^{-2}
47	4.75	1.73×10^{-3}
48	4.76	1.76×10^{-2}
49	4.77	2.90×10^{-2}
50	4.79	1.50×10^{-3}
51	4.81	3.32×10^{-4}
52	4.83	1.54×10^{-2}
53	4.83	5.55×10^{-3}
54	4.85	1.14×10^{-2}
55	4.86	3.99×10^{-3}
56	4.86	1.64×10^{-2}
57	4.87	2.83×10^{-3}
58	4.90	1.39×10^{-3}
59	4.90	5.20×10^{-4}

60	4.93	9.37×10^{-2}
61	4.93	3.24×10^{-2}
62	4.94	1.41×10^{-1}
63	4.94	3.83×10^{-3}
64	4.95	1.56×10^{-3}
65	4.97	8.42×10^{-4}
66	4.97	2.47×10^{-3}
67	4.98	1.10×10^{-1}
68	4.99	2.76×10^{-2}
69	4.99	1.18×10^{-1}
70	4.99	2.84×10^{-2}
71	5.01	1.91×10^{-2}
72	5.02	2.26×10^{-3}
73	5.03	1.42×10^{-2}
74	5.04	3.09×10^{-4}
75	5.06	4.69×10^{-3}
76	5.06	3.58×10^{-3}
77	5.07	2.18×10^{-3}
78	5.08	1.53×10^{-2}
79	5.09	8.92×10^{-4}
80	5.10	1.62×10^{-2}
81	5.11	4.54×10^{-3}
82	5.12	8.60×10^{-3}
83	5.13	3.57×10^{-2}
84	5.13	1.16×10^{-2}
85	5.14	2.92×10^{-2}
86	5.14	1.32×10^{-2}
87	5.15	1.24×10^{-2}
88	5.17	4.64×10^{-3}
89	5.17	7.73×10^{-3}
90	5.17	2.07×10^{-2}
91	5.20	2.86×10^{-4}
92	5.20	1.46×10^{-3}
93	5.22	2.18×10^{-3}
94	5.22	3.67×10^{-4}
95	5.24	1.68×10^{-3}
96	5.25	6.03×10^{-4}
97	5.25	2.66×10^{-3}
98	5.26	1.96×10^{-2}
99	5.26	7.89×10^{-3}
100	5.27	2.50×10^{-3}

Table S 4.2-6: Lowest 100 roots (singlet excitations) of $[dpfam_2Ag_3]^+$ (**5-(*thf*)$_2$-relaxed**) as obtained using TDDFT. The 2 THF molecules were removed and the geometry relaxed.

Excitation	Energy [eV]	Oscillator strength
1	3.64	2.14×10^{-4}
2	3.72	1.21×10^{-2}
3	3.85	1.78×10^{-1}
4	3.88	3.71×10^{-3}
5	3.94	7.93×10^{-2}
6	3.97	5.36×10^{-4}
7	4.04	6.18×10^{-2}
8	4.07	2.74×10^{-2}
9	4.10	7.80×10^{-6}
10	4.12	2.51×10^{-1}
11	4.13	1.00×10^{-2}
12	4.15	2.90×10^{-2}
13	4.16	2.64×10^{-3}
14	4.22	7.79×10^{-2}
15	4.26	3.13×10^{-3}
16	4.28	2.41×10^{-3}
17	4.31	4.70×10^{-3}
18	4.31	6.02×10^{-2}
19	4.32	1.43×10^{-1}
20	4.36	9.46×10^{-3}
21	4.37	2.66×10^{-2}
22	4.42	6.33×10^{-3}
23	4.42	3.86×10^{-2}
24	4.43	6.68×10^{-4}
25	4.46	4.48×10^{-4}
26	4.49	1.42×10^{-1}
27	4.49	5.37×10^{-6}
28	4.51	2.11×10^{-3}
29	4.51	1.42×10^{-3}
30	4.52	4.16×10^{-3}
31	4.53	4.12×10^{-3}
32	4.54	4.68×10^{-2}
33	4.57	2.96×10^{-2}
34	4.58	6.22×10^{-3}
35	4.60	8.47×10^{-4}
36	4.61	4.38×10^{-2}
37	4.64	1.19×10^{-1}
38	4.64	7.31×10^{-3}
39	4.65	5.34×10^{-2}
40	4.66	7.59×10^{-3}
41	4.68	1.31×10^{-2}
42	4.69	8.25×10^{-2}
43	4.71	8.66×10^{-4}
44	4.71	1.91×10^{-2}
45	4.73	6.68×10^{-3}
46	4.74	4.72×10^{-3}
47	4.75	2.33×10^{-4}
48	4.76	3.28×10^{-2}
49	4.77	2.42×10^{-3}
50	4.79	3.68×10^{-3}
51	4.80	5.37×10^{-4}
52	4.81	1.66×10^{-4}
53	4.81	7.89×10^{-3}
54	4.82	1.11×10^{-2}
55	4.85	5.87×10^{-3}
56	4.85	1.18×10^{-2}
57	4.87	3.19×10^{-4}
58	4.88	3.73×10^{-2}
59	4.88	1.96×10^{-3}

60	4.90	2.64×10^{-1}
61	4.92	1.84×10^{-2}
62	4.94	2.37×10^{-2}
63	4.94	3.22×10^{-2}
64	4.94	2.77×10^{-2}
65	4.95	5.71×10^{-3}
66	4.96	9.51×10^{-3}
67	4.96	4.62×10^{-4}
68	4.98	4.60×10^{-2}
69	5.00	1.71×10^{-2}
70	5.00	2.60×10^{-2}
71	5.02	6.20×10^{-3}
72	5.02	4.84×10^{-4}
73	5.03	1.38×10^{-3}
74	5.04	3.64×10^{-3}
75	5.04	1.22×10^{-2}
76	5.05	1.19×10^{-4}
77	5.06	3.44×10^{-2}
78	5.06	3.56×10^{-2}
79	5.07	7.50×10^{-3}
80	5.09	3.98×10^{-3}
81	5.09	2.86×10^{-2}
82	5.10	4.56×10^{-2}
83	5.11	3.75×10^{-3}
84	5.12	4.78×10^{-4}
85	5.13	7.86×10^{-3}
86	5.14	5.26×10^{-3}
87	5.16	2.60×10^{-2}
88	5.17	2.49×10^{-3}
89	5.18	5.13×10^{-2}
90	5.19	4.78×10^{-3}
91	5.19	1.90×10^{-2}
92	5.20	3.13×10^{-3}
93	5.21	1.06×10^{-2}
94	5.23	8.47×10^{-3}
95	5.23	1.48×10^{-2}
96	5.24	1.21×10^{-3}
97	5.24	1.69×10^{-2}
98	5.25	1.28×10^{-4}
99	5.26	1.21×10^{-2}
100	5.26	7.42×10^{-3}

4.3 Non-relaxed difference densities for 1-3

Table S 4.3-1: Contour plots of non-relaxed difference densities for **1-3**. A density loss is depicted in red, while a density gain is shown in blue. The isovalue was set to 0.002 a_0^{-3}.

System	Energy interval in eV	Non-relaxed difference density	Energy interval in eV	Non-relaxed difference density
(**1**)	2.80-3.54	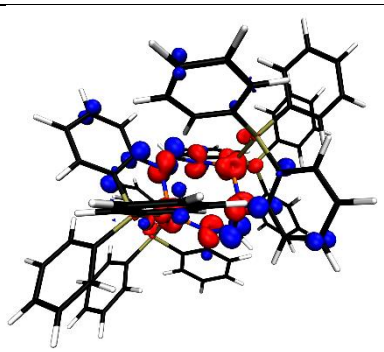	3.54-4.62	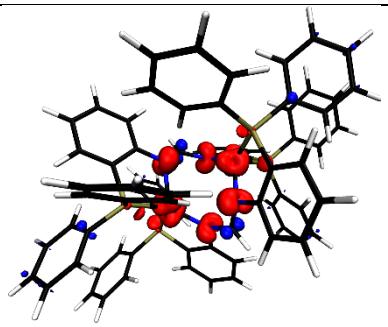
(**2**)	3.00-3.80	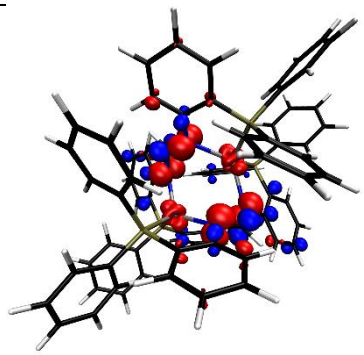	3.80-5.00	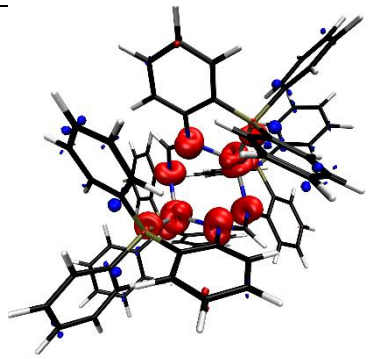
(**3**)	2.80-3.79	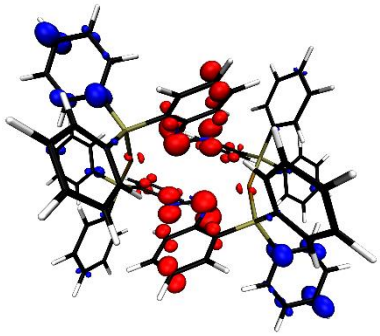	3.79-5.00	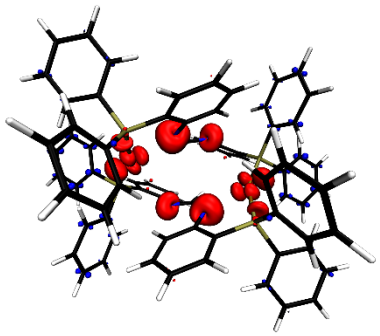

4.4 Non-relaxed difference densities for 4, 4a and 5

Table S 4.4-1: Contour plots of non-relaxed difference densities for **4**, **4a** and **5**. A density loss is depicted in red, while a density gain is shown in blue. The isovalue was set to 0.002 a_0^{-3}.

System	Energy interval in eV	Non-relaxed difference density	Energy interval in eV	Non-relaxed difference density
(**4**)	3.00-4.10	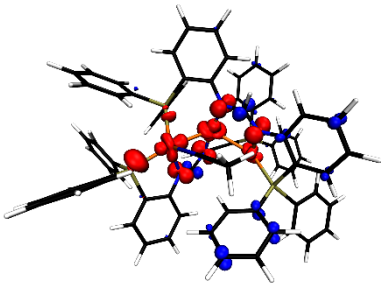	4.10-5.30	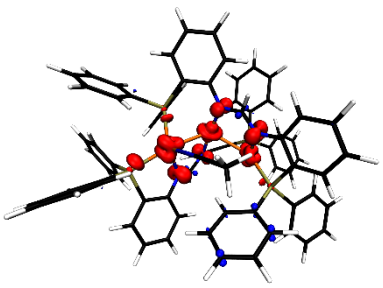
(**4a**)	3.00-4.15	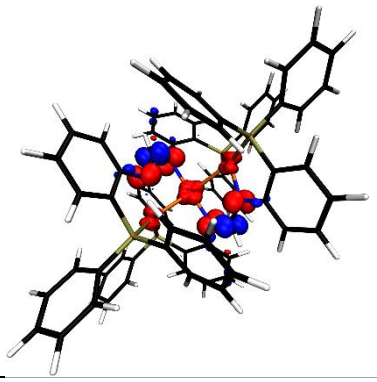	4.15-5.30	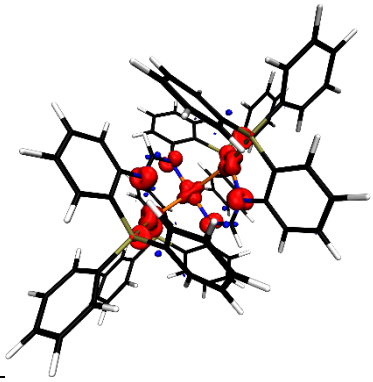
(**5**)	3.50-4.20	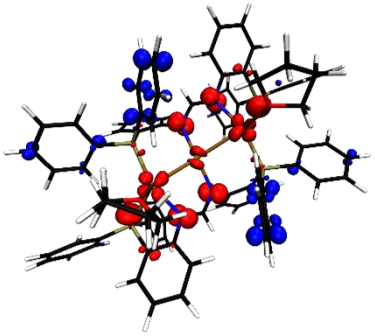	4.20-5.50	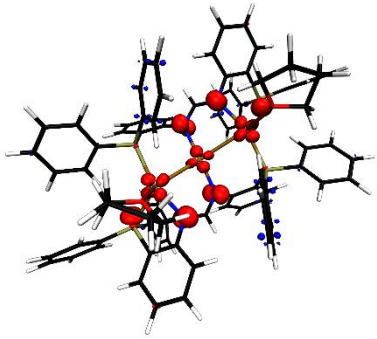

4.5 Calculated triplet excitation energies of bimetallic complexes 1-3

Table S 4.5-1: Lowest 5 roots (triplet excitations) of $dpfam_2Cu_2$ (**1**) as obtained using TDDFT. Listed oscillator strengths only include the spatial contributions, as oscillator strength including the spin contributions is zero for non-relativistic one-component calculations.

Excitation	Energy [eV]	Oscillator strength
1	2.53	$1.01x10^{0}$
2	2.54	$7.76x10^{-1}$
3	3.05	$1.42x10^{-3}$
4	3.06	$3.88x10^{-2}$
5	3.12	$8.83x10^{-2}$

Table S 4.5-2: Lowest 5 roots (triplet excitations) of $dpfam_2Ag_2$ (**2**) as obtained using TDDFT. See Table S 4-5-1 for further information.

Excitation	Energy [eV]	Oscillator strength
1	2.60	$1.27x10^{0}$
2	2.60	$7.10x10^{-1}$
3	3.18	$1.95x10^{-1}$
4	3.19	$3.05x10^{-2}$
5	3.25	$3.83x10^{-1}$

Table S 4.5-3: Lowest 5 roots (triplet excitations) of $dpfam_2Au_2$ (**3**) as obtained using TDDFT. See Table S 4-5-1 for further information.

Excitation	Energy [eV]	Oscillator strength
1	2.70	$1.32x10^{0}$
2	2.71	$4.49x10^{-1}$
3	3.14	$4.35x10^{-2}$
4	3.15	$3.38x10^{-2}$
5	3.31	$2.81x10^{-2}$

4.6 Calculated triplet excitation energies of trimetallic complexes 4, 4a and 5

Table S 4.6-1: Lowest 5 roots (triplet excitations) of $[dpfam_2Cu_3(MeCN)]^+$ (**4**) as obtained using TDDFT See Table S 4-5-1 for further information.

Excitation	Energy [eV]	Oscillator strength
1	2.75	$8.14x10^{-1}$
2	2.91	$7.45x10^{-1}$
3	3.12	$3.04x10^{-3}$
4	3.24	$1.07x10^{-1}$
5	3.26	$5.25x10^{-3}$

Table S 4.6-2: Lowest 5 roots (triplet excitations) of $[dpfam_2Cu_3]^+$ (**4a**) as obtained using TDDFT. See Table S 4-5-1 for further information.

Excitation	Energy [eV]	Oscillator strength
1	2.75	$8.87x10^{-1}$
2	2.76	$7.36x10^{-1}$
3	2.99	$2.19x10^{-2}$
4	3.18	$5.02x10^{-2}$
5	3.28	$1.68x10^{-2}$

Table S 4.6-3: Lowest 5 roots (triplet excitations) of $[dpfam_2Ag_3]^+$ (**5**) as obtained using TDDFT. See Table S 4-5-1 for further information.

Excitation	Energy [eV]	Oscillator strength
1	3.18	$1.49x10^{-1}$
2	3.19	$8.97x10^{-1}$
3	3.31	$3.43x10^{-3}$
4	3.33	$8.55x10^{-2}$
5	3.36	$9.82x10^{-2}$

5 Spectra

5.0 Kdpfam

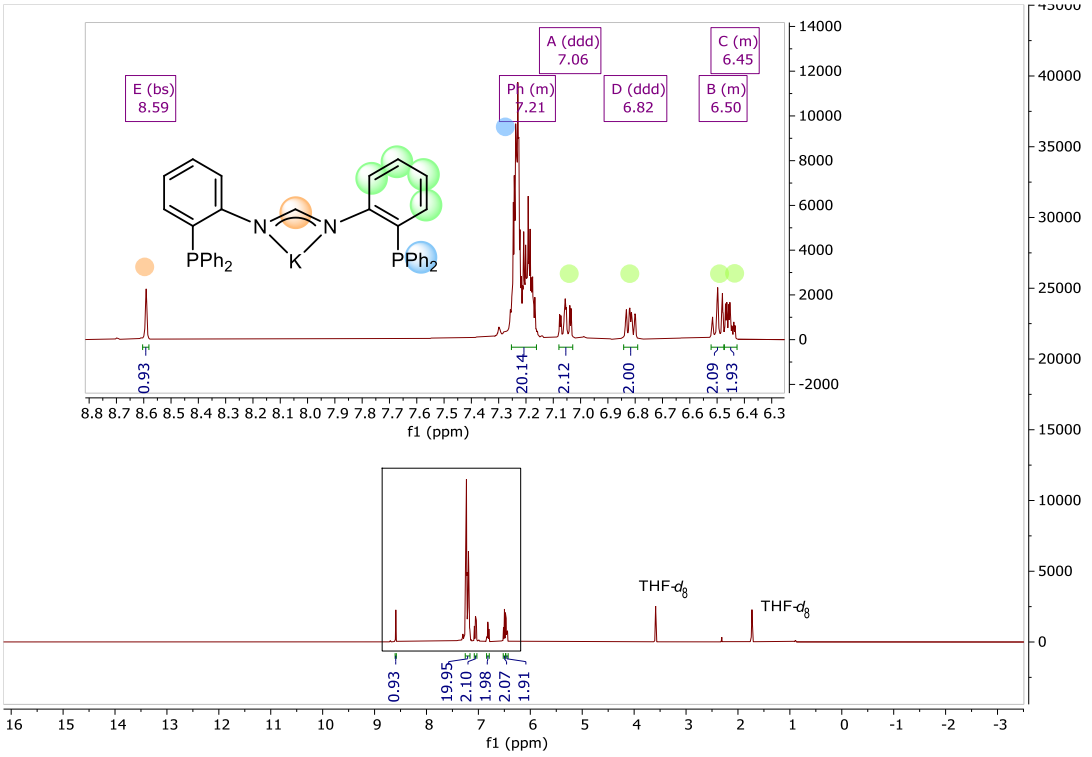

Figure S 5.0-1: ^{1}H NMR (400 MHz, THF-d_8) spectrum of Kdpfam.

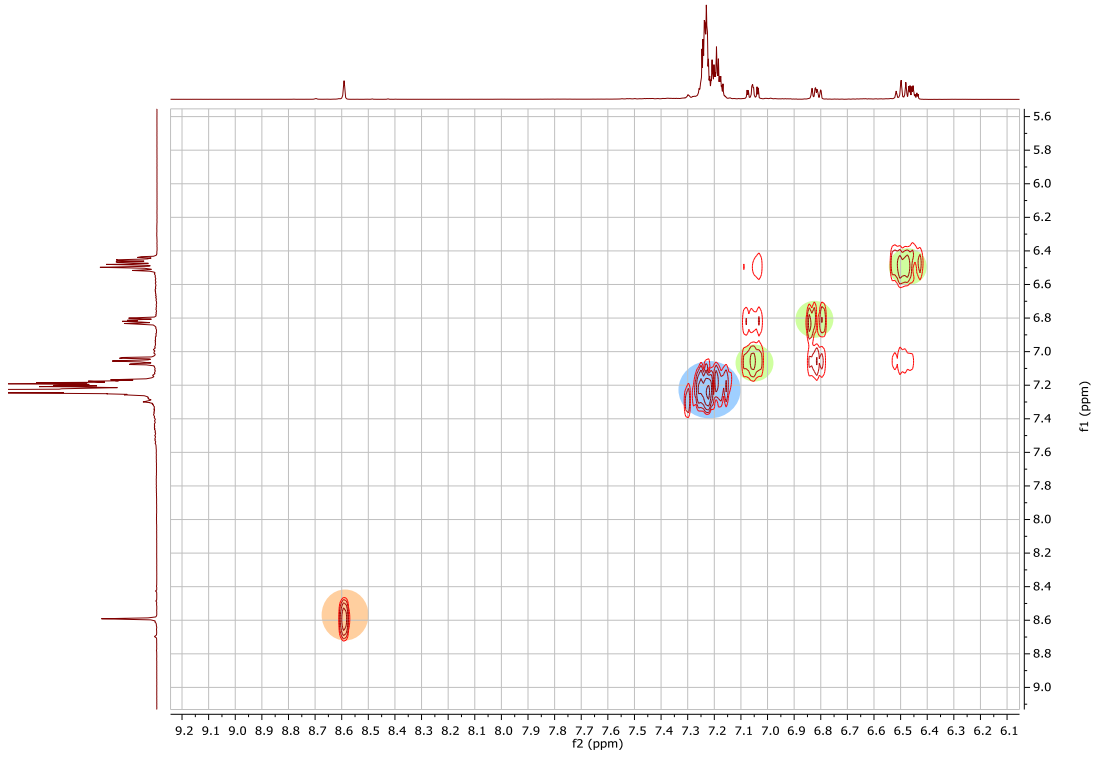

Figure S 5.0-2: ^{1}H-COSY NMR (300 MHz, THF-d_8) of Kdpfam.

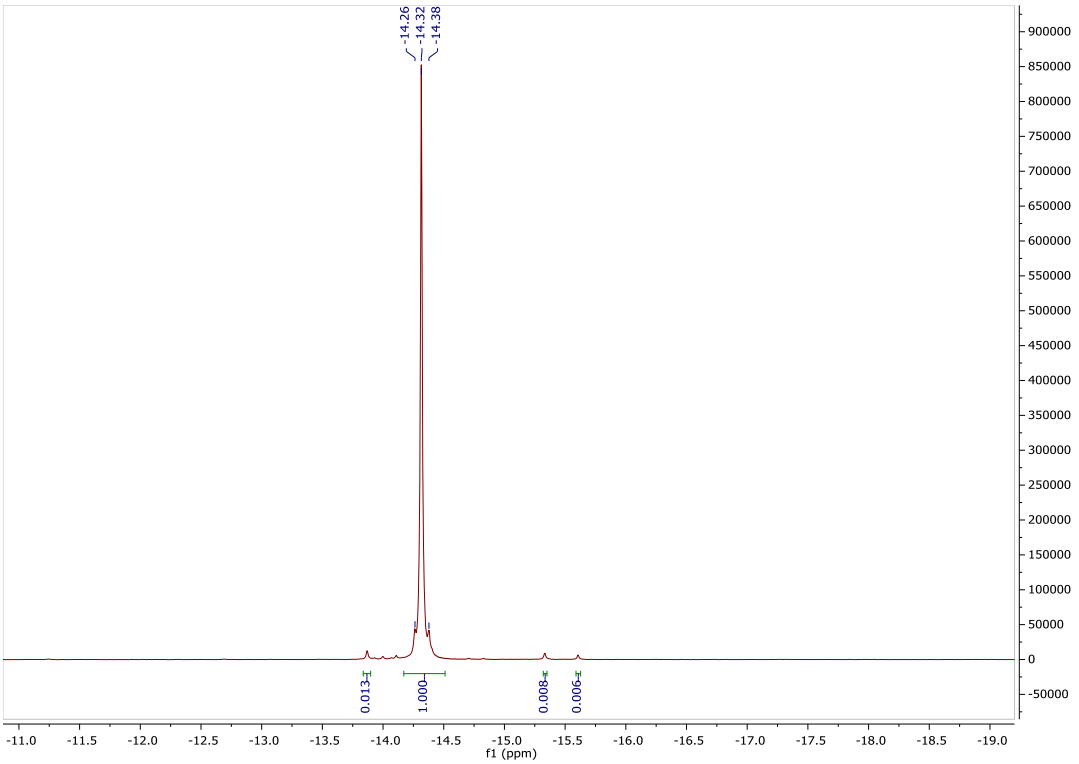

Figure S 5.0-3: $^{31}P\{^{1}H\}$ NMR (162 MHz, THF-d_8) spectrum of Kdpfam.

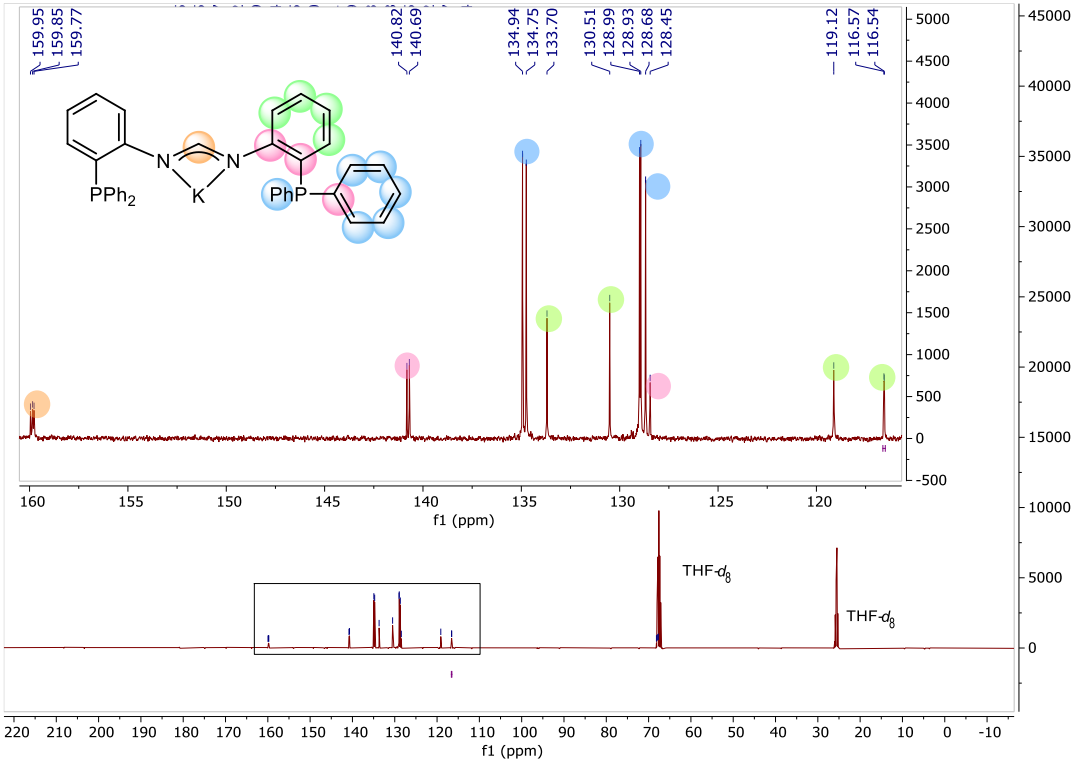

Figure S 5.0-4: $^{13}C\{^{1}H\}$ NMR (101 MHz, THF-d_8): spectrum of Kdpfam.

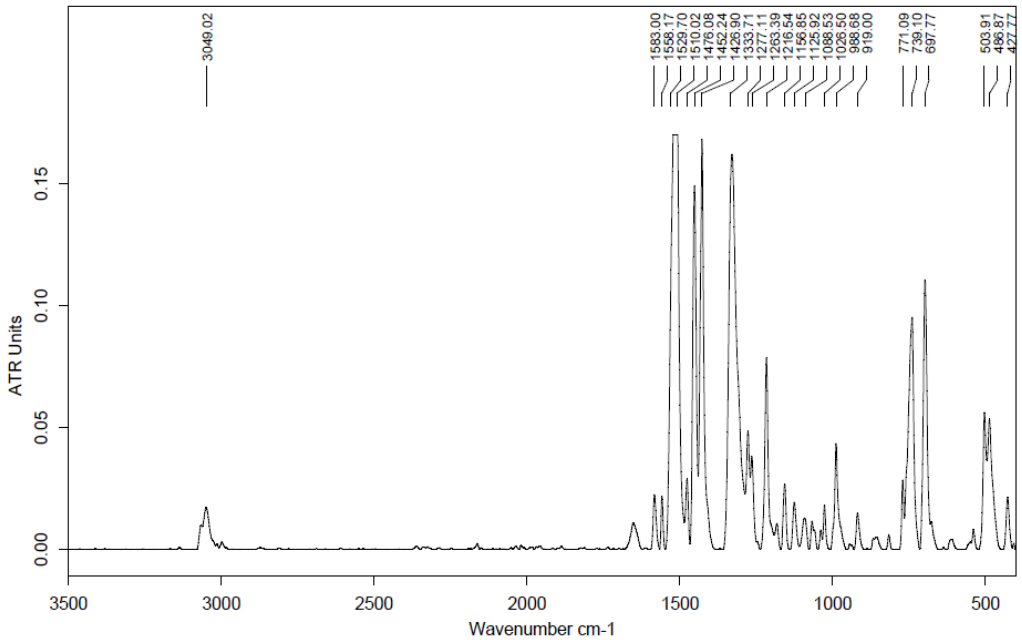

Figure S 5.0-5: ATR-IR spectrum of Kdpfam.

5.1 [dpfam$_2$Cu$_2$] (1)

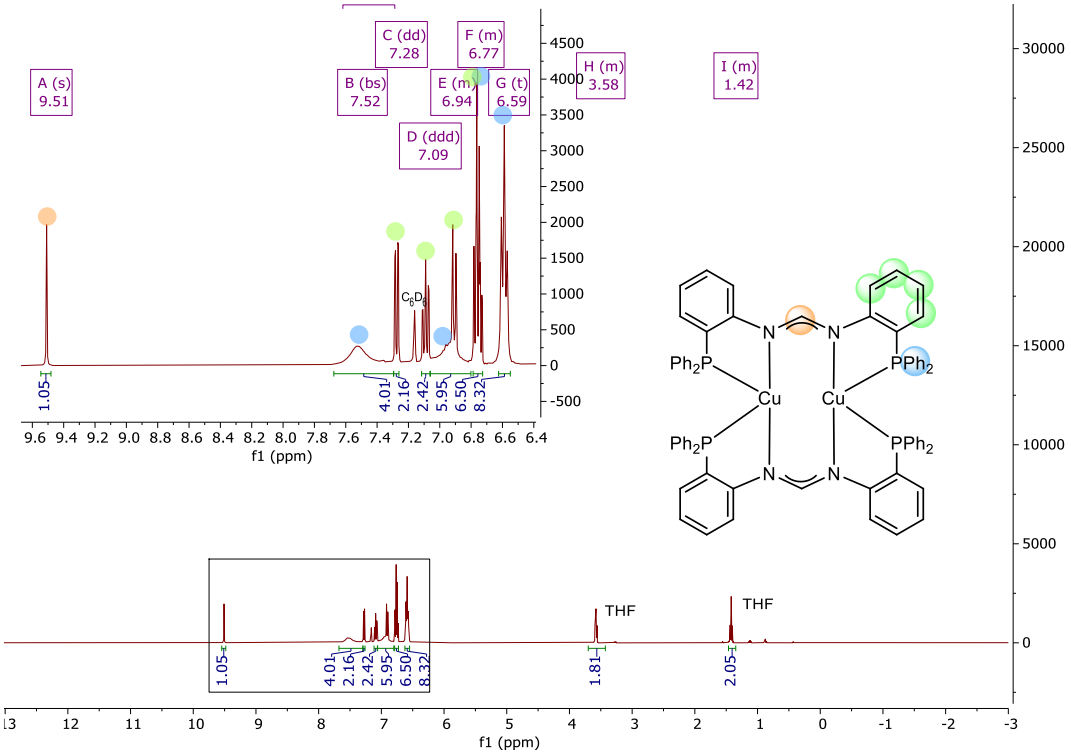

Figure S 5.1-1: ^{1}H NMR{^{31}P (-18.43 ppm)} (400 MHz, benzene-d_6) spectrum of **1**. Phosphorous nuclei decoupled at -18.4 ppm. Residual THF is originated from the crystals used.

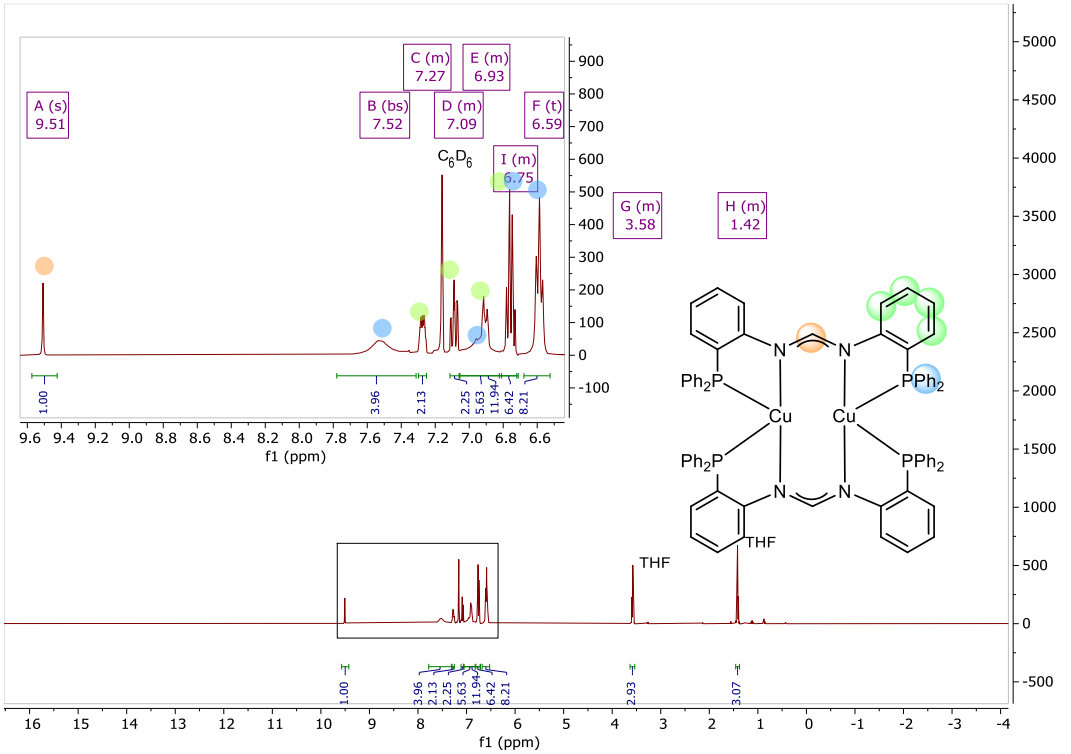

Figure S 5.1-2: ^{1}H NMR (400 MHz, benzene-d_6) spectrum of **1**. Residual THF is originated from the crystals used.

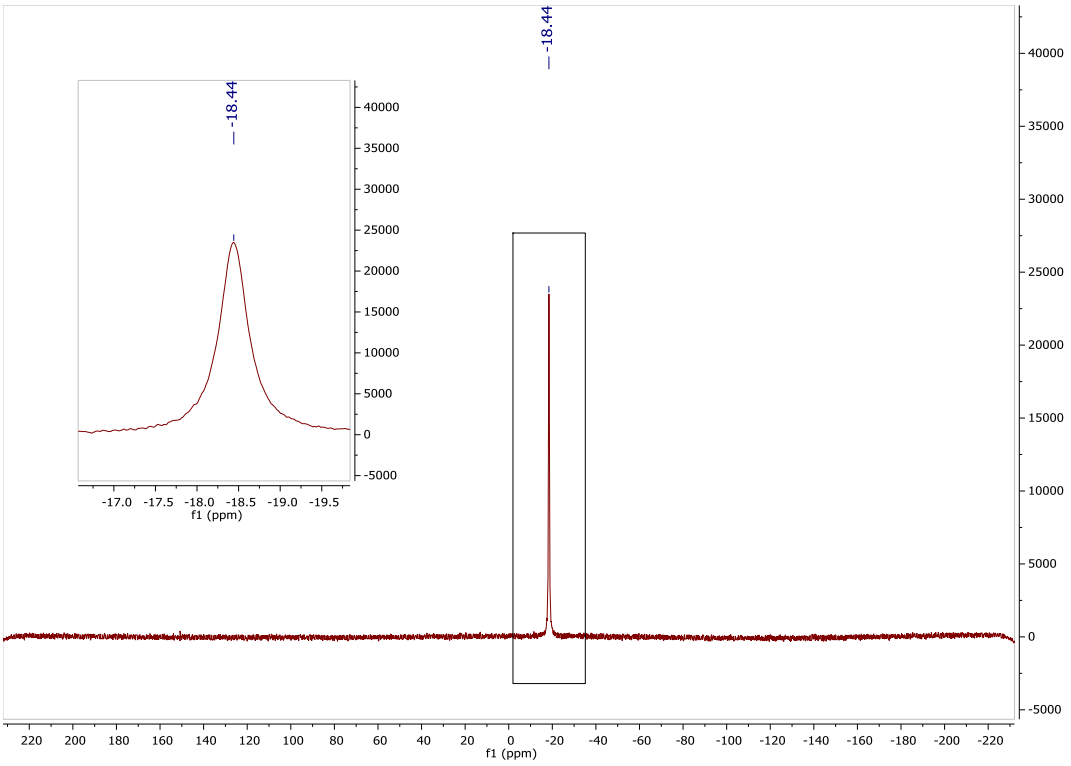

Figure S 5.1-3: $^{31}P\{^{1}H\}$ NMR (162 MHz, benzene-d_6 spectrum of **1**.

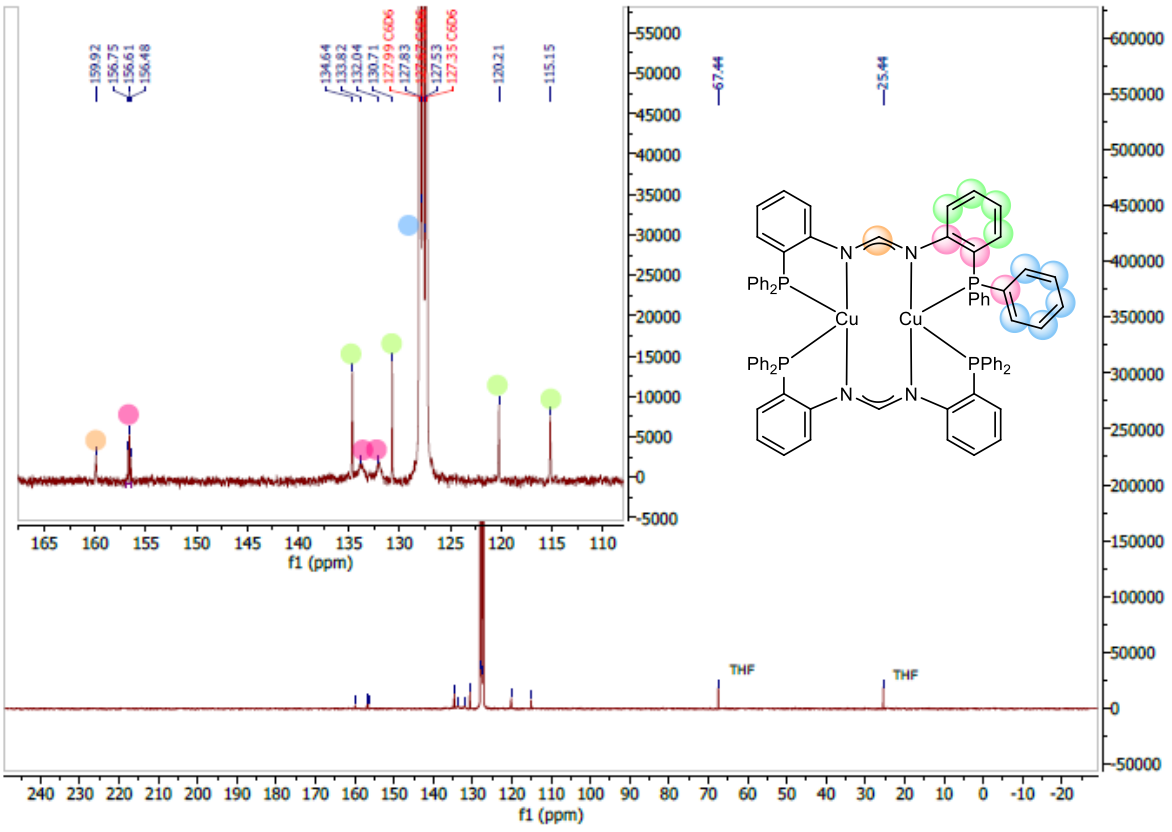

Figure S 5.1-4: $^{13}C\{^{1}H\}$ NMR (75 MHz, Benzene-d_6 spectrum of **1**. Residual THF is originated from the crystals used.

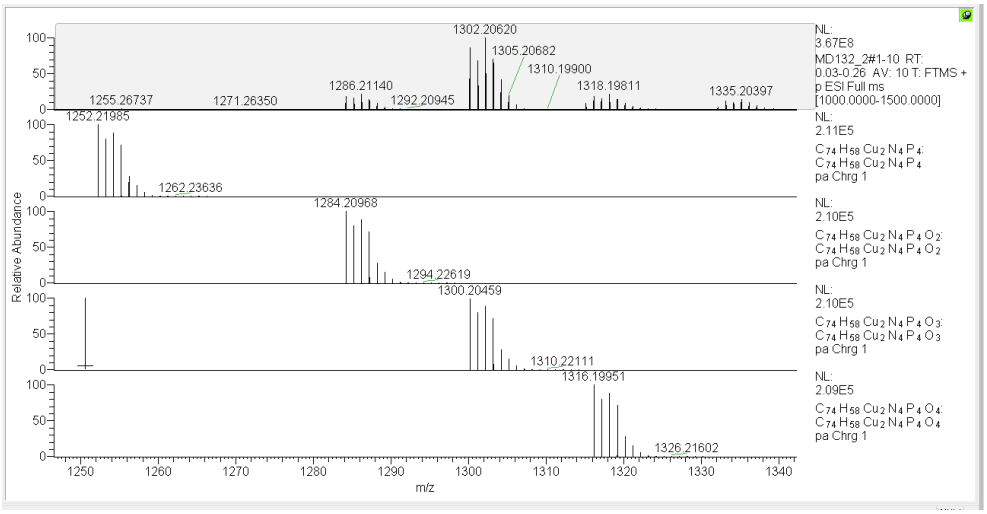

Figure S 5.1-5: ESI MS analysis of **1**, $[M]^+$ could not be detected but several oxygen adducts. Top line: experimental spectrum; Bottom lines: simulated signals.

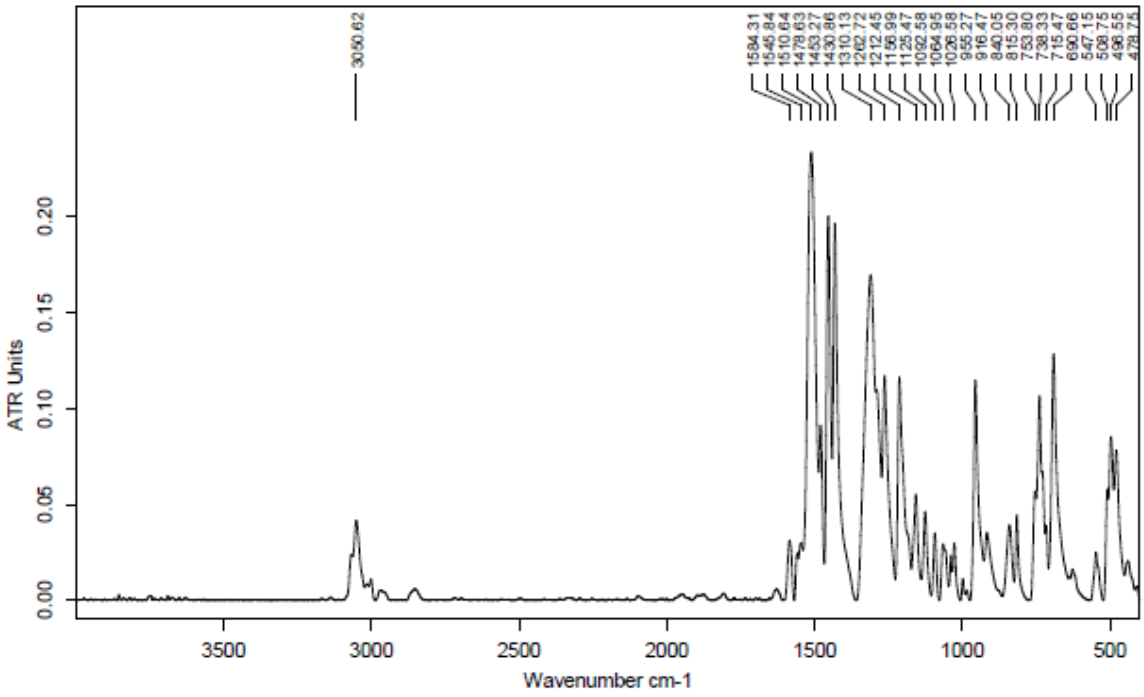

Figure S 5.1-6: ATR-IR spectrum of **1**.

5.2 [dpfam$_2$Ag$_2$] (2)

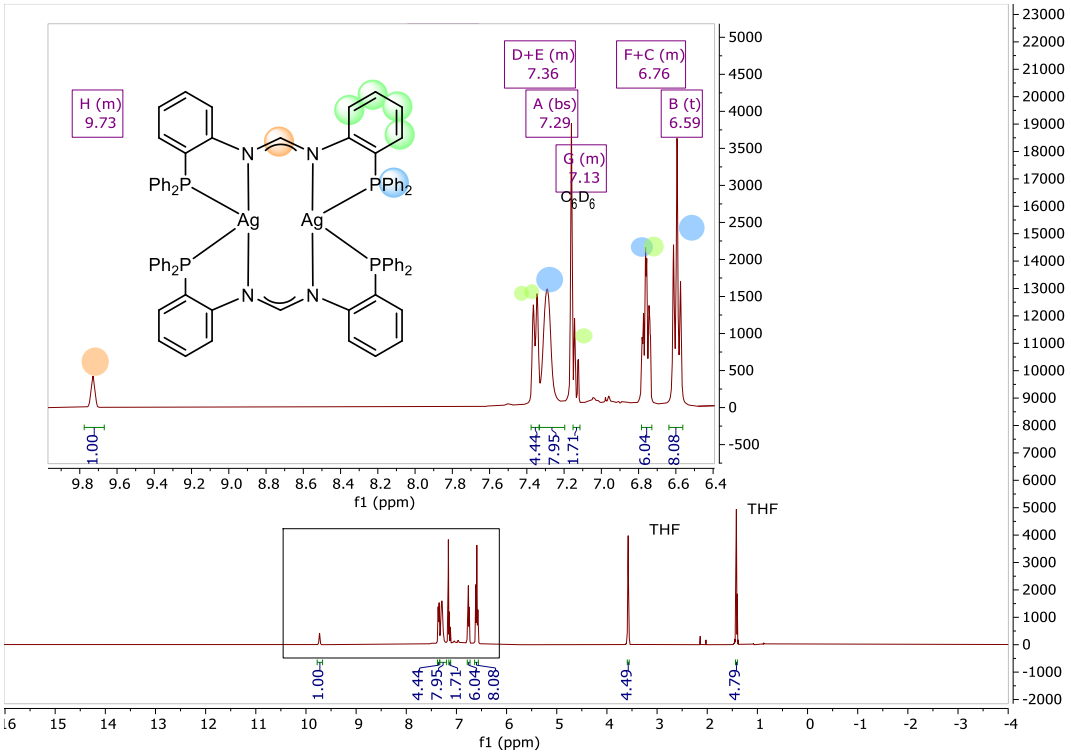

Figure S 5.2-1: ^{1}H NMR (400 MHz, benzene-d_6) spectrum of **2**. Residual toluene is originated from the crystals used.

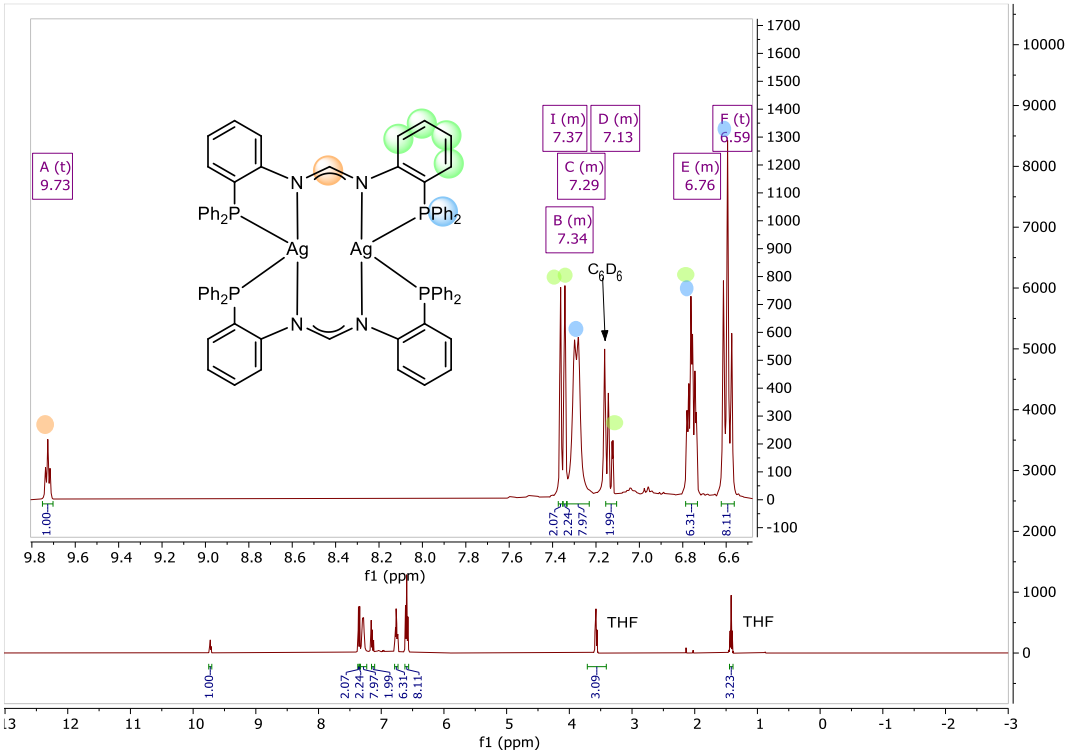

Figure S 5.2-2: ^{1}H{^{31}P} NMR (400 MHz, benzene-d_6) spectrum of **2**. Phosphorous nuclei decoupled at -16.7 ppm. Residual THF is originated from the crystals used.

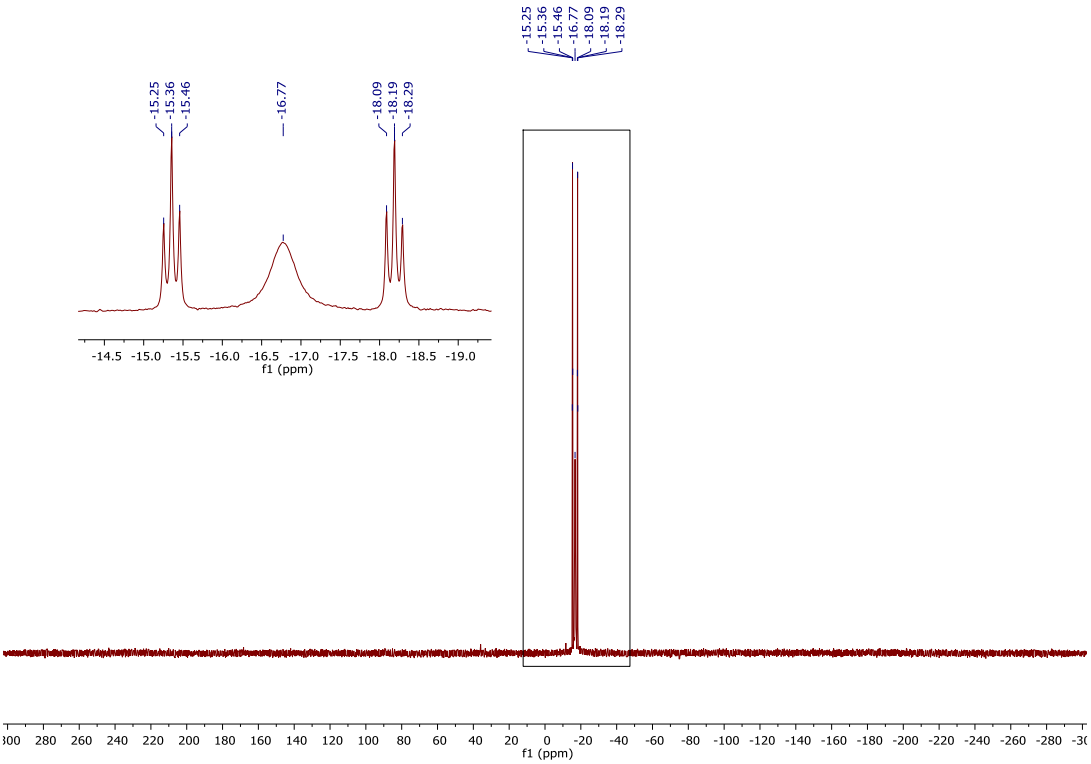

Figure S 5.2-3: $^{31}P\{^{1}H\}$ NMR (162 MHz, benzene-d_6) spectrum of **2**.

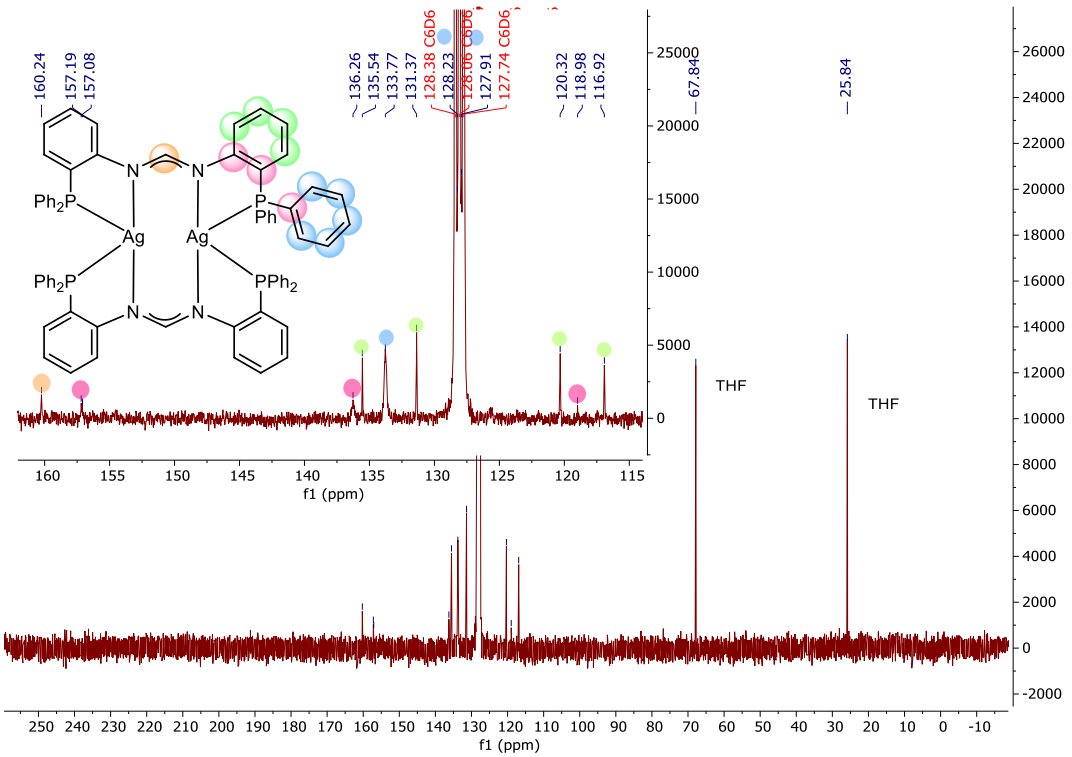

Figure S 5.2-4: $^{13}C\{^{1}H\}$ NMR (75 MHz, benzene-d_6) spectrum of **2**. Residual THF is originated from the crystals used.

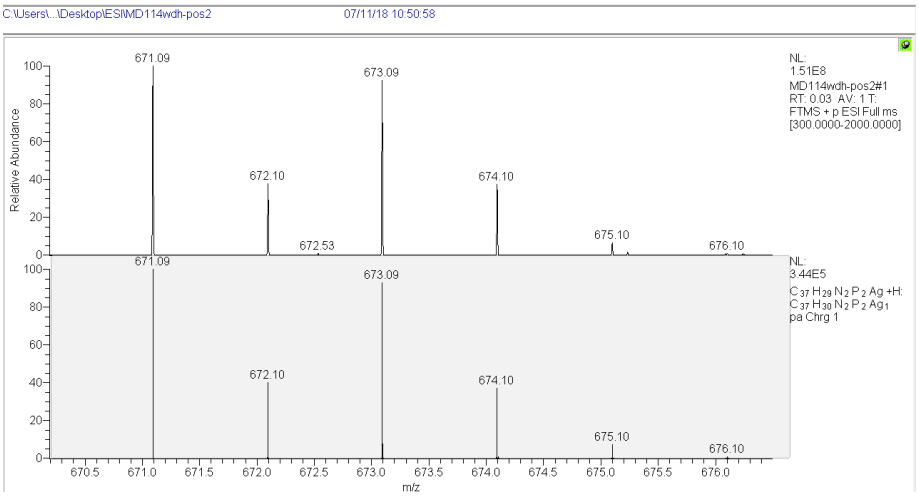

Figure S 5.2-5: ESI-MS analytics of **2**. Top: experimental spectrum; Bottom: simulated signals.

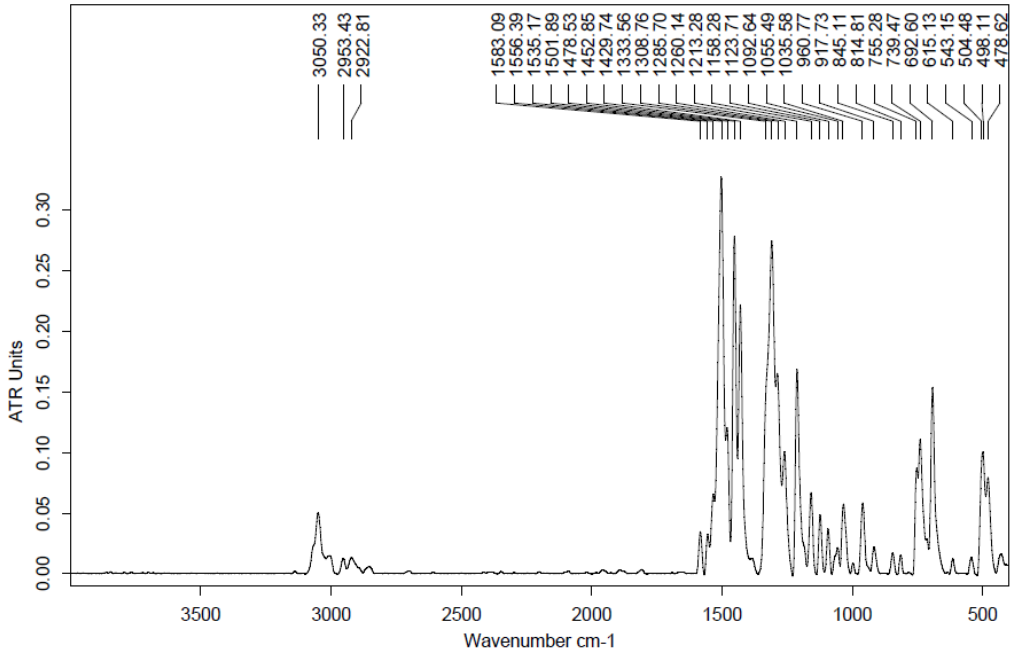

Figure S 5.2-6: IR ATR spectra of **2**.

5.3 [dpfam$_2$Au$_2$] (3)

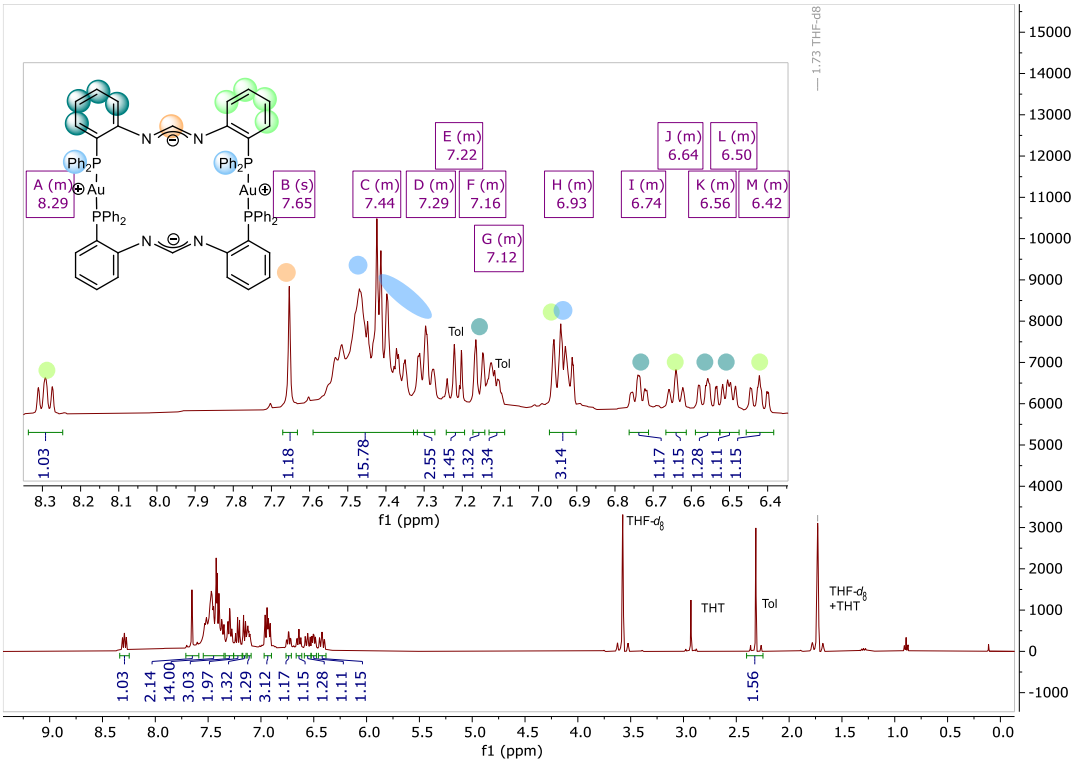

Figure S 5.3-1: ^{1}H NMR (400 MHz, THF-d_8, 213 K) spectrum of **3**. Residual toluene is originated from the crystals used.

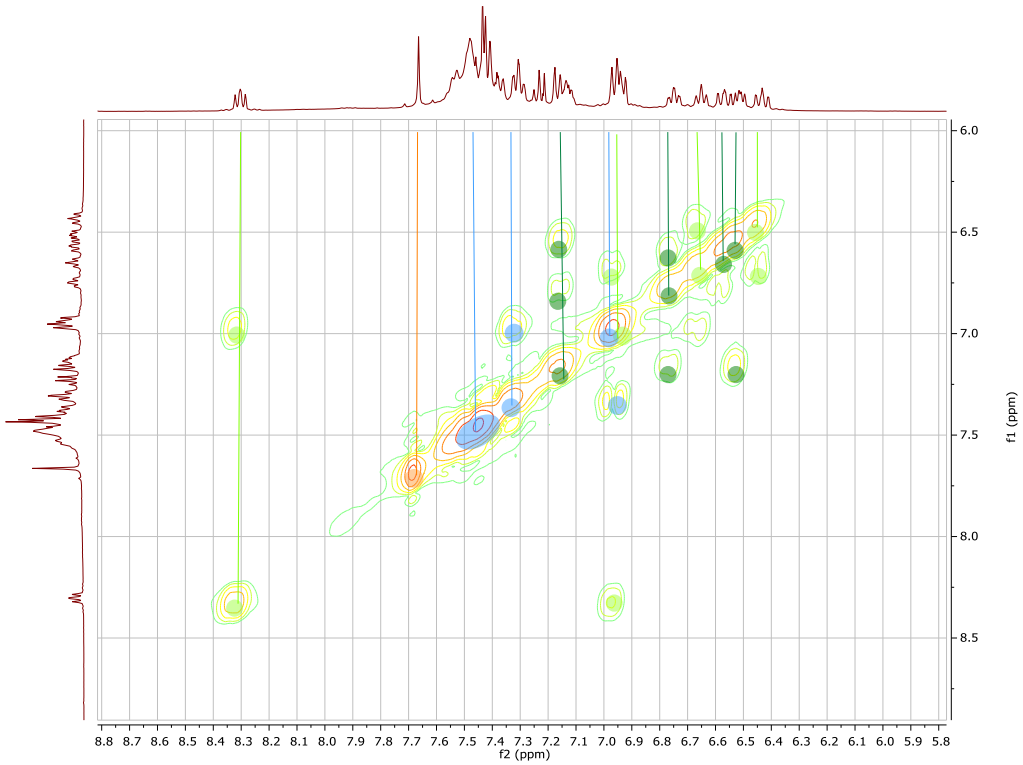

Figure S 5.3-2: ^{1}H-COSY NMR (400 MHz, THF-d_8, 213 K) spectrum of **3**.

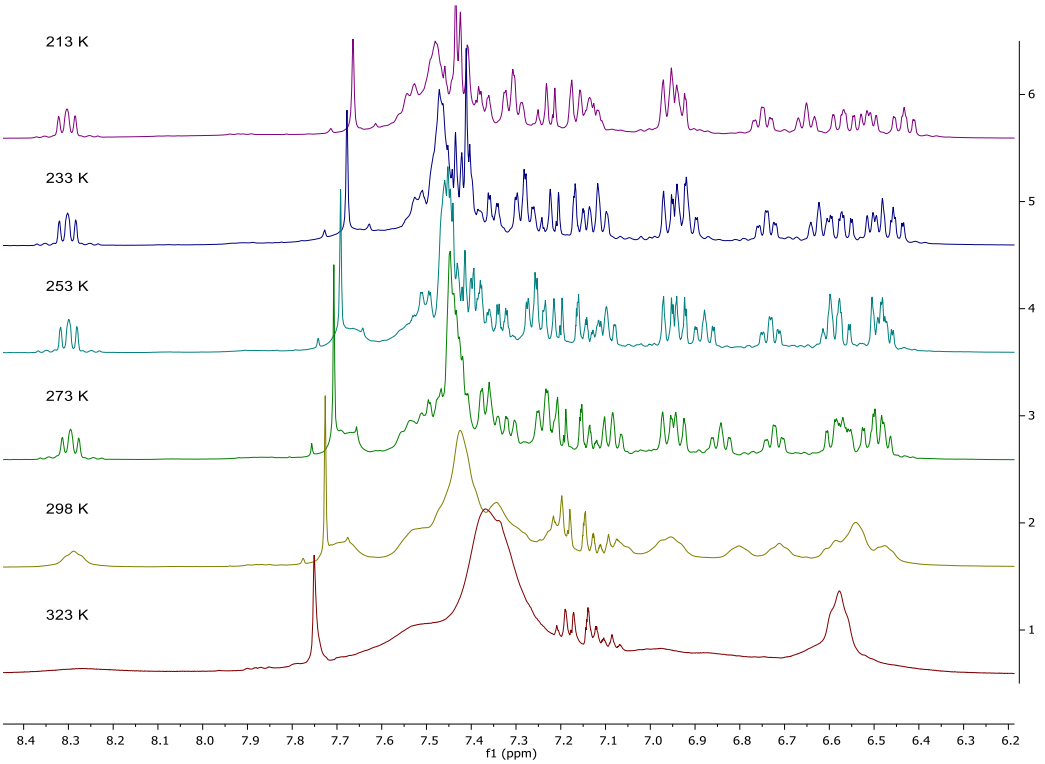

Figure S 5.3-3: VT ^{1}H NMR (400 MHz, THF-d_8) spectra of **3**.

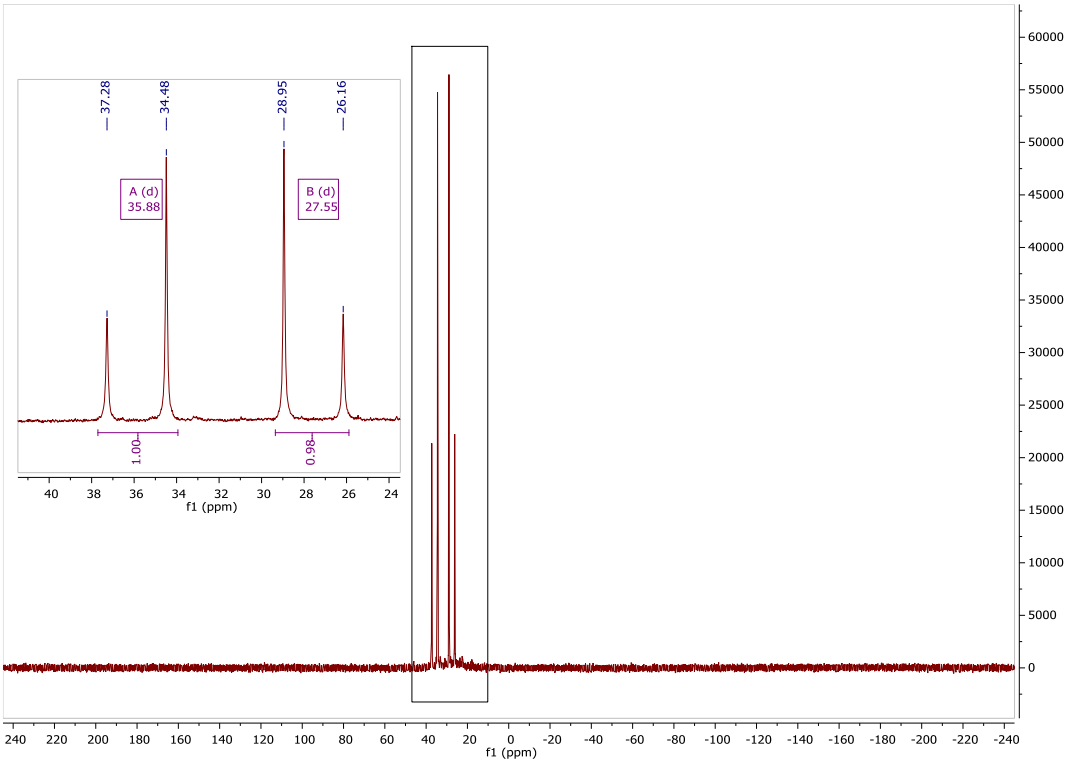

Figure S 5.3-4: ^{31}P{^{1}H} NMR (121 MHz, THF-d_8) spectrum of **3**.

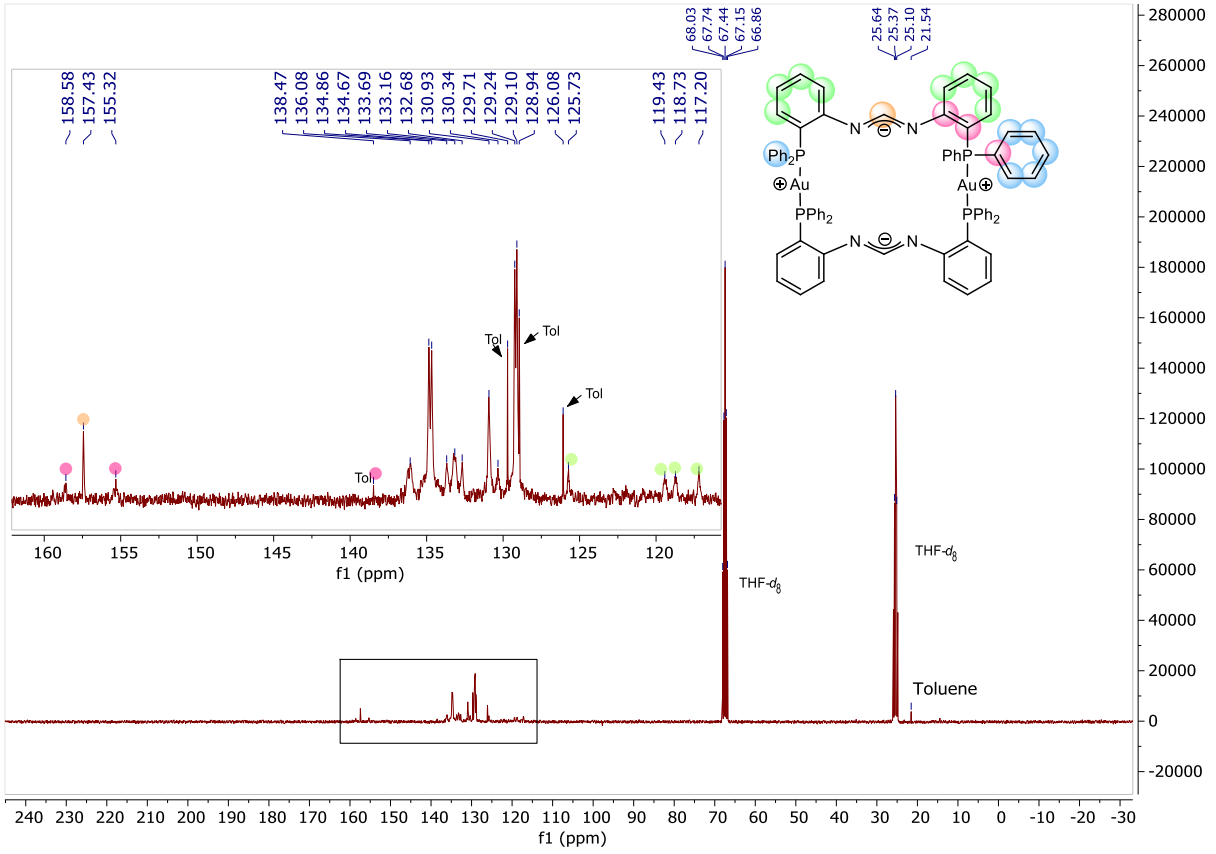

Figure S 5.3-5: $^{13}C\{^1H\}$ NMR (75 MHz, THF-d_8) spectrum of **3**. Residual toluene is originated from the crystals used.

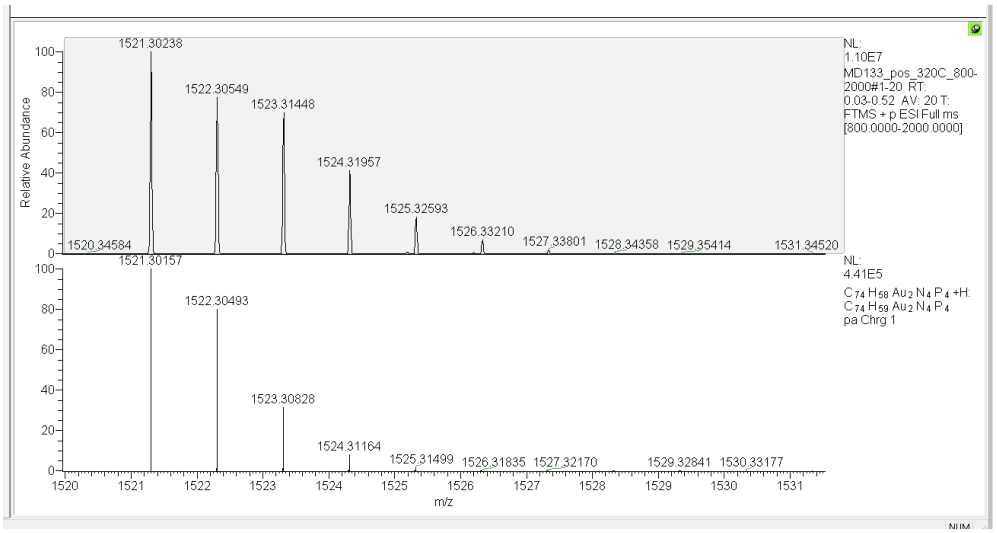

Figure S 5.3-6: ESI-MS analytics of **3**. Top: experimental spectrum; Bottom: simulated signals.

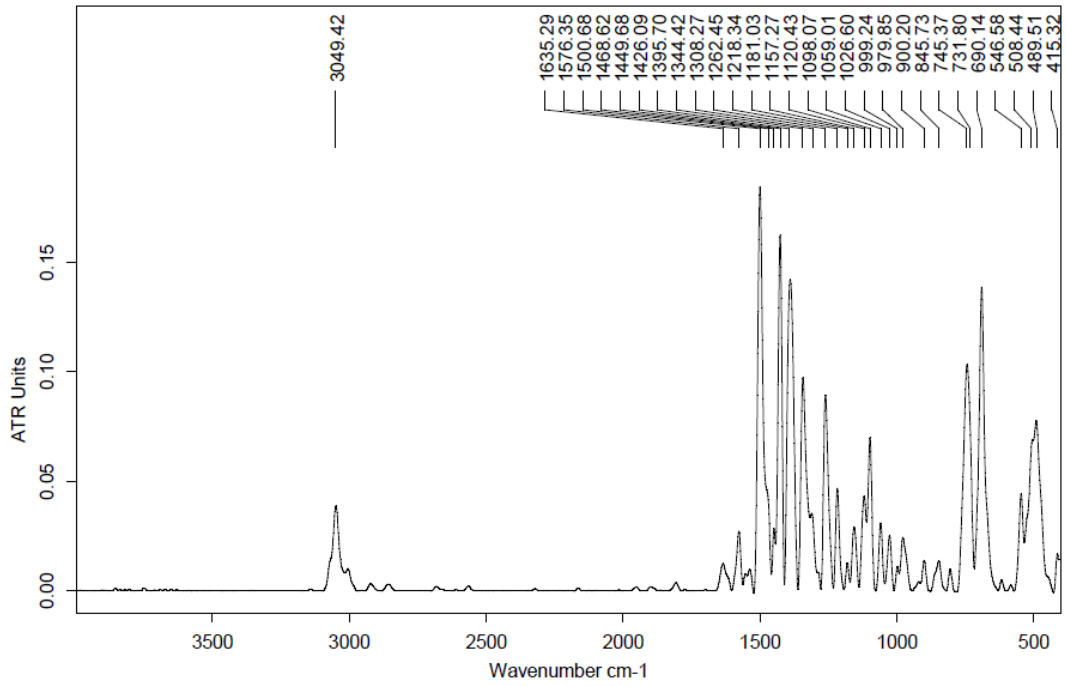

Figure S 5.3-7: IR ATR spectra of **3**.

5.4 [dpfam$_2$Cu$_3$(MeCN)][PF$_6$] (4)

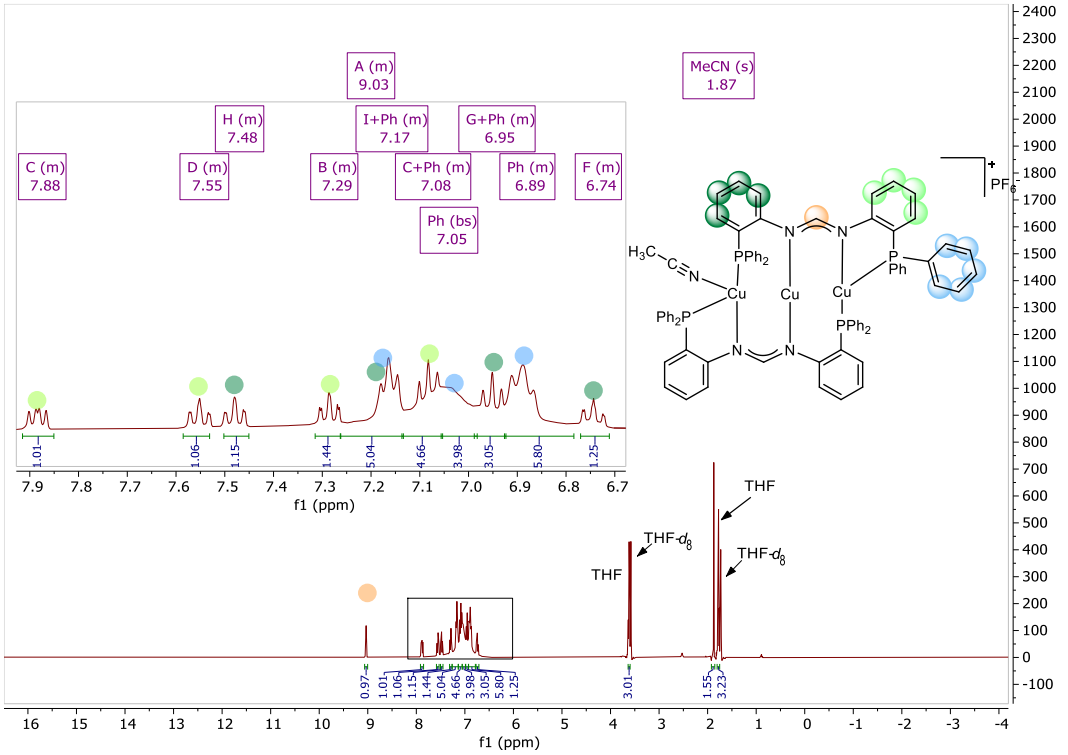

Figure S 5.4-1: ^{1}H NMR (400 MHz, THF-d_8) spectrum of **4**. Residual THF is originated from the crystals used.

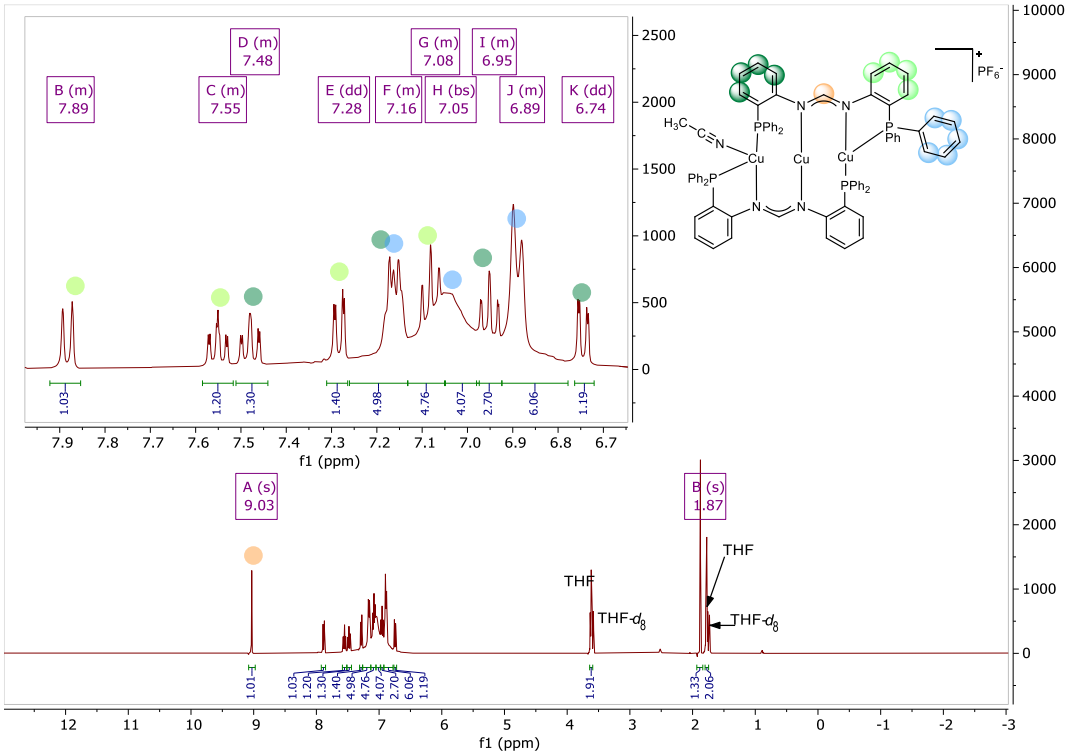

Figure S 5.4-2: ^{1}H{^{31}P(-18.2 ppm)} NMR (400 MHz, THF-d_8) spectrum of **4**. Residual THF is originated from the crystals used.

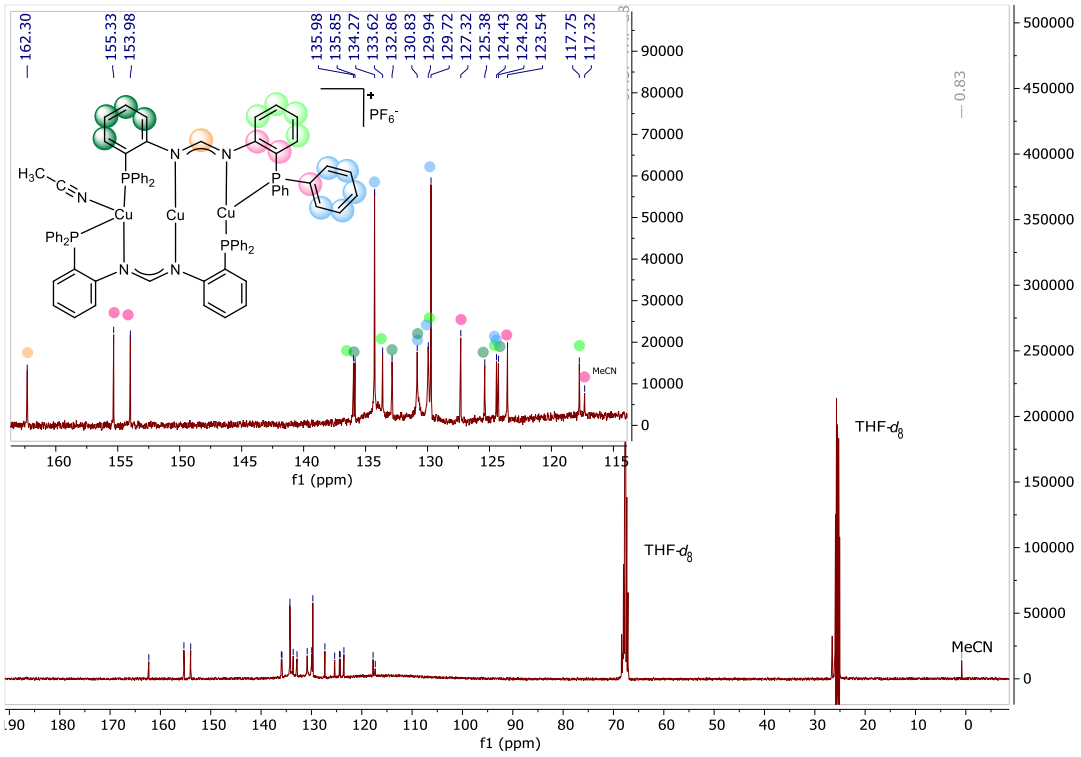

Figure S 5.4-3: $^{13}C\{^{1}H,^{31}P\}$ NMR (101 MHz, THF-d_8) NMR spectrum of **4**. Phosphor nuclei decoupled at -18.2 ppm.

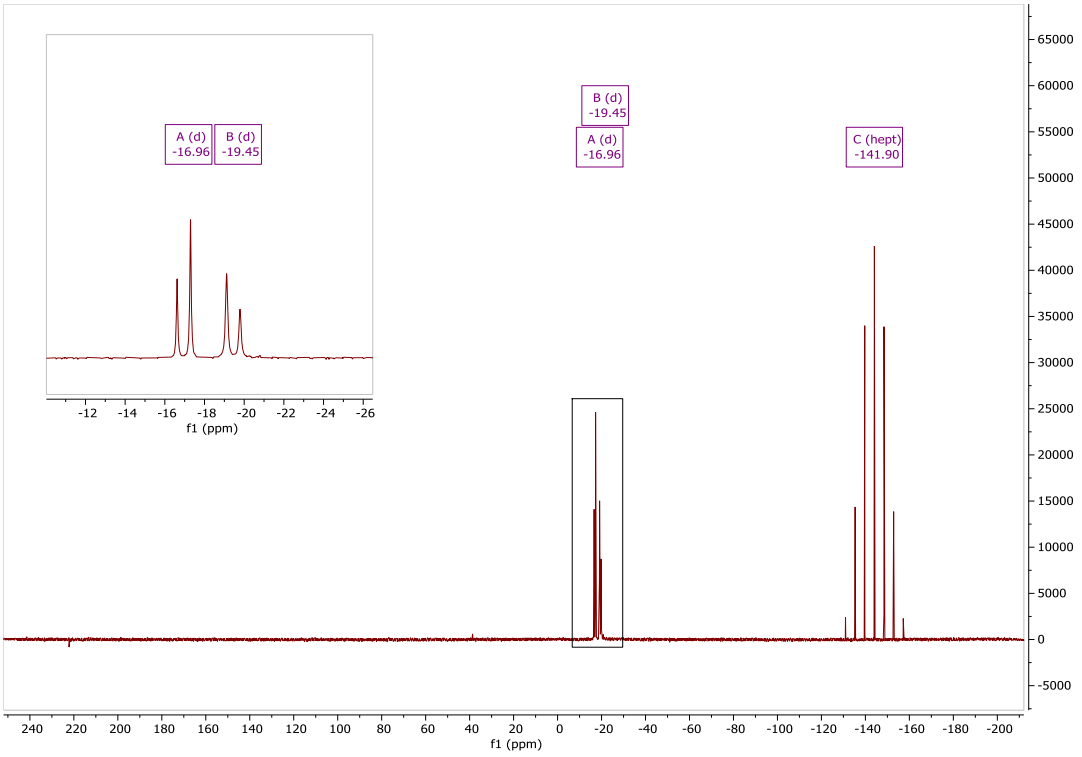

Figure S 5.4-4: $^{31}P\{^{1}H\}$ NMR (162 MHz, THF-d_8) spectrum of **4**.

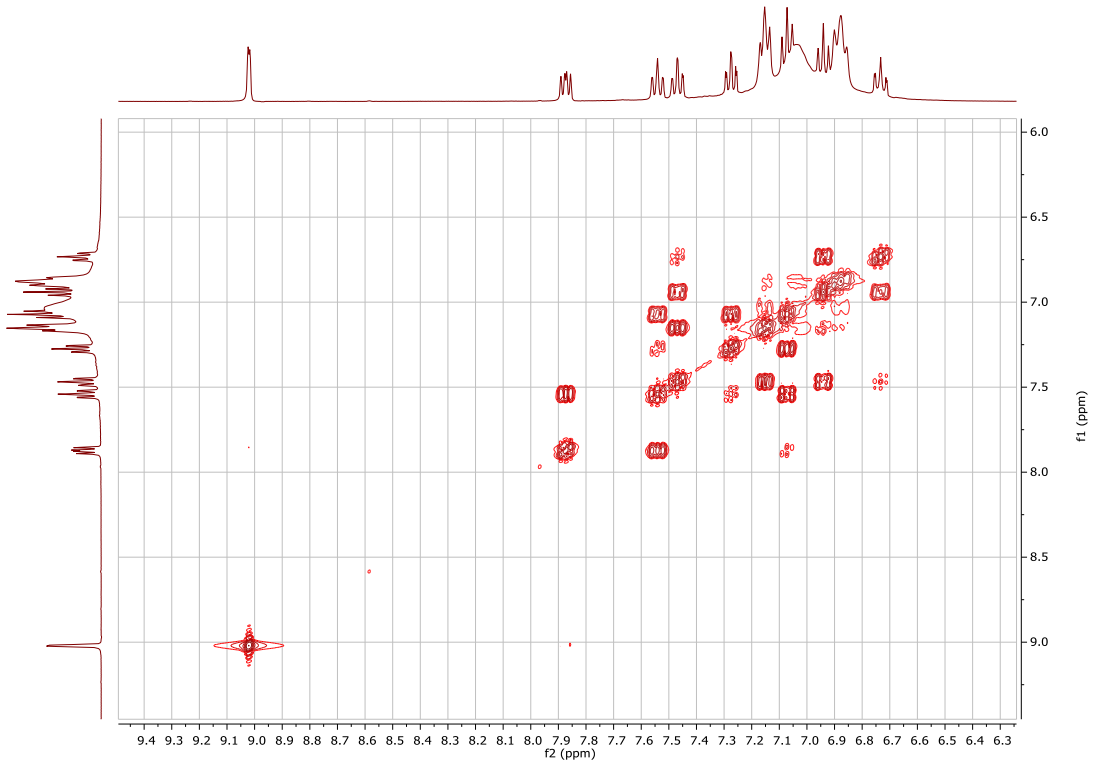

Figure S 5.4-5: ^{1}H-COSY NMR (400 MHz, THF-d_8) NMR spectrum of **4**.

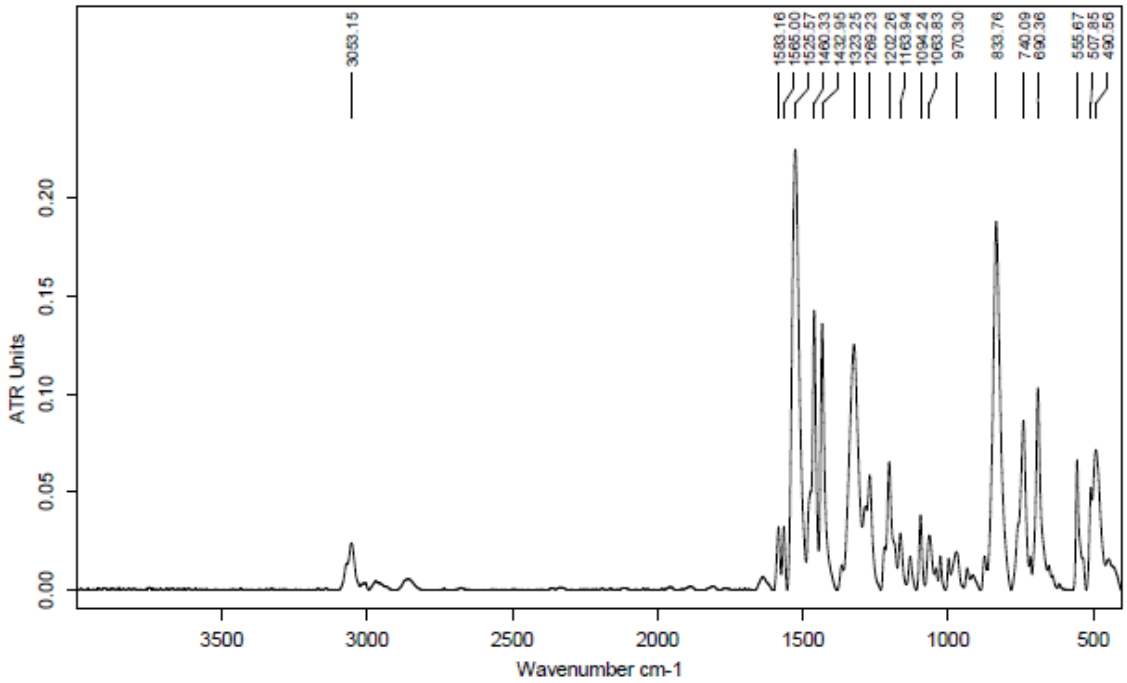

Figure S 5.4-6: ATRIR spectra of **4**.

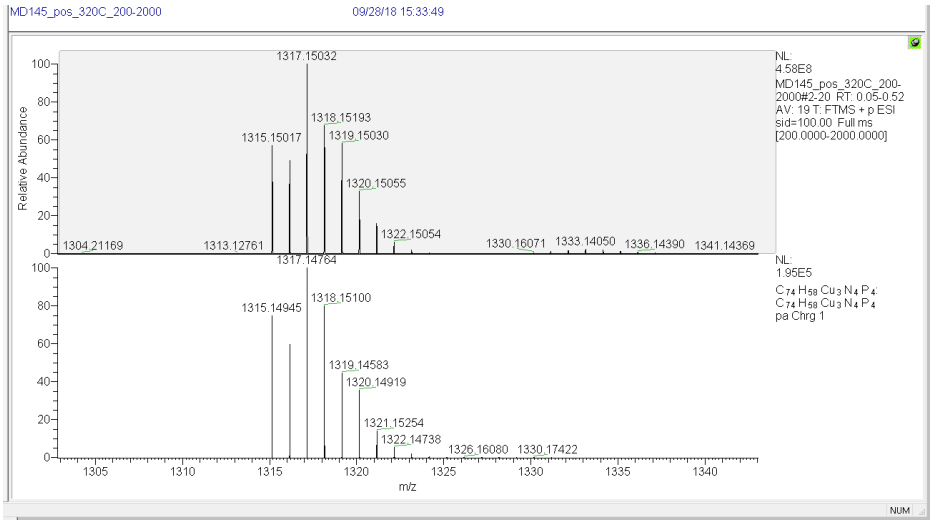

Figure S 5.4-7: ESI-MS analytics of **4**. Top: experimental spectrum; Bottom: simulated signals.

5.5 [dpfam$_2$Cu$_3$][PF$_6$] (4a)

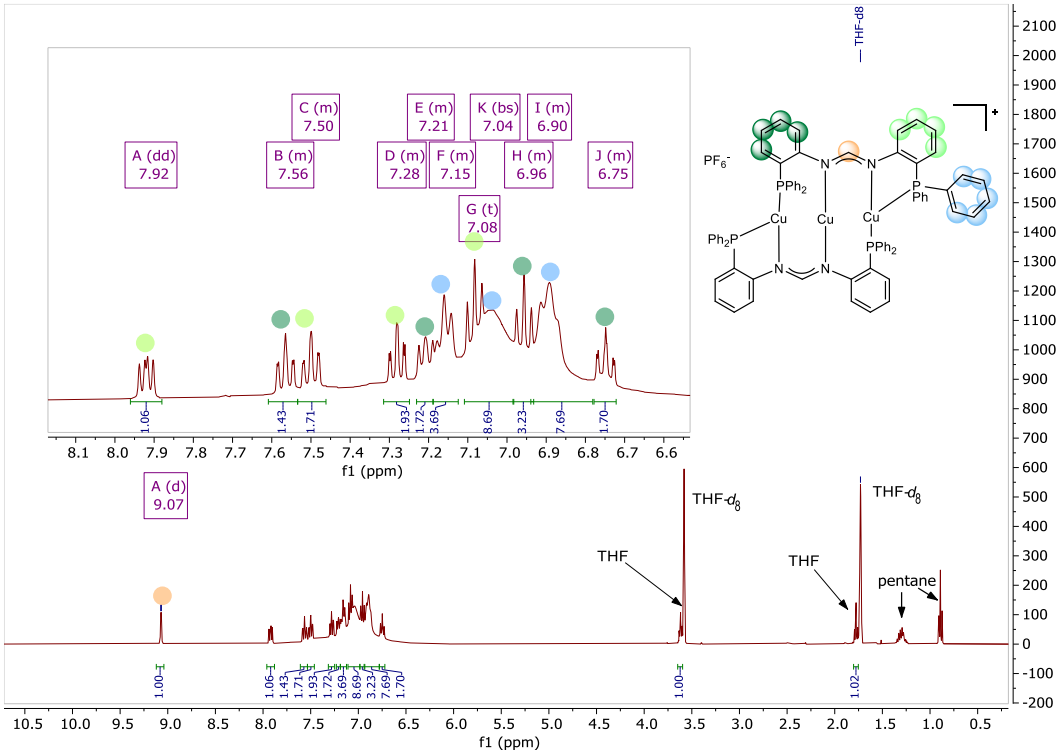

Figure S 5.5-1: ^{1}H NMR (400 MHz, THF-d_8) spectrum of **4a**. Residual THF is originated from the crystals used. Remaining *n*-pentane is most likely due to incomplete drying of the crystals before measuring.

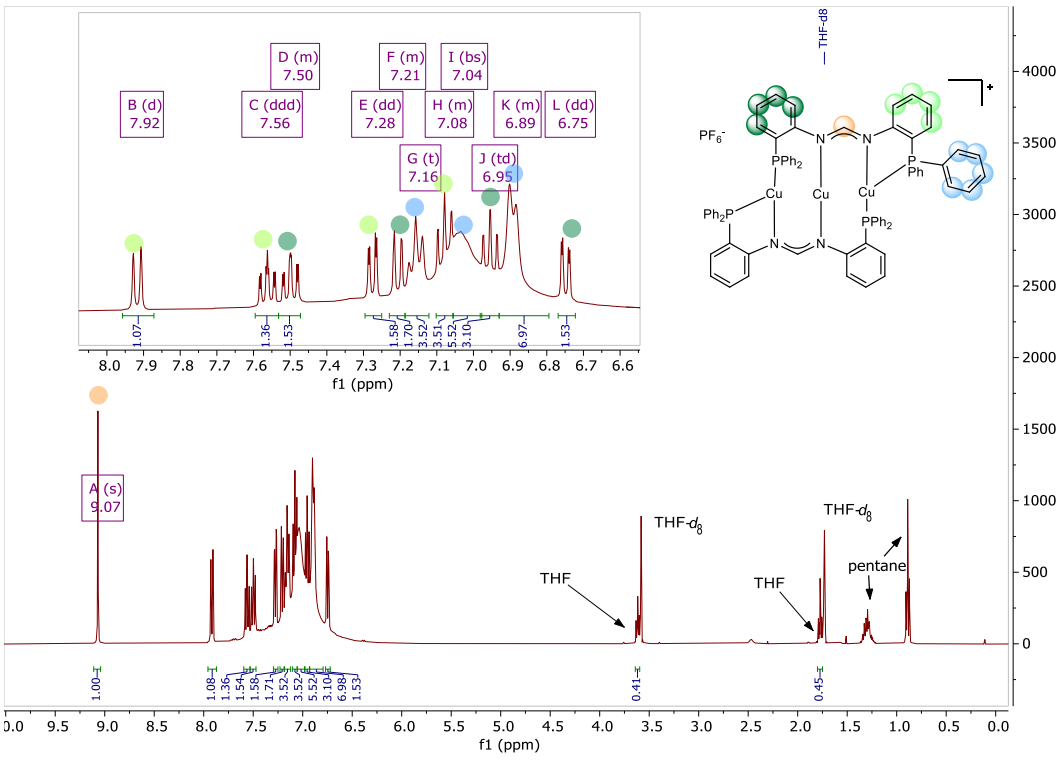

Figure S 5.5-2: ^{1}H{^{31}P(-18.3ppm)} NMR (400 MHz, THF-d_8) spectrum of **4a**. Residual THF is originated from the crystals used. Remaining *n*-pentane is most likely due to incomplete drying of the crystals before measuring.

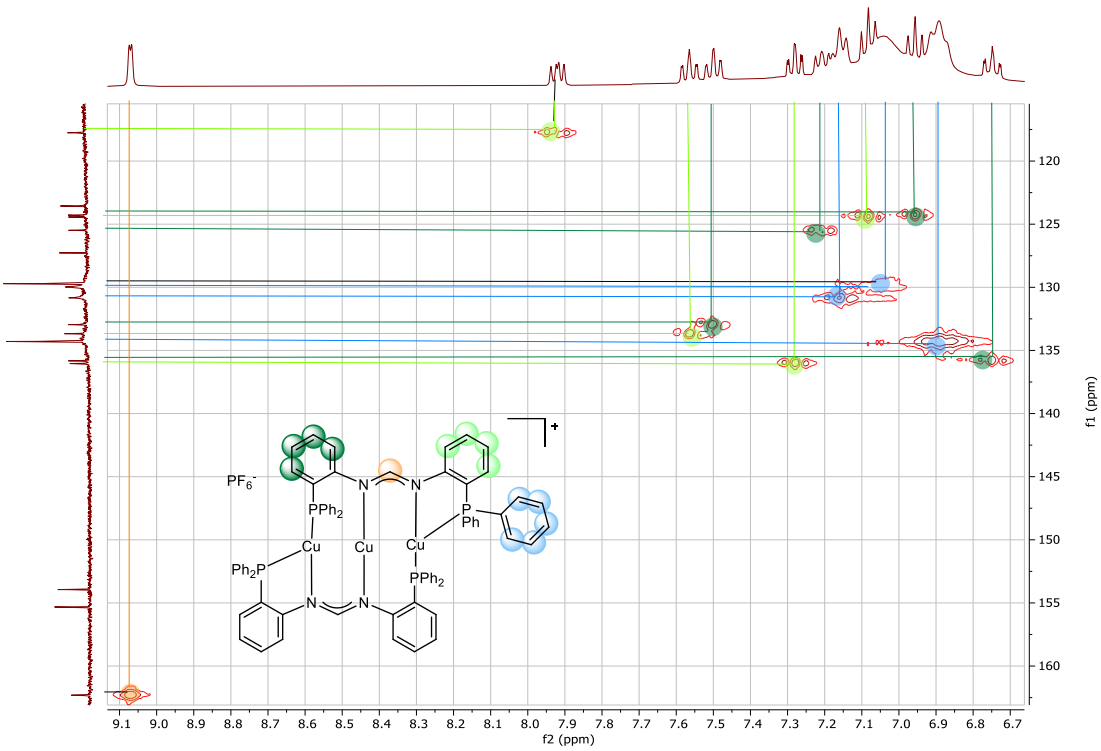

Figure S 5.5-3: HMQC NMR (75 MHz, THF-d_8) spectrum of **4a**. Horizontal trace: ^{1}H NMR; Vertical trace: ^{13}C{^{1}H, ^{31}P}.

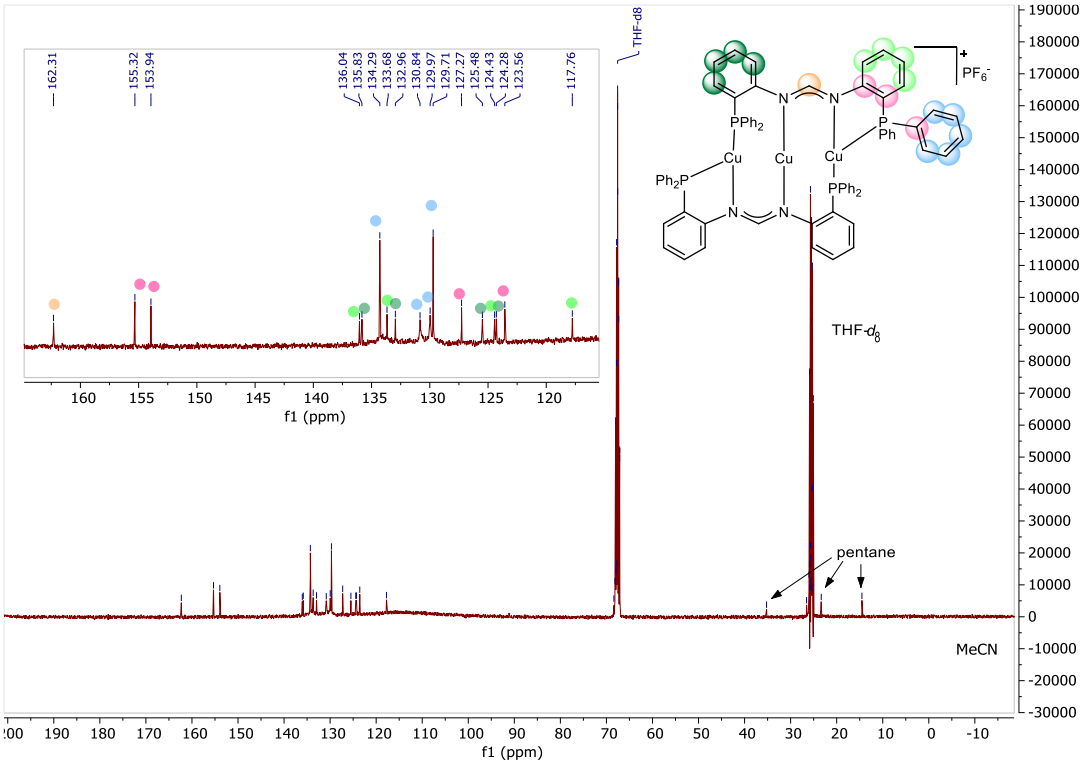

Figure S 5.5-4: ^{13}C{^{1}H,^{31}P} NMR (101 MHz, THF-d_8) NMR spectrum of **4a**. Phosphor nuclei decoupled at -18.3 ppm. Residual THF is originated from the crystals used. Remaining *n*-pentane is most likely due to incomplete drying of the crystals before measuring.

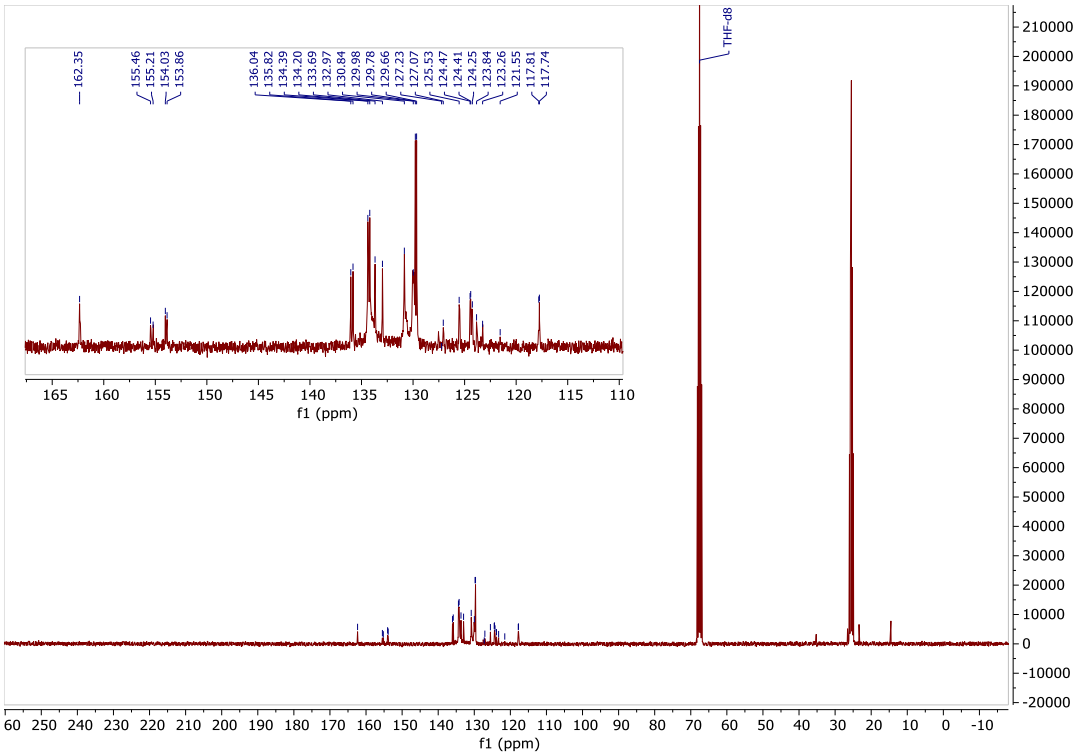

Figure S 5.5-5: $^{13}C\{^{1}H\}$ NMR (75 MHz, THF-d_8) NMR spectrum of **4a**.

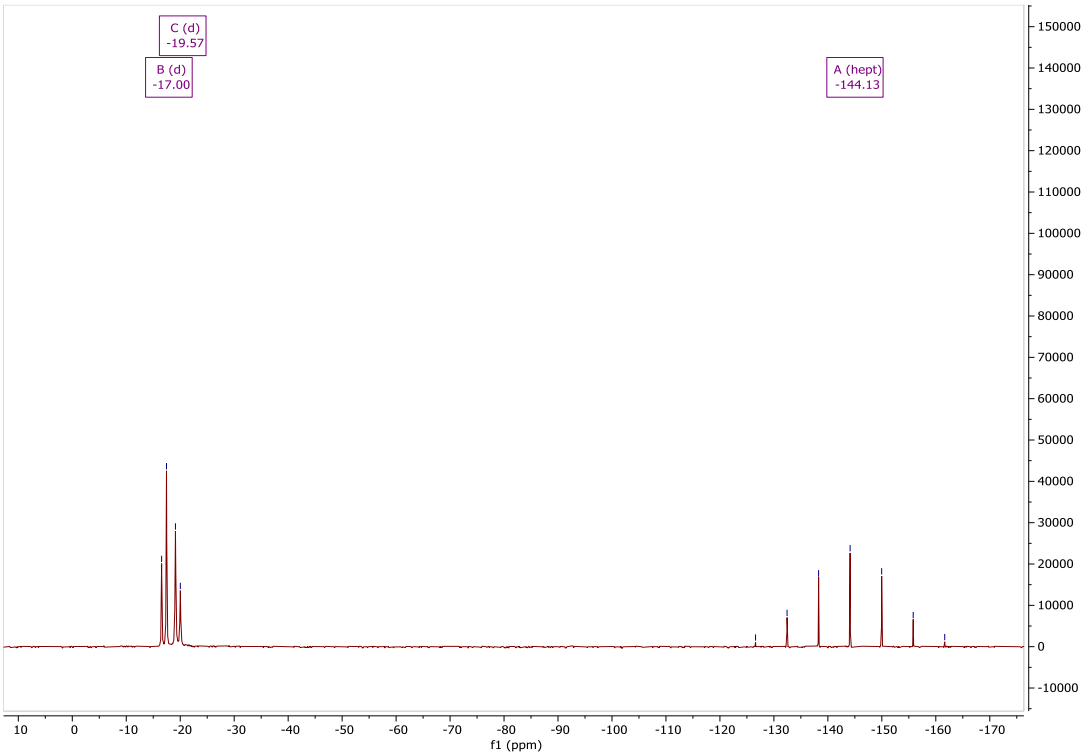

Figure S 5.5-6: $^{31}P\{^{1}H\}$ NMR (121 MHz, THF-d_8) spectrum of **4a**.

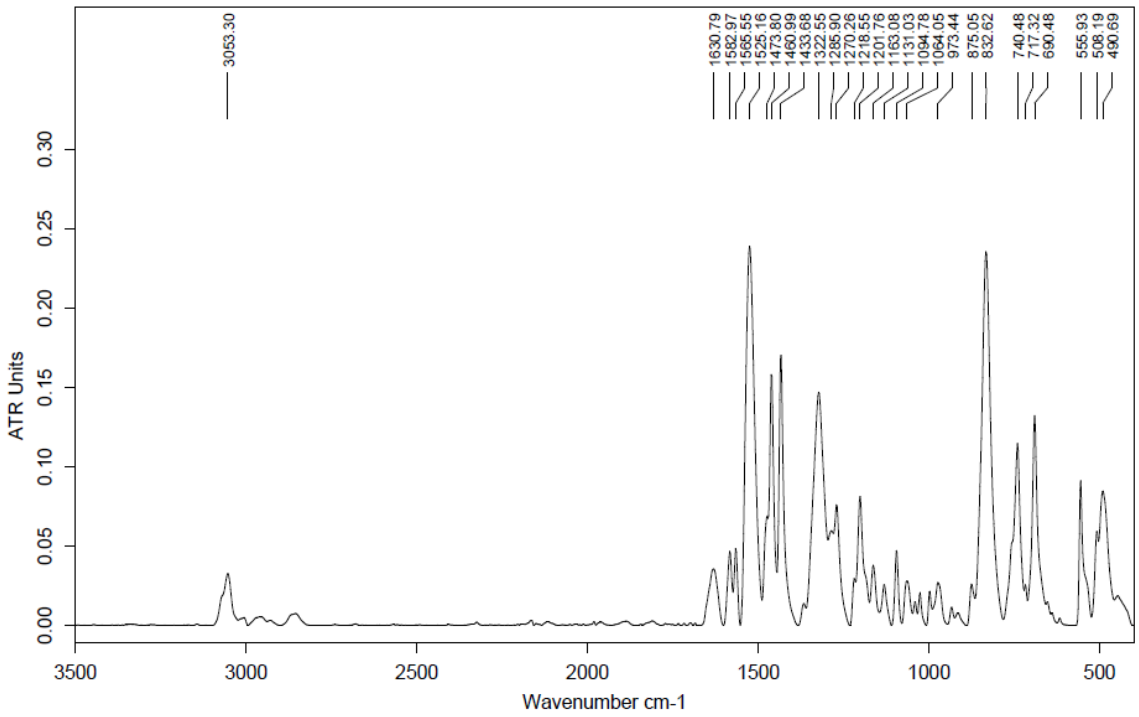

Figure S 5.5-7: IR ATR spectrum of **4a**.

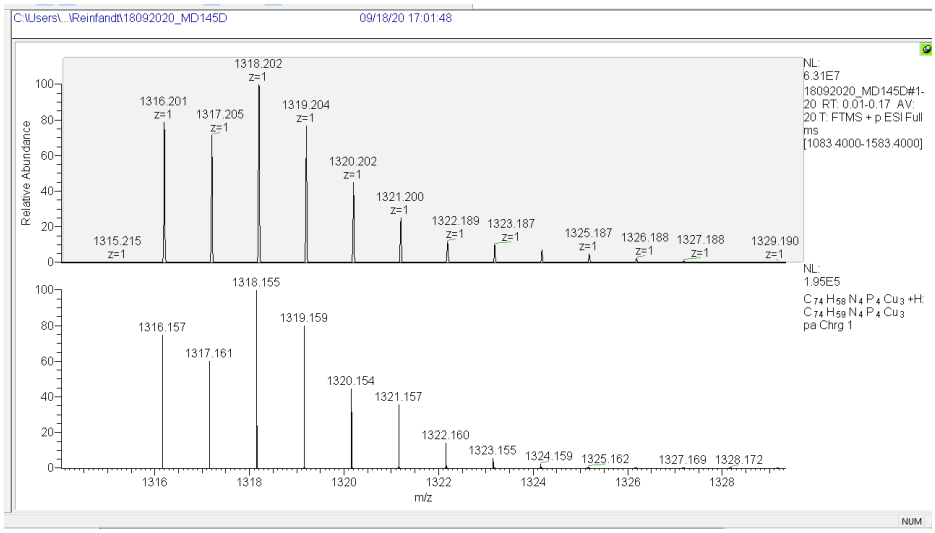

Figure S 5.5-8: ESI-MS analytics of **4a**. Top: experimental spectrum; Bottom: simulated signals.

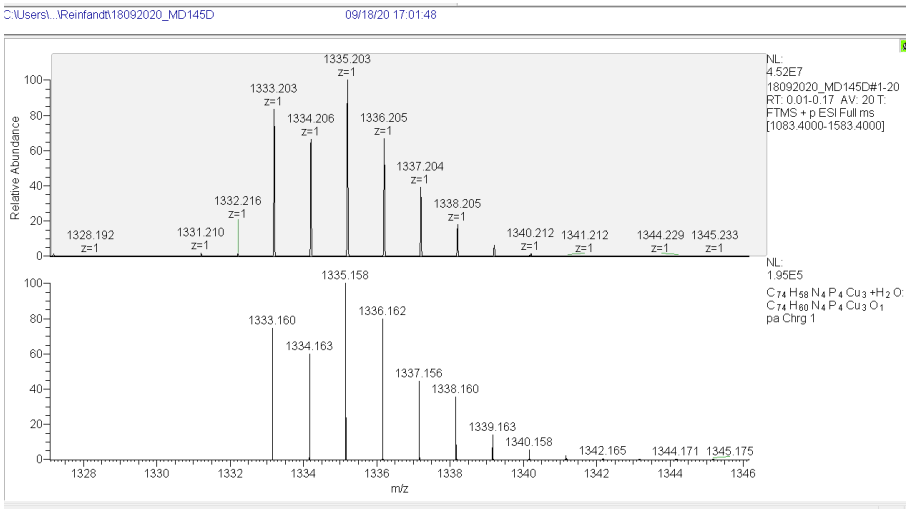

Figure S 5.5-9: ESI-MS analytics of **4a**. Top: experimental spectrum; Bottom: simulated signals.

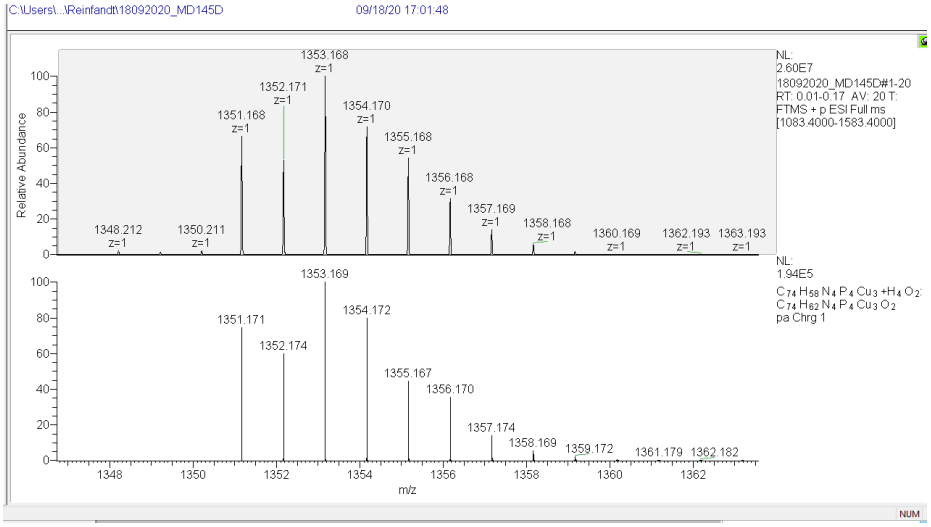

Figure S 5.5-10: ESI-MS analytics of **4a**. Top: experimental spectrum; Bottom: simulated signals.

5.6 [dpfam$_2$Ag$_3$(*thf*)$_2$][BF$_4$] (5)

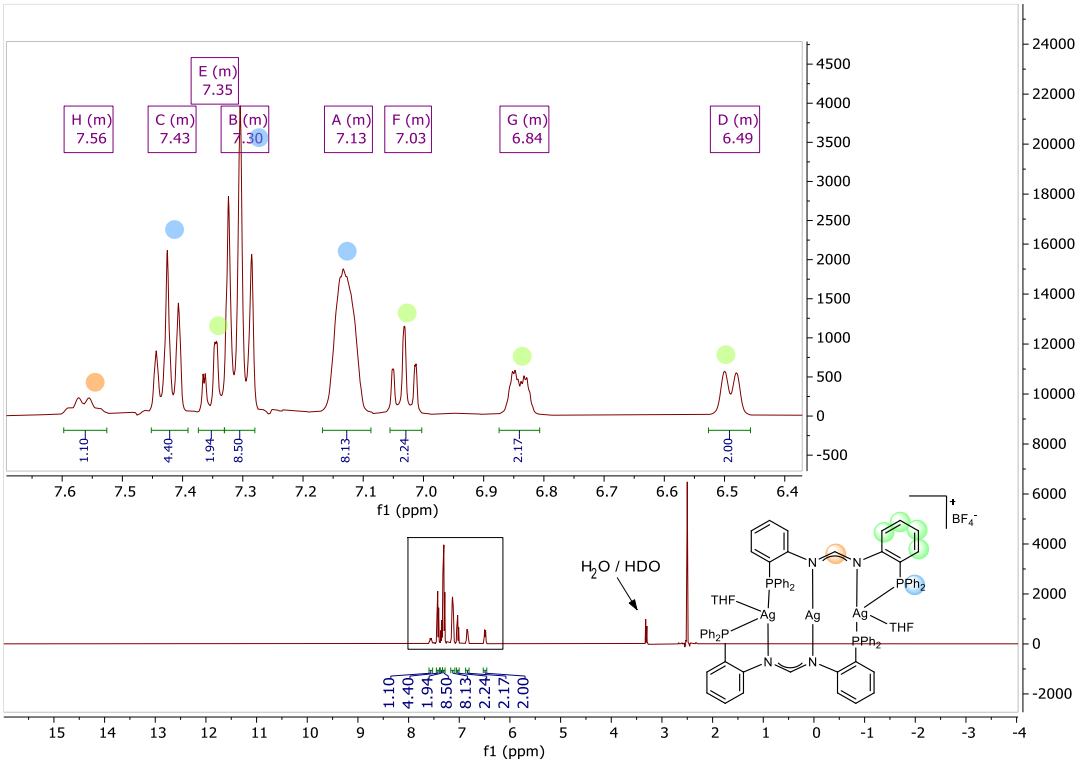

Figure S 5.6-1: ^{1}H NMR (400 MHz, DMSO-d_6) spectrum of **5**.

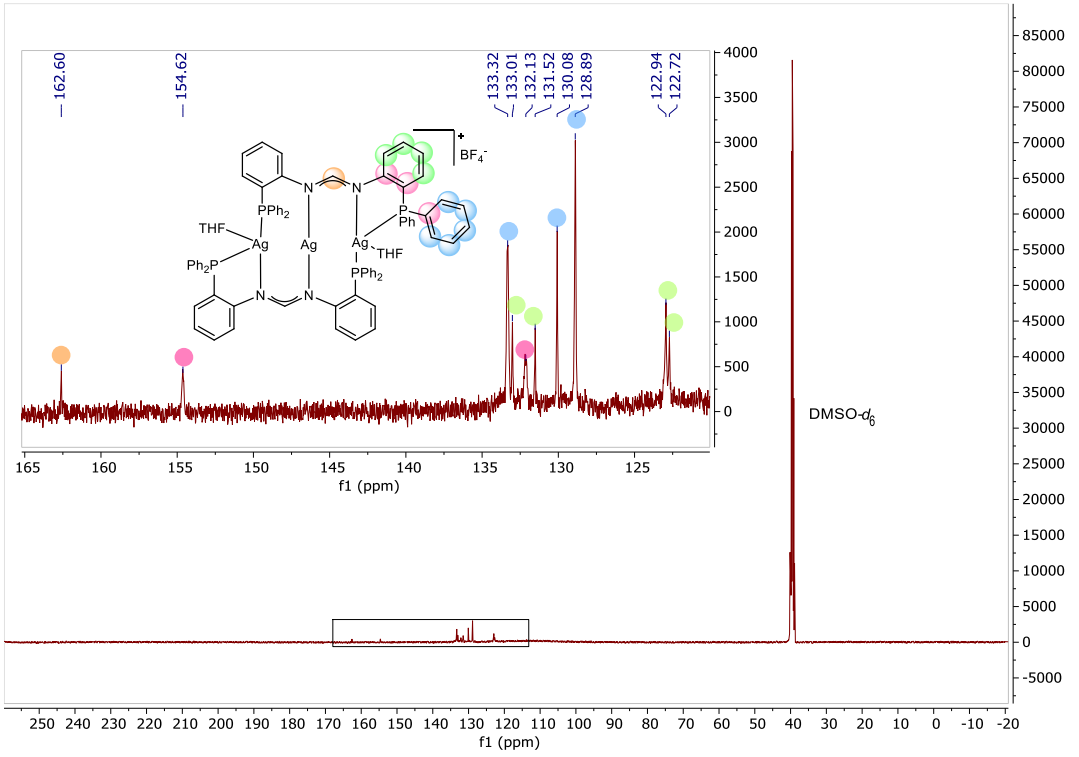

Figure S 5.6-2: ^{13}C{^{1}H} NMR (101 MHz, DMSO-d_6 spectrum of **5**.

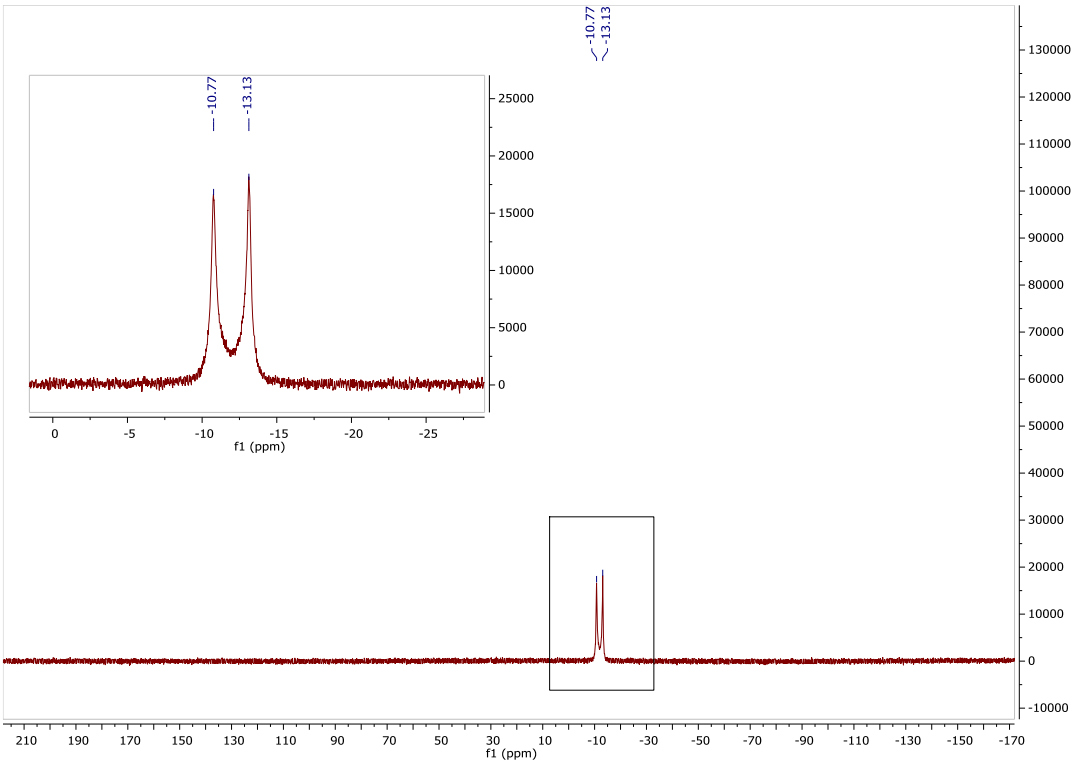

Figure S 5.6-3: $^{31}P\{^{1}H\}$ NMR (162 MHz, DMSO-$d_6$spectrum of **5**.

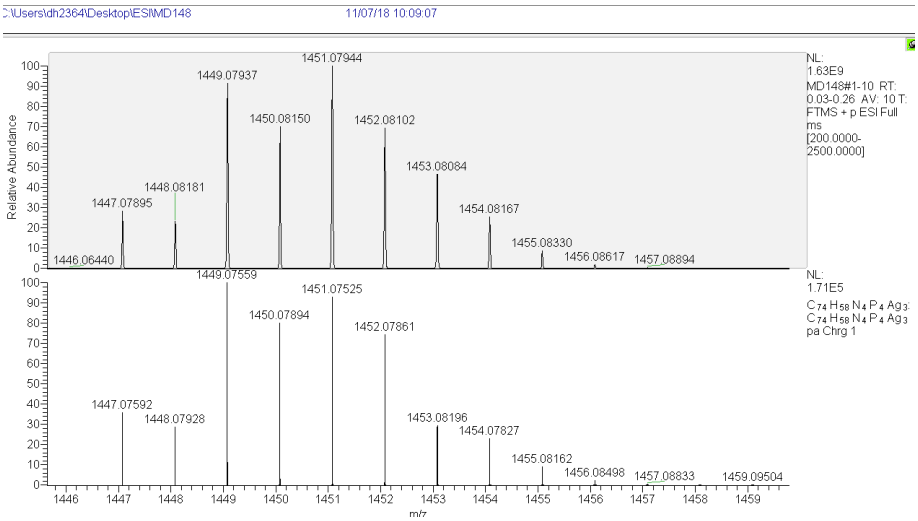

Figure S 5.6-4: ESI-MS analytics of **5**. Top: experimental spectrum; Bottom: simulated signals.

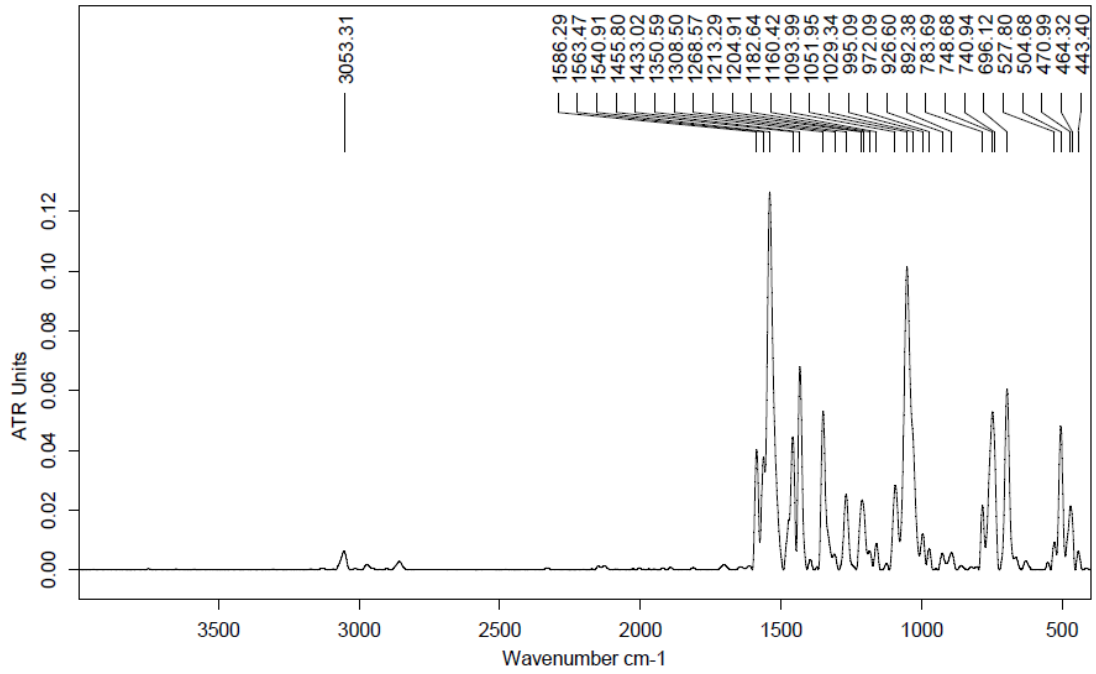

Figure S 5.6-5: IR ATR spectrum of **5**.

6 Crystallographic Data

A crystal suitable for single X-ray diffraction was covered in mineral oil (Aldrich) and mounted on a glass fiber. The selected crystal was directly transferred to the cold stream of a STOE IPDS 2 or a STOE StadiVari diffractometer. All structures were solved by using the programs SHELXS/T[22-24] and Olex2.[25] Remaining non-hydrogen atoms were located from successive difference Fourier map calculations. The refinements were carried out by using full-matrix least-squares techniques on F^2 by using the program SHELXL.[22-24] In each case, the locations of the largest peaks in the final difference Fourier map calculations, as well as the magnitude of the residual electron densities, were of no chemical significance. Crystallographic data (excluding structure factors) for the structures reported in this paper have been deposited with the Cambridge Crystallographic Data Centre as a supplementary publication no. 2094052 (Kdpfam) and 2041033-2041038 (**1**-**5**). Copies of the data can be obtained free of charge on application to CCDC, 12 Union Road, Cambridge CB21EZ, UK (fax: (+(44)1223-336-033; email: deposit@ccdc.cam.ac.uk).

Table S6-1: Crystal data and structure refinement of **1-3**.

Substance	**Kdpfam**	**1** [dpfam$_2$Cu$_2$]	**2** [dpfam$_2$Ag$_2$]	**3** [dpfam$_2$Au$_2$]
Identification code	MD125	MD132	MD114wdh	MD133
Empirical formula	$C_{37}H_{29}KN_2P_2$	$C_{74}H_{58}Cu_2N_4P_4$, [2 THF]	$C_{74}H_{58}Ag_2N_4P_4$, [2 THF]	$C_{74}H_{58}Au_2N_4P_4$, toluene
Formula weight	602.66	1254.20	1342.86	1613.19
Temperature/K	150.0	210.0	150.0	100.0
Crystal system	monoclinic	monoclinic	triclinic	monoclinic
Space group	Cc	*C*2/*c*	$P\bar{1}$	$P2_1/c$
a/Å	29.7304(9)	25.4339(7)	14.1675(5)	21.9289(4)
b/Å	9.4819(2)	14.1329(4)	17.0221(6)	26.2967(12)
c/Å	22.7870(7)	39.1265(10)	18.4683(6)	11.7368(8)
α/°	90		65.032(3)	90
β/°	102.235(2)	94.038(2)	88.399(3)	104.246(3)
γ/°	90		74.850(3)	90
Volume/Å^3	6277.8(3)	14029.3(7)	3880.0(3)	6560.0(6)
Z	8	8	2	4
ρ_{calc}g/cm^3	1.275	1.188	1.149	1.633
μ/mm^{-1}	0.300	0.739	0.625	4.615
F(000)	2512.0	5184.0	1368.0	3192.0
Crystal size/mm^3	0.502 × 0.315 × 0.112	0.285 × 0.212 × 0.071	0.483 × 0.368 × 0.145	0.101 × 0.064 × 0.039
Radiation	Mo Kα (λ = 0.71073 Å)	MoKα (λ = 0.71073 Å)	MoKα (λ = 0.71073 Å)	Mo Kα (λ = 0.71073 Å)
2Θ range for data collection/°	2.804 to 53.616	3.298 to 51.158	3.458 to 59.048	4.134 to 59.17
Index ranges	-37 ≤ h ≤ 37, -11 ≤ k ≤ 11, -28 ≤ l ≤ 28	-30 ≤ h ≤ 24, -17 ≤ k ≤ 17, -47 ≤ l ≤ 47	-19 ≤ h ≤ 19, -23 ≤ k ≤ 23, -22 ≤ l ≤ 25	-25 ≤ h ≤ 29, -35 ≤ k ≤ 35, -15 ≤ l ≤ 16
Reflections collected	27376	29245	39797	40288
Independent reflections	13226 [R_{int} = 0.0445, R_{sigma} = 0.0455]	12956 [R_{int} = 0.0718, R_{sigma} = 0.0825]	21186 [R_{int} = 0.0205, R_{sigma} = 0.0268]	16297 [R_{int} = 0.0548, R_{sigma} = 0.0952]
Data/restraints/parameters	13226/2/758	12956/0/757	21186/0/757	16297/256/943
Goodness-of-fit on F^2	1.016	1.027	1.098	1.029
Final R indexes [I>=2σ (I)]	R_1 = 0.0435, wR_2 = 0.1079	R_1 = 0.0697, wR_2 = 0.1681	R_1 = 0.0302, wR_2 = 0.0883	R_1 = 0.0546, wR_2 = 0.0993
Final R indexes [all data]	R_1 = 0.0538, wR_2 = 0.1130	R_1 = 0.1038, wR_2 = 0.1887	R_1 = 0.0401, wR_2 = 0.0922	R_1 = 0.1047, wR_2 = 0.1155
Largest diff. peak/hole / e Å^{-3}	0.42/-0.23	0.74/-0.97	0.38/-0.39	1.38/-1.17
Flack parameter	0.45(5)			

Table S6-2: Crystal data and structure refinement of **4**, **4a**, and **5.**

Substance	**4** [dpfam$_2$Cu$_3$(MeCN)][PF$_6$]	**4a** [dpfam$_2$Cu$_3$][PF$_6$]	**5** [dpfam$_2$Ag$_3$(*thf*)$_2$][BF$_4$]
Identification code	MD145	MD_L2Cu3DCM_Z	MD148D
Empirical formula	$C_{76}H_{61}Cu_3N_5P_4$, 2 ($P_{0.5}F_3$) ·2 THF	$C_{74}H_{58}Cu_3N_4P_5F_6$, [2.5 THF]	$C_{78}H_{66}Ag_3N_4O_1P_4$, BF_4, 3.5 THF
Formula weight	1647.97	1643.04	1862.01
Temperature/K	150	150.0	150
Crystal system	triclinic	triclinic	triclinic
Space group	$P\bar{1}$	$P\bar{1}$	$P\bar{1}$
a/Å	12.9637(3)	13.9670(7)	14.7569(3)
b/Å	13.9113(3)	16.5443(8)	14.5740(4)
c/Å	23.1423(6)	18.8209(9)	21.5672(5)
α/°	96.538(2)	65.314(4)	74.423(2)
β/°	99.897(2)	88.001(4)	68.661(2)
γ/°	111.353(2)	73.153(4)	84.842(2)
Volume/Å^3	3757.71(16)	3763.4(3)	4161.56(18)
Z	2	2	2
ρ_{calc}g/cm^3	1.456	1.450	1.486
μ/mm^{-1}	1.015	1.017	0.840
F(000)	1696.0	1752.0	1904.0
Crystal size/mm^3	0.417 × 0.35 × 0.287	0.308 × 0.162 × 0.086	0.424 × 0.365 × 0.324
Radiation	MoKα (λ = 0.71073 Å)	Mo Kα (λ = 0.71073 Å)	MoKα (λ = 0.71073 Å)
2Θ range for data collection/°	3.204 to 59.012	4.428 to 60.672	2.902 to 54.232
Index ranges	-17 ≤ h ≤ 17, -19 ≤ k ≤ 19, -30 ≤ l ≤ 31	-18 ≤ h ≤ 18, -23 ≤ k ≤ 22, -25 ≤ l ≤ 26	-17 ≤ h ≤ 18, -18 ≤ k ≤ 18, -27 ≤ l ≤ 27
Reflections collected	37989	33239	34037
Independent reflections	20464 [R_{int} = 0.0345, R_{sigma} = 0.0444]	18281 [R_{int} = 0.0510, R_{sigma} = 0.1243]	18209 [R_{int} = 0.0281, R_{sigma} = 0.0303]
Data/restraints/parameters	20464/12/986	18281/141/1037	18209/90/1045
Goodness-of-fit on F^2	1.027	0.929	1.026
Final R indexes [I>=2σ (I)]	R_1 = 0.0401, wR_2 = 0.0932	R_1 = 0.0584, wR_2 = 0.1269	R_1 = 0.0377, wR_2 = 0.1014
Final R indexes [all data]	R_1 = 0.0636, wR_2 = 0.1038	R_1 = 0.1183, wR_2 = 0.1471	R_1 = 0.0480, wR_2 = 0.1074
Largest diff. peak/hole / e Å^{-3}	0.56/-0.41	0.70/-0.81	1.42/-1.02

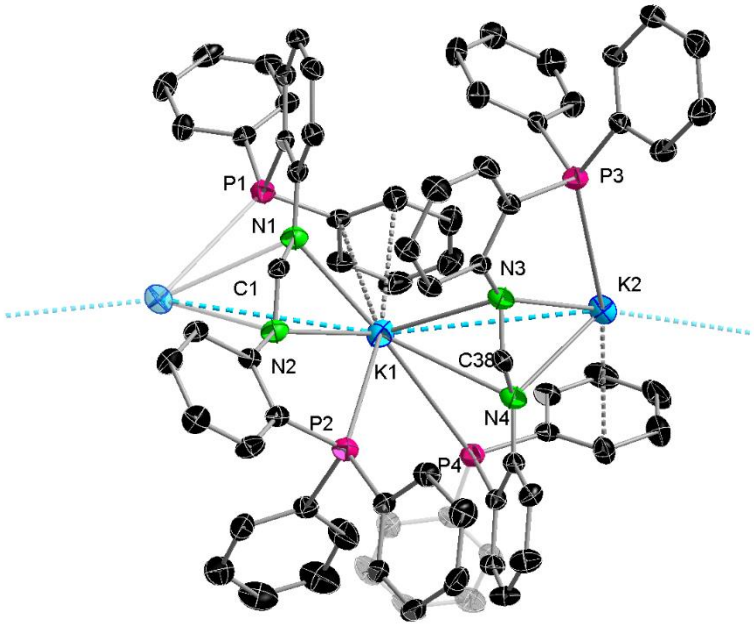

Figure S 6-0: Molecular structure of **Kdpfam** in the solid state. Hydrogen atoms are omitted for clarity. Thermal ellipsoids displayed to encompass 40% probability. Selected bond lengths [Å] and angles [°]: K1-K2 4.7697(14), K1-K2 4.7948(14), K1-P4 3.8320(14), K1-P2 3.663(2), K1-N1 2.834(4), K1-N4 3.153(4), K1-N3 2.978(3), K1-N2 2.947(3), K2-P1 3.8316(14), K2-P3 3.6466(14), K2-N1 3.173(4), K2-N4 2.852(3), K2-N3 2.919(3), K2-N2 2.998(3), N1-C1 1.324(5), N2-C1 1.311(5), N3-C38 1.318(5), N4-C38 1.326(5), K2-K1-K2 164.93(3), N2-C1-N1 122.1(4), N3-C38-N4 122.0(4).

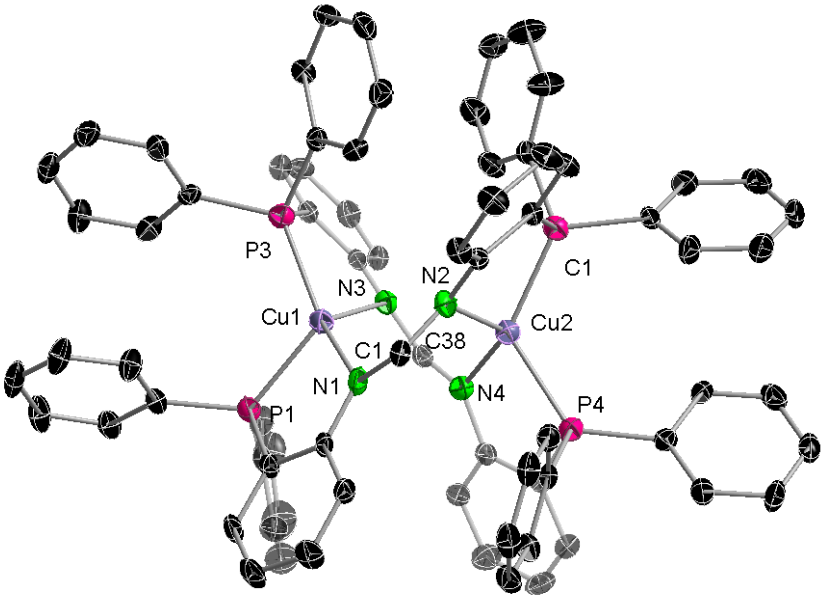

Figure S 6-1: Molecular structure of **1** in the solid state. Hydrogen atoms and non-coordinating solvent molecules are omitted for clarity. Thermal ellipsoids displayed to encompass 40% probability. Selected bond lengths [Å] and angles [°]: Cu1-P1 2.2529(13), Cu1-P3 2.2266(14), Cu1-N1 2.042(4), Cu1-N3 2.095(4), Cu2-P2 2.2289(14), Cu2-P4 2.2648(14), Cu2-N2 2.120(4), Cu2-N4 2.043(4), N1-C1 1.307(6), N2-C1 1.319(6), N3-C38 1.321(6), N4-C38 1.322(6), P3-Cu1-P1 116.41(5), N1-Cu1-P1 86.27(12), N1-Cu1-P3 140.34(12), N1-Cu1-N3 118.8(2), N1-C1-N2 120.8(4), N3-C38-N4 120.6(4).

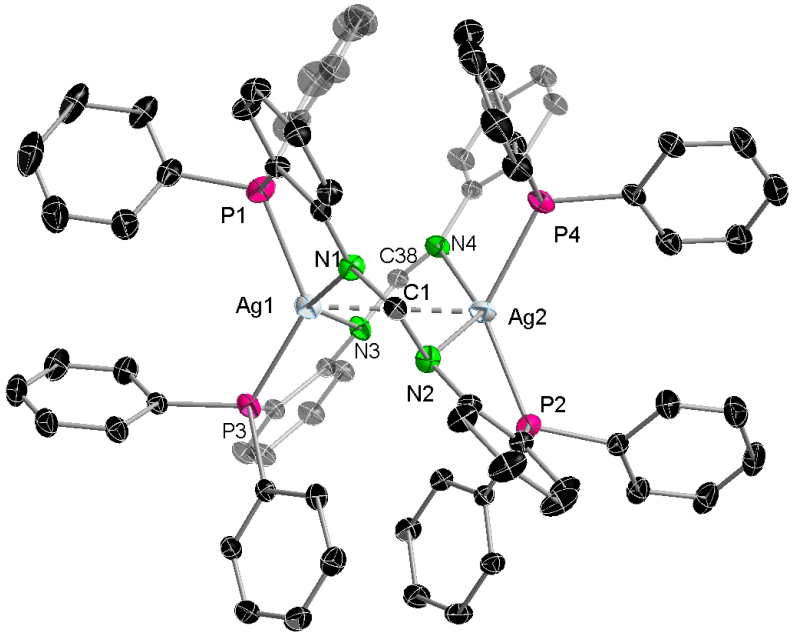

Figure S 6-2: Molecular structure of **2** in the solid state. Hydrogen atoms and non-coordinating solvent molecules are omitted for clarity. Thermal ellipsoids displayed to encompass 40% probability. Selected bond lengths [Å] and angles [°]: Ag1-Ag2 3.435, Ag1-P1 2.4793(5), Ag1-P3 2.4280(5), Ag1-N1 2.302(2), Ag1-N3 2.377 (2), Ag2-P2 2.4263(5), Ag2-P4 2.4668(5), Ag2-N2 2.453(2), Ag2-N4 2.3223(14), N1-C1 1.315(2), N2-C1 1.315(2), N3-C38 1.319(2), N4-C38 1.314(2), P3-Ag1-P1 125.97(2), N1-Ag1-P1 77.43(4), N1-Ag1-P3 136.50(4), N1-Ag1-N3 131.88(5), N3-Ag1-P1 112.91(4), N3-Ag1-P3 77.12(4), N1-C1-N2 121.9(2), N4-C38-N3 121.0(2).

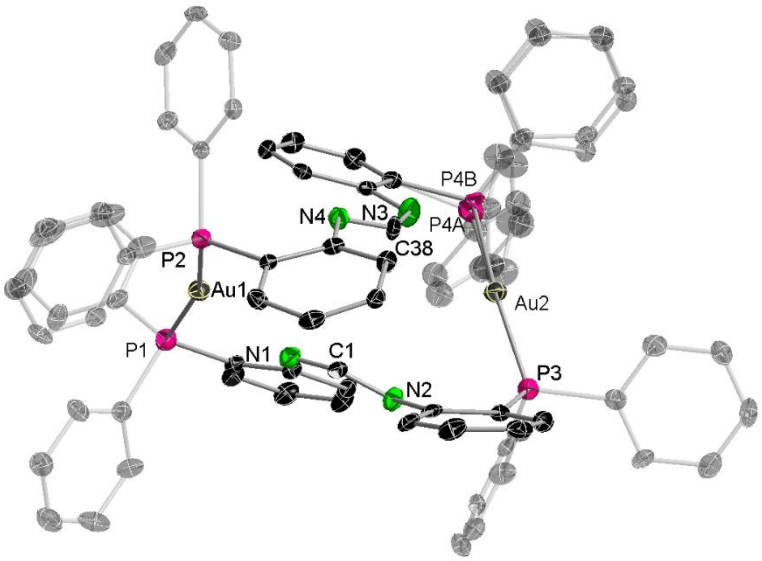

Figure S 6-3: Molecular structure of **3** in the solid state. Hydrogen atoms and non-coordinating solvent molecules are omitted for clarity. Thermal ellipsoids displayed to encompass 40% probability. Selected bond lengths [Å] and angles [°]: Au1-P1 2.332(2), Au1-P2 2.285(2), Au2-P3 2.277(2), Au2-P4A 2.26(2), Au2-P4B 2.323(10), N1-C1 1.326(8), N2-C1 1.316(8), N3-C38 1.321(8), N4-C38 1.309(8), P2-Au1-P1 163.60(6), P3-Au2-P4B 168.6(3), P4A-Au2-P3 163.5(4), N2-C1-N1 130.5(7), N4-C38-N3 129.6(6).

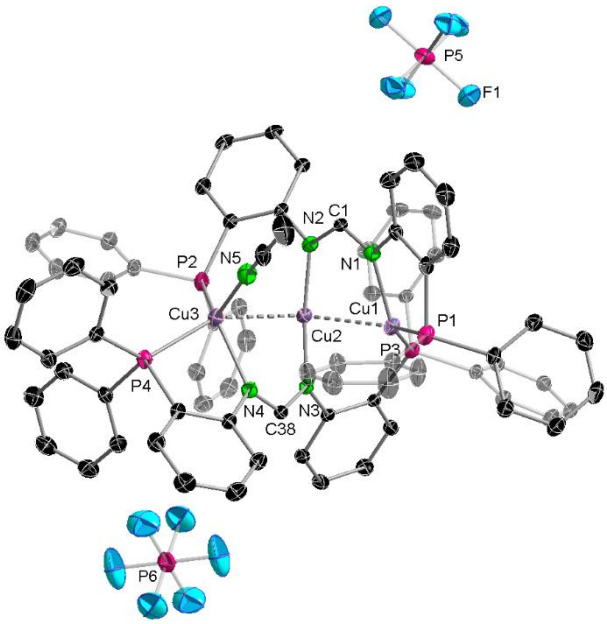

Figure S 6-4: Molecular structure of **4** in the solid state. Hydrogen atoms and non-coordinating solvent molecules are omitted for clarity. Thermal ellipsoids displayed to encompass 40% probability. Please note that the PF_6 anion only have an occupancy of 0.5 each. Selected bond lengths [Å] and angles [°]: Cu1-Cu2 2.5984(4), Cu2-Cu3 2.7792(4), Cu1-P1 2.2326(6), Cu1-P3 2.2126(6), Cu3-P2 2.2595(6), Cu3-P4 2.3158(6), Cu1-N1 2.042(2), Cu2-N2 1.880(2), Cu2-N3 1.872(2), Cu3-N4 2.098(2), Cu3-N5 2.032(2), N1-C1 1.315(3), N2-C1 1.325(3), N3-C38 1.329(3), N4-C38 1.311(3), Cu1-Cu2-Cu3 117.835(13), N1-C1-N2 122.5(2), N4-C38-N3 123.2(2).

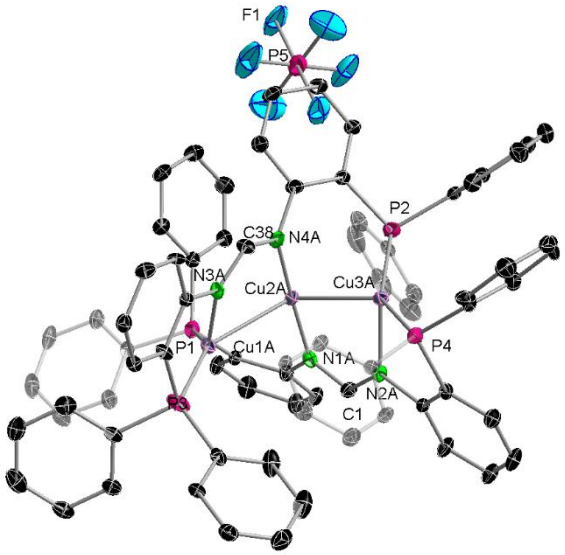

Figure S 6-5: Molecular structure of **4a** in the solid state. Hydrogen atoms and non-coordinating solvent molecules are omitted for clarity. Thermal ellipsoids displayed to encompass 40% probability. Please note that the Cu_3 chain is partly disordered as well as the nitrogen atoms. Only the main part (84 %) is displayed. Selected bond lengths [Å] and angles [°]: Cu1A-Cu2A 2.5736(7), Cu2A-Cu3A 2.5577(8), P1-Cu1A 2.1755(11), P3-Cu1A 2.2345(11), P2-Cu3A 2.1978(11), P4-Cu3A 2.2372(11), Cu1A-N3A 2.005(3), Cu2A-N1A 1.874(3), Cu2A-N4A 1.875(3), Cu3A-N2A 2.027(3), N1A-C1A 1.318(3), N3A-C38A 1.327(4), N4A-C38A 1.327(4), N3A-C38A 1.327(4), N4A-C38A 1.327(4), Cu3A-Cu2A-Cu1A 122.07(3), N2A-C1A-N1A 121.5(5), N3A-C38A-N4A 121.2(6).

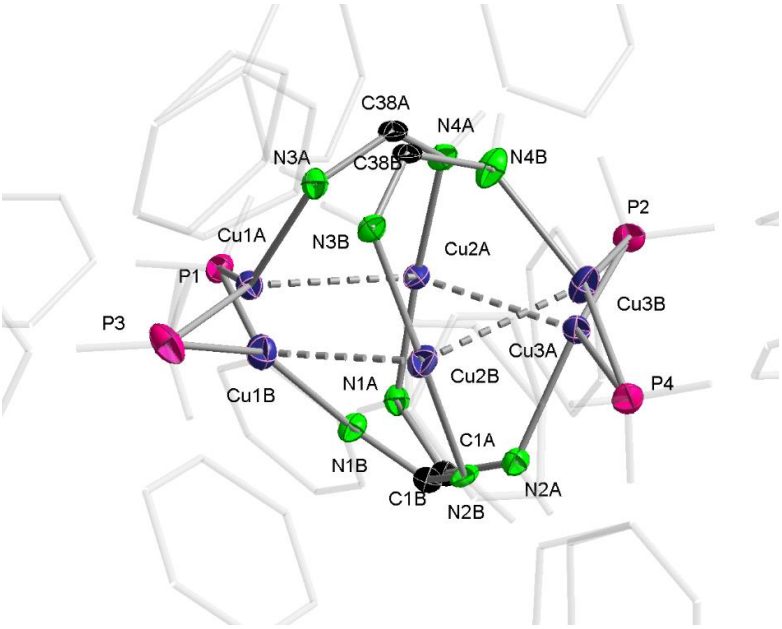

Figure S 6-6: Zoom in picture of molecular structure of **4a** in the solid state. Hydrogen atoms and non-coordinating solvent molecules and counter anion are omitted for clarity. Thermal ellipsoids displayed to encompass 40% probability. Please note that the Cu_3 chain is partly disordered as well as the nitrogen atoms and some carbon atoms (Part A: 84%; Part B: 16%.) Selected bond lengths [Å] and angles [°]: Cu1A-Cu2A 2.5736(7), Cu2A-Cu3A 2.5577(8), Cu1B-Cu2B 2.564(4), Cu2B-Cu3B 2.567(5), P1-Cu1A 2.1755(11), P1-Cu1B 2.396(3), P3-Cu1A 2.2345(11), P2-Cu3A 2.1978(11), P2-Cu3B 2.249(4), P4-Cu3A 2.2372(11), P4-Cu3B 2.211(4), Cu1A-N3A 2.005(3), Cu2A-N1A 1.874(3), Cu2A-N4A 1.875(3), Cu3A-N2A 2.027(3), Cu1B-N1B 2.058(19), Cu2B-N2B 1.95(2), Cu2B-N3B 1.92(2), Cu3B-N4B 2.02(2), N1A-C1A 1.318(3), N3A-C38A 1.327(4), N4A-C38A 1.327(4), Cu1B-Cu2B 2.564(4), Cu1B-N1B 2.06(2), Cu2B-Cu3B 2.567(5), Cu2B-N2B 1.95(2), Cu2B-N3B 1.92(2), Cu3B-N4B 2.02(2), N3A-C38A 1.327(4), N4A-C38A 1.327(4), C38B-N3B 1.327(4), C38B-N4B 1.327(4), C1B-N2B 1.317(4), C1B-N1B 1.318(4), Cu3A-Cu2A-Cu1A 122.07(3), Cu1B-Cu2B-Cu3B 122.4(2), N2A-C1A-N1A 121.5(5), N3A-C38A-N4A 121.2(6), N2B-C1B-N1B 121(2), N4B-C38B-N3B 117.6(19).

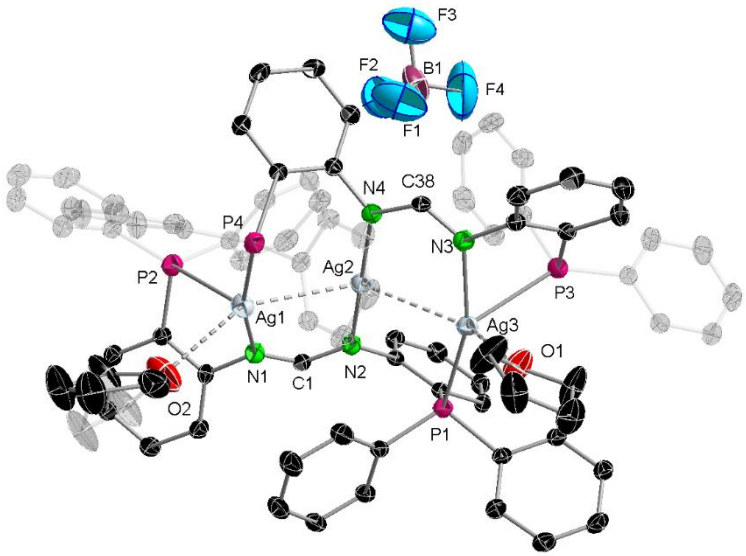

Figure S 6-7: Molecular structure of **5** in the solid state. Hydrogen atoms and non-coordinating solvent molecules are omitted for clarity. Thermal ellipsoids displayed to encompass 40% probability. Selected bond lengths [Å] and angles [°]: Ag1-Ag2 2.8987(3), Ag2-Ag3 2.8893(3), Ag1-P2 2.8457(8), Ag1-P4 2.3645(7), Ag3-P1 2.3539(7), Ag3-P3 2.6320(8), Ag1-N1 2.174(2), Ag2-N2 2.126(2), Ag2-N4 2.129(2), Ag3-N3 2.215(2), Ag3-O1 2.552(2), N1-C1 1.309(4), N2-C1 1.319(4), N3-C38 1.303(4), N4-C38 1.317(4), Ag3-Ag2-Ag1 133.861(10), N2-Ag2-N4 173.66(9), C1-N1-C2 125.6(3) N3-C38-N4 125.5(3).

7 References

1. G. R. Fulmer, A. J. M. Miller, N. H. Sherden, H. E. Gottlieb, A. Nudelman, B. M. Stoltz, J. E. Bercaw and K. I. Goldberg, *Organometallics*, 2010, **29**, 2176-2179.
2. G. B. Deacon, P. C. Junk and D. Werner, *Polyhedron*, 2016, **103**, 178-186.
3. S. Ahrland, K. Dreisch, B. Norén and Å. Oskarsson, *Mater. Chem. Phys.*, 1993, **35**, 281-289.
4. C. Kaub, PhD thesis, *Synthese multi- und heterometallischer Goldkomplexe mit Ferrocendithiocarboxylat und bipyridyl-funktionalisierten N-heterozyklischen-Carbenliganden*, Karlsruhe Institute of Technology, 2016.
5. C. Zovko, S. Bestgen, C. Schoo, A. Görner, J. M. Goicoechea and P. W. Roesky, *Chem. Eur. J.*, 2020, **26**, 13191-13202.
6. G. S. Day, B. Pan, D. L. Kellenberger, B. M. Foxman and C. M. Thomas, *Chem. Commun.*, 2011, **47**, 3634-3636.
7. L.-C. Liang, P.-S. Chien, J.-M. Lin, M.-H. Huang, Y.-L. Huang and J.-H. Liao, *Organometallics*, 2006, **25**, 1399-1411.
8. J. C. de Mello, H. F. Wittmann and R. H. Friend, *Adv. Mater.*, 1997, **9**, 230-232.
9. J. P. Perdew, K. Burke and M. Ernzerhof, *Phys. Rev. Lett.*, 1996, **77**, 3865-3868.
10. C. Adamo and V. Barone, *J. Chem. Phys.*, 1999, **110**, 6158–6170.
11. F. Weigend and A. Baldes, *J. Chem. Phys.*, 2010, **133**, 174102.
12. F. Weigend and R. Ahlrichs, *Phys. Chem. Chem. Phys.*, 2005, **7**, 3297–3305.
13. D. Figgen, G. Rauhut, M. Dolg and H. Stoll, *Chem. Phys.*, 2005, **311**, 227–244.
14. R. Ahlrichs, M. Bär, M. Haser, H. Horn and C. Kolmel, *Chem. Phys. Lett.*, 1989, **162**, 165-169.
15. F. Furche, R. Ahlrichs, C. Hättig, W. Klopper, M. Sierka and F. Weigend, *Wiley Interdiscip. Rev.: Comput. Mol. Sci.*, 2014, **4**, 91–100.
16. TURBOMOLE GmbH, *Journal*, 1989-2007, A development of University of Karlsruhe and Forschungszentrum Karlsruhe GmbH.
17. O. Treutler and R. Ahlrichs, *J. Chem. Phys.*, 1995, **102**, 346–354.
18. K. Eichkorn, F. Weigend, O. Treutler and R. Ahlrichs, *Theor. Chim. Acta*, 1997, **97**, 119–124.
19. F. Weigend, *Phys. Chem. Chem. Phys.*, 2006, **8**, 1057-1065.
20. P. Plessow and F. Weigend, *J. Comput. Chem.*, 2012, **33**, 810-816.
21. F. Neese, F. Wennmohs, A. Hansen and U. Becker, *Chem. Phys.*, 2009, **356**, 98–109.
22. G. M. Sheldrick, *Journal*, 1997.
23. G. M. Sheldrick, *Acta Crystallogr., Sect. A: Found. Crystallogr.*, 2008, **64**, 112-122.
24. G. M. Sheldrick, *Acta Crystallogr., Sect. C: Struct. Chem.*, 2015, **71**, 3-8.
25. O. V. Dolomanov, L. J. Bourhis, R. J. Gildea, J. A. K. Howard and H. Puschmann, *J. Appl. Crystallogr.*, 2009, **42**, 339-341.